1-1-2006

Parametric effects on concrete-dowel behavior

Nathan Joel Pierson
Iowa State University

Parametric effects on concrete-dowel behavior

by

Nathan Joel Pierson

A thesis submitted to the graduate faculty

in partial fulfillment of the requirements for the degree of

MASTER OF SCIENCE

Major: Civil Engineering (Structural Engineering)

Program of Study Committee:
Max L. Porter, Major Professor
Fouad S. Fanous
Lester W. Schmerr, Jr.

Iowa State University

Ames, Iowa

2006

Graduate College

Iowa State University

This is to certify that the master's thesis of

Nathan Joel Pierson

has met the thesis requirements of Iowa State University

Signatures have been redacted for privacy

TABLE OF CONTENTS

LIST OF TABLES

LIST OF FIGURES

ABSTRACT

Dowel bars are a useful tool for transferring loads from one concrete slab to another across joints. Dowels have usefulness in highway slab and building slab applications. While dowels are used to increase load transfer capabilities across joints, they also introduce new problems, including stress concentrations and corrosion.

Most dowel bars have circular cross sections. The regions of stress concentration for circular dowels are at the top and bottom of the cross section. Therefore, the sides of the dowel give little aid in providing bearing against dowel loading. Circular steel dowels have performed well in handling stress concentrations. However, alternative materials and shapes may perform better.

Much research has been conducted at Iowa State University and nationally concerning the performance of dowels with various parameters. Parameters include dowel material, dowel shape, joint width, and dowel spacing and have been used to evaluate bearing stress performance. Laboratory testing, field testing, and finite element analysis have all been performed to study these parameters.

Altogether, ten types of dowels were tested. The six highway dowels studied were adequate to transfer load. Cost and environment are criteria that should be considered when choosing among these six dowel types.

All four of the building slab dowel types studied were able to transfer a load of at least 3000 pounds between adjacent slabs without a factor of safety (an appropriate factor of safety should be applied as deemed necessary by a jurisdictional authority). Slab thickness, dowel spacing, and dowel cost should all be considered when selecting among these four dowel types.

1. INTRODUCTION

1.1 Background

Dowel bars are a useful tool for transferring loads from one concrete slab to another across joints. Dowels have usefulness in highway slab and building slab applications. While dowels are used to increase load transfer capabilities across joints, they also introduce new problems.

Repeated loading of a dowel across a joint leads to oblonging within the concrete that contacts the dowel. The oblonging is a result of stress concentrations and creates void spaces around the dowel. The repetitive loading over time leads to the concrete surrounding the dowel to crush and void spaces to become bigger. The voids reduce the ability of the dowels to effectively transfer loads.

Steel is the most commonly used dowel material for transferring loads between concrete slabs. Steel's susceptibility to corrode—even when epoxy coated—can lead to many joint problems. Corrosion can bind joints and, thus, not allow for thermal expansion. Corrosion deteriorates the dowel over time and reduces the dowel's effectiveness. Concrete cracking can occur as a result of the binding of joints and deterioration of the dowels, which can lead no load transfer across a joint. When load ceases to be transferred across joints the load is transferred to the subgrade. When load is not transferred, adjacent slabs settle independent of each other creating unwanted vertical discontinuities at the joints.

Most dowel bars have circular cross sections. The regions of stress concentration for circular dowels are at the top and bottom of the cross section. Therefore, the sides of the dowel give little aid in providing bearing against dowel loading. Circular steel dowels have

performed well in handling stress concentrations. However, alternative materials and shapes may perform better.

Much research has been conducted at Iowa State University (*1-21*) and nationally (*22-26, 34-36*) (see Section 1.4 for more details) about the performance of dowels with various parameters. Parameters include dowel material, dowel shape, joint width, and dowel spacing and have been used to evaluate bearing stress performance (*15-20*). Laboratory testing, field testing, and finite element analysis have all been performed to study these parameters.

An emphasis of much of the research has been evaluating fiber reinforced polymer (FRP) as a non-corrosive alternative to steel. Other FRP dowel bar research is being and has been conducted in Illinois, Ohio, Minnesota, and Wisconsin (*26*). Research in Iowa and Ohio has suggested that corrosion deterioration comparisons between FRP and steel dowels used in highway applications require longer-term evaluation. Research from all these states have shown that steel provides better load transfer efficiency than FRP for similar size round dowels. Studies of the performance of larger size FRP dowels and smaller spacing to improve load transfer efficiency are therefore needed. Studies conducted at Iowa State University (ISU) as well as in Illinois have recommended the evaluation of elliptically-shaped dowels (both FRP and steel) to improve load transfer efficiency.

1.2 Objective

The objective of this study was to investigate the effects of different dowel shapes and materials on the dowel behavior for concrete pavement and building slabs. The focus was on dowels researched for two independent projects. One project centered on dowels for highway use sponsored by the United States Department of Transportation, while the other

focused on industry dowels used for building slabs. The combination of these two projects provides a good set of parameters to study although the highway dowels and building slab dowels should not be directly compared to each other since their sizes and applications are different.

The Modified AASHTO T253 method (and variations of the method) for determining the modulus of dowel support was the main method of testing the dowels. The test method was used to determine the following:

1. Modulus of dowel support
2. Effects of joint width
3. Effects of dowel shape
4. Effects of dowel material
5. Effects of dowel flexural rigidity
6. Dowel deflections
7. Bearing stresses

A select portion of the testing included the use of strain gages to determine dowel behavior (e.g. bending moment and deflection behavior) along the length of the dowel.

Ultimately, a comparison and evaluation of the bearing stresses of the dowels on concrete was performed and the adequacy of dowel bars was determined. The focus of this work was to investigate the dowel-to-concrete interface behavior and the associated shear, deflection and bending moments of the dowel transfer modeling per se, neglecting the effects of soil support.

1.3 Scope

The scope of this study includes the testing and analysis of the following:

- Ten dowel types
    - Six highway dowel types
    - Four building slab dowel types
- Twenty-eight test configurations
    - Ten dowel types
    - Three joint widths
    - Use of dowel sleeves
- Eighty-four total specimens
- Concrete compressive strength tests
- FRP loss on ignition tests

1.4 Literature Review

The literature review included theses, research reports, journal articles, proceedings, and assessments about dowel bar theory and performance. These references included a variety of topics. Different dowel materials were evaluated, including steel (*2,9-11,15,17*), fibercomposites (*1-9,11,16,19,20,25*), and aluminum and copper (*9,11*). Testing has involved laboratory evaluation (*8,9,11,15,19-21*), field evaluation (*9-11,16,17,19*), and finite element analysis (*8-11*). Much of the laboratory testing has utilized the AASHTO T253 method (*27*) and some modifications to the test have been recommended (*15*) and utilized (*20*).

There has been extensive research on parameters such as dowel spacing (*8,10,11,15-17, 19*) but not as much research on joint width. There has been a theoretical evaluation (*14*) of joint width and recommendations for more research into the effects of joint width (*13*). Some of the past research conducted at ISU has involved analysis of the theory used (*14,18*) and development of more complex theory (*18*).

Other studies have conducted an assessment of dowel research (*12,13,26*) to determine the overlaps and gaps in knowledge. A significant amount of reference documents were found relating to the dowel-to-concrete interface theory and the modulus of dowel support (*28-33*). This background will be discussed later in Chapters 3 and 4. In addition, other studies have been conducted (*34-36*). Much of the research at ISU has had an emphasis on alternatives to round steel dowels and has been presented at national conventions (*22-24*). More recently, elliptically-shaped dowels have been researched (*15-17,19,20*) and more evaluation is needed. The modified AASHTO method of evaluation for plate dowels in building slabs are a new topic of research at ISU (*21*).

Additional discussion of references can be found throughout this study. A list of references can be found at the end of this study.

2. TESTING

2.1 Test Matrices

Ten different dowels were tested in 28 different configurations. Six of the dowels were designed for use in highway construction to transfer load across transverse joints. These six dowels are referred to as *highway dowels* in this study. The other four dowels tested are used primarily in construction joints in building floor slabs. These four dowels are referred to as *building slab dowels* in this study.

2.1.1 Highway Dowels

Table 2.1 shows the test matrix for the highway dowels. The six dowels are tested for three different joint widths for a total of 18 configurations. Each configuration has three specimens for a total of 54 specimens.

The main differences among the six highway dowels are shape and material. Three dowels have circular cross sections and three have elliptical cross sections. Three of the dowels are epoxy-coated steel, one dowel is stainless steel, and two dowels are glass fiber reinforced polymer (GFRP).

2.1.2 Building Slab Dowels

Table 2.2 shows the test matrix for the building slab dowels. The four dowels are tested with and without a dowel sleeve and one dowel type was tested for two different size specimens—6 inches and 12 inches in depth (i.e. slab thickness)—for a total of ten configurations. Each configuration has three specimens for a total of 30 specimens.

Table 2.1. Highway dowel test matrix

Dowel Material	Dowel Shape	Dowel Size, in.	Gap Width, in.	Quantity
Steel (epoxy-coated)	Circular	1.5	0	3*
Steel (epoxy-coated)	Circular	1.5	1/8	3
Steel (epoxy-coated)	Circular	1.5	1/2	3*
Steel (epoxy-coated)	Elliptical	2.00 x 1.375	0	3
Steel (epoxy-coated)	Elliptical	2.00 x 1.375	1/8	3
Steel (epoxy-coated)	Elliptical	2.00 x 1.375	1/2	3*
Steel (epoxy-coated)	Elliptical	1.66 x 1.13	0	3*
Steel (epoxy-coated)	Elliptical	1.66 x 1.13	1/8	3
Steel (epoxy-coated)	Elliptical	1.66 x 1.13	1/2	3*
Stainless Steel	Circular	1.5	0	3
Stainless Steel	Circular	1.5	1/8	3*
Stainless Steel	Circular	1.5	1/2	3
GFRP	Circular	1.875	0	3
GFRP	Circular	1.875	1/8	3*
GFRP	Circular	1.875	1/2	3
GFRP	Elliptical	2.25 x 1.25	0	3*
GFRP	Elliptical	2.25 x 1.25	1/8	3*
GFRP	Elliptical	2.25 x 1.25	1/2	3

*Indicates one specimen in test series of three specimens has strain gages
Note: The dimension for circular dowels is diameter and the dimensions for elliptical dowels are strong axis diameter (width) x weak axis diameter (height)

Table 2.2. Building slab dowel test matrix

	Dowel		Specimen	
Dowel Type	Dimensions, in.	Cross Section, in.	Depth, in.	Quantity
Square Plate	4½ x 4½ x ¼	4½ x ¼	6	3
Diamond Plate	4½ x 4½ x ¼	6.36 x ¼	6	3
Rectangular Plate	12 x 2 x ⅜	2 x ⅜	6	3
Round Bar	14 x ¾	¾ diameter	6	3
Round Bar	14 x ¾	¾ diameter	12	3
Square Plate w/sleeve	4½ x 4½ x ¼	4½ x ¼	6	3
Diamond Plate w/sleeve	4½ x 4½ x ¼	6.36 x ¼	6	3
Rectangle Plate w/sleeve	12 x 2 x ⅜	2 x ⅜	6	3
Round Bar w/sleeve	14 x ¾	¾ diameter	6	3
Round Bar w/sleeve	14 x ¾	¾ diameter	12	3

All four dowels are steel. Each dowel is a different shape. Figure 2.1 shows the four shapes which are (from left to right) rectangle, square, diamond, and round. The dashed lines

show the position of the joint. The dowels can be used with or without a sleeve. The dowel sleeve is used in practice where a joint needs to expand or contract and dowels are still needed to provide load transfer. A sleeve is added to one half of a dowel to allow the dowel to move within one of the slabs while remaining fixed in the other slab.

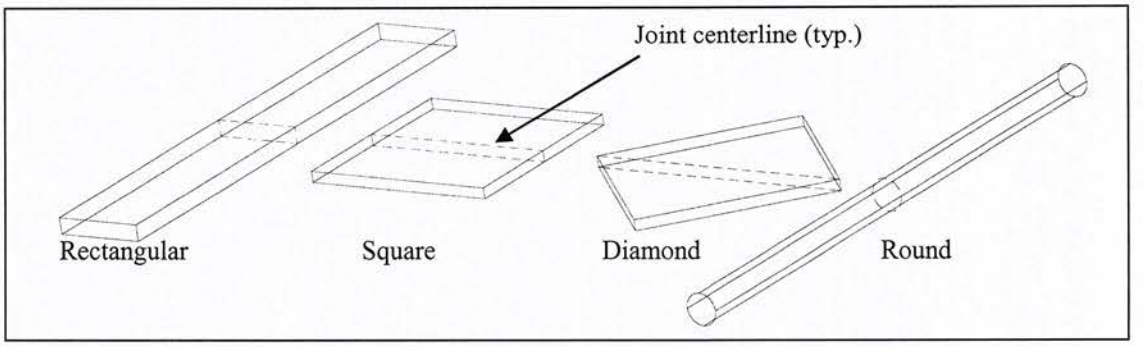

Figure 2.1. Building slab dowel shapes

2.2 Test Descriptions

2.2.1 Modified AASHTO T253

The American Association of State Highway and Transportation Officials (AASHTO) developed a test (Figure 2.2) to measure a dowel's ability to limit joint deflection (*27*).

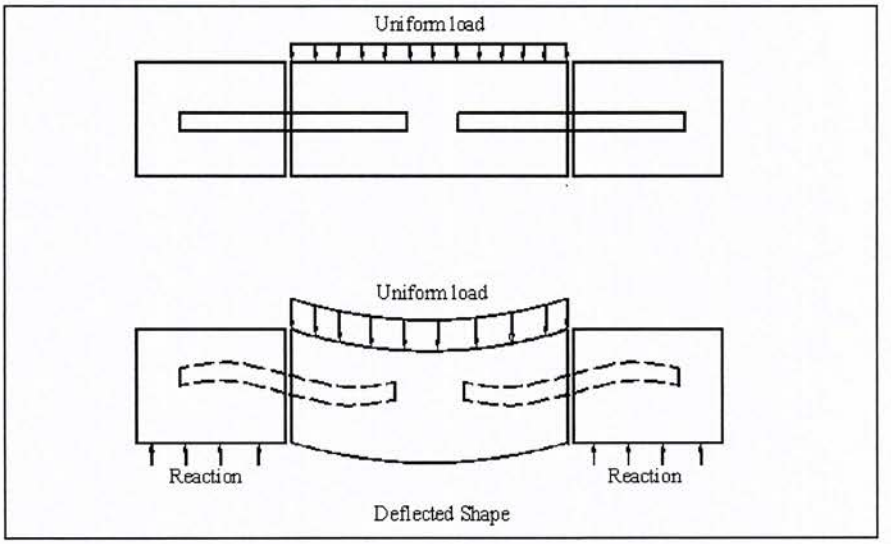

Figure 2.2. AASHTO T253

Researchers have made several modifications to the AASHTO T253 over the years. The Modified AASHTO T253 (*15*) was developed and is currently in use at Iowa State University as shown in Figure 2.3. The biggest difference is the load application. Porter and others (*3*) recommend two point loads on the center block instead of one uniform load across the center block. This loading reduces the flexural behavior of the center block and provides a more pure shear load transfer across the joints. The Modified AASHTO T253 specimens have 12-inch long end blocks and a 21-inch long center block with 12-inch height and 12-inch width.

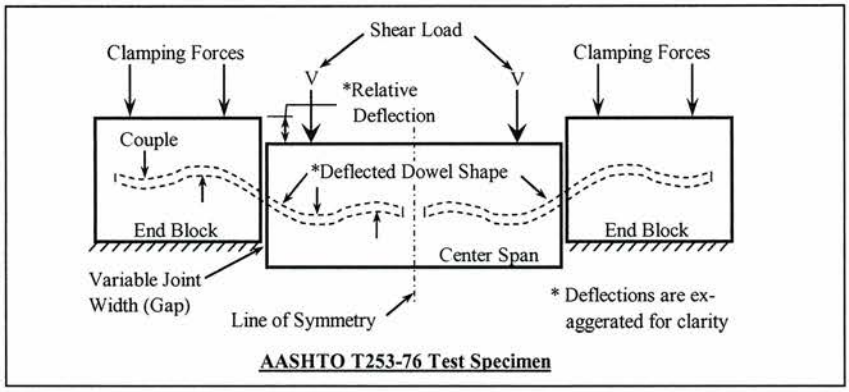

Figure 2.3. Modified AASHTO T253

The load frame shown in Figure 2.4 was constructed to test the specimens. The specimens were centered on a stiffened test beam, which was secured to the laboratory structural tie-down floor. The top cross beam was supported by two ductile iron structural tubes that were post-tensioned to the laboratory floor to counteract forces from the hydraulic actuator. The actuator was positioned between the top cross beam and a spreader beam. The spreader beam was used to distribute the actuator load to two line loads located three inches from the ends of the center block. The distance of three inches between the end of the center block and the line load is to accommodate instrumentation. Two square steel tubes were wrench-tightened down to the test beam over each end block to provide a fixed-end condition

to prevent rotation of the end blocks. Pieces of neoprene were placed between the concrete specimens and steel parts of the test frame (line load application and end-block fixity) to prevent localized crushing of concrete and to better distribute forces. Although neoprene is a relatively softer material it does not increase a specimen's ability to rotate because the neoprene provides better clamping force distribution over the rough concrete surface.

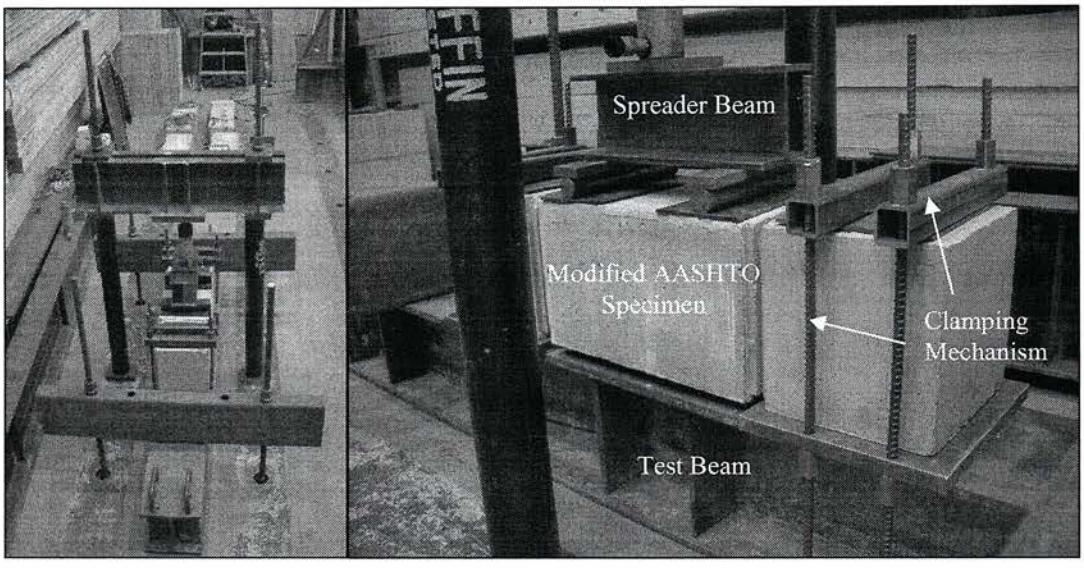

Figure 2.4. Load test frame

Eight direct current deflection transducers (DCDTs) were used to measure deflections during testing. Four DCDTs were used to measure relative deflection across each of the two joints, while the remaining four DCDTs were used to monitor rotations of the end blocks and test beam. A data acquisition system was used to simultaneously read the applied actuator load and eight deflections.

2.2.2 Building Slab Dowel Testing

The specimens used for the building slab dowels were small-scale versions of the Modified AASHTO T253 with a few modifications. The specimens were 12 inches wide

like the Modified AASHTO T253 but only 6 inches in height to better represent building slab thickness. The center block is 16 inches long and the end blocks are 8 inches long. Steel reinforcement was added to the center block to help prevent concrete failure during testing due to the reduced thickness of the specimens. The reinforcement consisted of #2 bars in an "H" configuration 1 inch from the bottom of the specimens (see Figure 2.5).

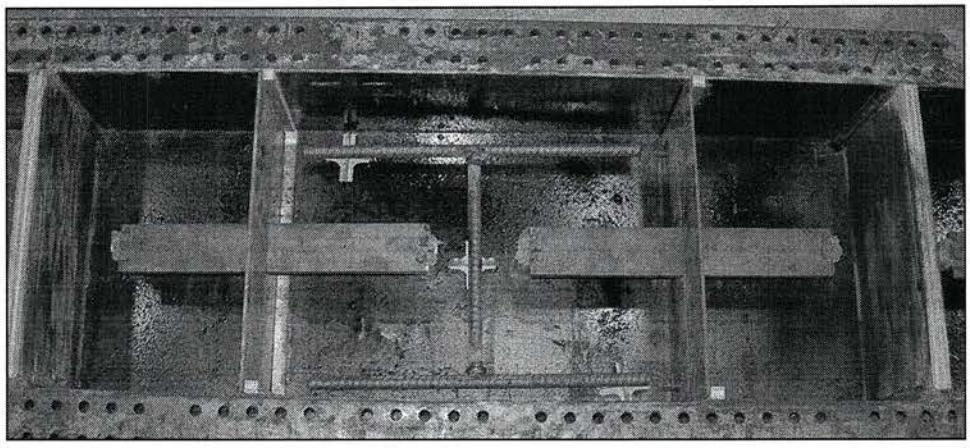

Figure 2.5. Building slab specimen in forms

The same test frame was used for the building slab dowel specimens with a few modifications to accommodate the smaller height. Instead of using a spreader beam to apply two line loads, the actuator was placed at the center of the center block and a single load was applied. This was done to mimic testing procedures used by industry for the building slab dowels.

Six round dowel specimens (three without sleeves and three with sleeves) were constructed as Modified AASHTO T253 specimens (12-inch deep specimens as opposed to 6-inch deep specimens) to observe the effects of increased concrete thickness around the dowel.

2.3 Construction

2.3.1 Modified AASHTO T253 Specimens

The Modified AASHTO T253 specimens were constructed using steel forms built in 12-inch by 12-inch troughs (see Figure 2.6). Specimens were separated within the troughs by 3/4-inch plywood sheets. The joints between the end blocks and center blocks were created using 1/8-inch PVC sheets cut to accommodate a dowel through the center. The PVC sheets were removed after the concrete was cured. One piece of the PVC sheet was used for the 1/8-inch joint and four sheets were used for the 1/2-inch joints. Each end of the dowels was set on a chair.

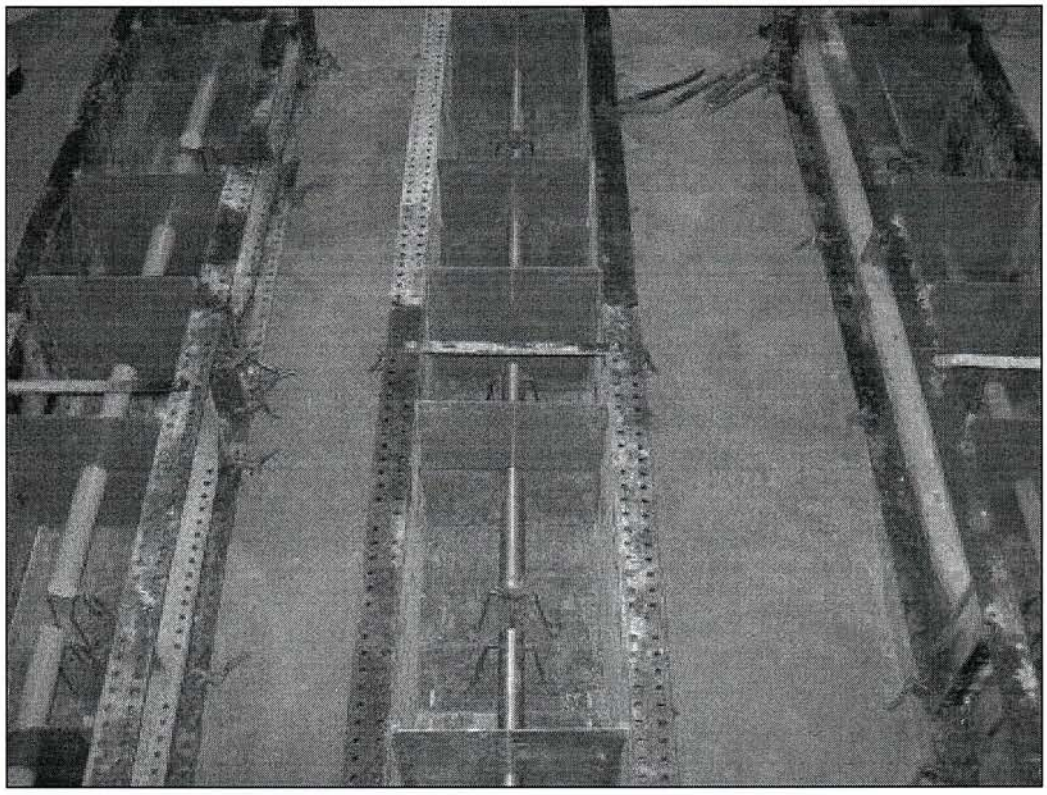

Figure 2.6. Troughs for constructing Modified AASHTO T253 specimens

A Class-C Portland Cement mix with a target compressive strength of 4000 psi was used for the concrete. The concrete was placed in the troughs with shovels and by hand. The concrete was vibrated to ensure proper consolidation. Care was taken to not disturb the dowels while placing concrete so as not to develop dowel misalignment. The 0-inch joint specimens were constructed by placing concrete for the end blocks and allowing that concrete to set before placing the concrete for the center blocks.

2.3.2 Building Slab Dowel Specimens

The building slab dowel specimens were constructed in the same manner as the Modified AASHTO T253 specimens. The troughs were 12-inch wide by 6-inch tall (refer to Figure 2.5). The steel reinforcement for the center blocks were placed on 3/4-inch chairs. Dowel sleeves for the specimens containing the sleeves were glued to one side of the PVC-sheet joint dividers and supported on the end by a piece of 3/4-inch PVC pipe (these are shown glued to the ends of the rectangular dowels in Figure 2.5).

The concrete for the building slab dowel specimens was placed by hand scoops to prevent displacing the dowels. Care was taken to provide adequate concrete consolidation on the undersides of the plate dowels.

2.3.3 Strain Gages

Nine of the highway dowel specimens had strain gages applied to the dowels as shown in Figure 2.7 to measure the behavior of the dowels while load was applied. Twelve gages were applied to each dowel—six on top and six on bottom. The gages were placed 1.5, 5.5, and 7 inches from the center of the dowel. Strain readings were obtained by the same data acquisition system as used for the deflection and load measurements. The readings were

used to determine stresses and calculate moment at different points along the dowels. These calculated moments can be compared to the theoretical moments.

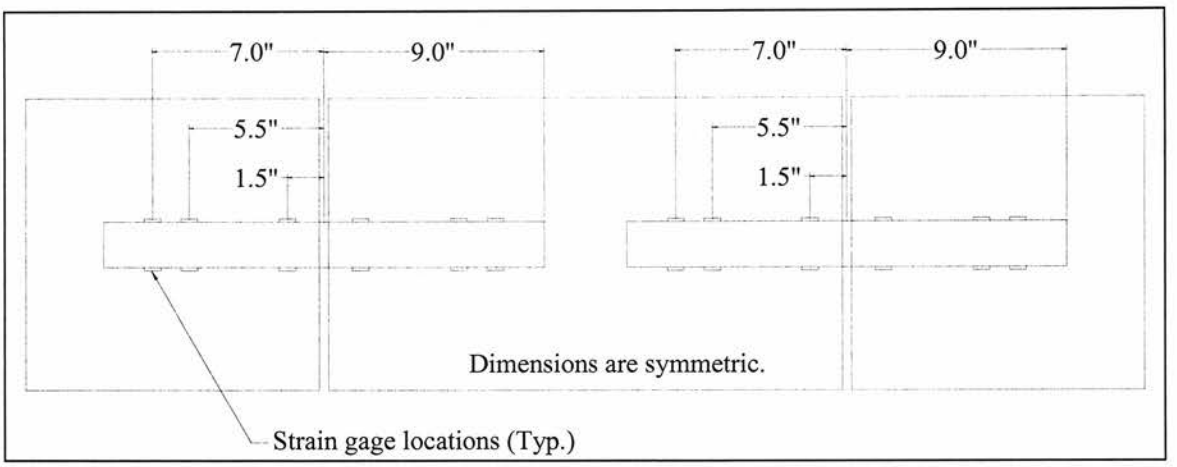

Figure 2.7. Strain gage placement

2.4 Other Testing

Other testing included concrete compressive strength tests for both the highway dowels and building slab dowels and FRP loss on ignition testing. The concrete compressive strength tests were used to determine if the concrete used for the test specimens met the minimum strength requirements and were used for calculating the allowable stresses for the highway dowels. The loss on ignition testing was used to determine the ratio of fiber to resin in the GFRP dowels.

3. THEORY AND MODELING OF DOWEL-TO-CONCRETE BEHAVIOR

3.1 Modulus of Dowel Support

Several researchers utilized Timoshenko's (*28*) model of beam on an elastic foundation (see Figure 3.1) to investigate the performance of dowel bars in pavement structures. Figure 3.1 shows a specific case where a load, P, and moment, M_0, area applied at the end of the beam.

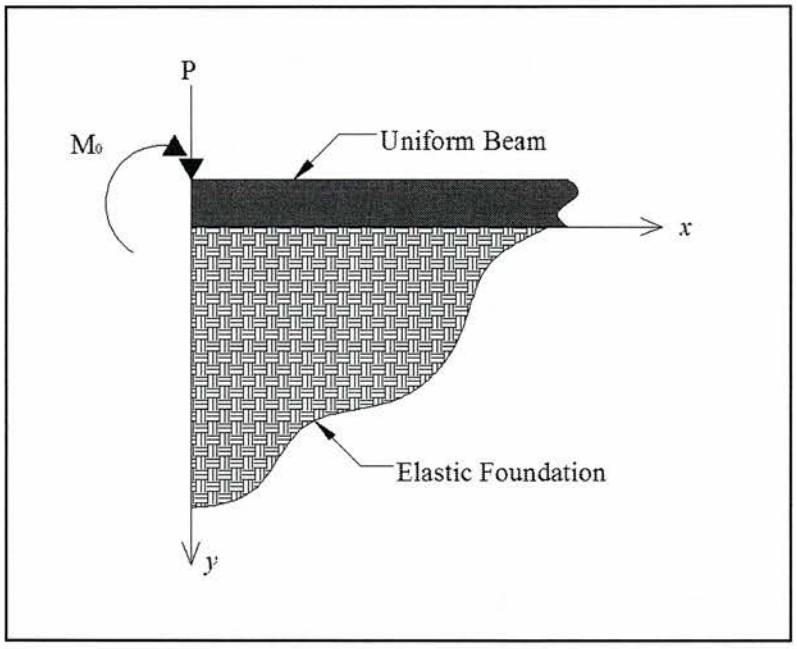

Figure 3.1. Beam on an elastic foundation

The following briefly describes the analytical model of an infinite beam that is resting on a concrete foundation. This model, which is a Winkler model (*29*), assumes a linear force-deflection relationship, so that if the beam (dowel in this case) imposes a deflection, y, on the foundation, the beam (dowel) will be resisted with a pressure ky, where k is the foundation modulus (see Figures 3.2 and 3.3 where z represents the joint width). When analyzing a dowel in pavement structures, the modulus, k, will be replaced by k_0b where b is the width

(or diameter, in the case of circular cross-sections) of the dowel bar and k_0 is referred to as the modulus of dowel support. The units of k_0 are psi/in. The units of k_0 will be denoted throughout this report as pounds per cubic inch (pci) for simplicity.

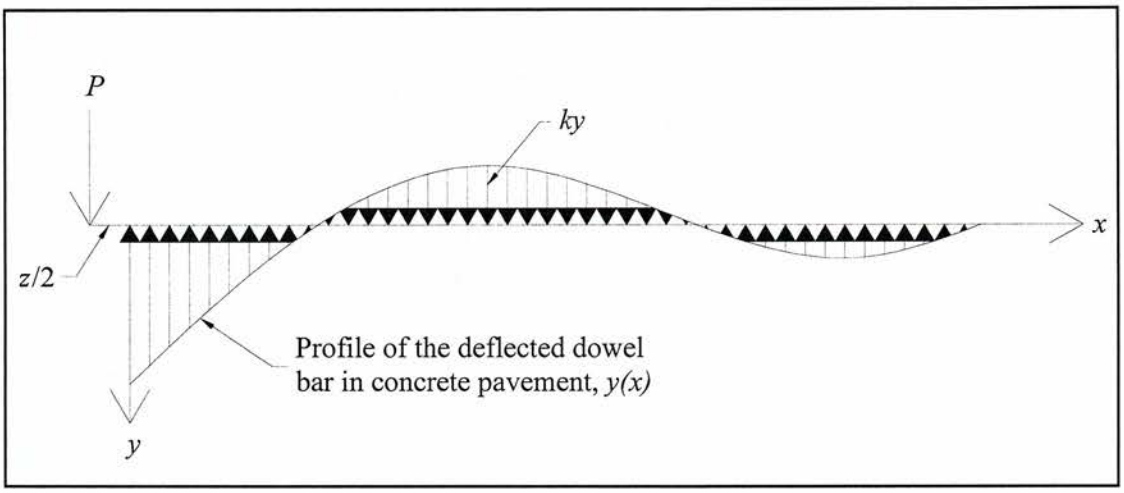

Figure 3.2. Reactions along a deflected beam on an elastic foundation

Following Timoshenko's model, the following relationship can be written:

$$EI\frac{d^4y}{dx^4} = -(k_0 b)y \tag{3.1}$$

Where EI is the rigidity of the dowel and y is the deflection of the dowel.

The general solution of the differential equation in Equation 3.1 is

$$y = \frac{e^{-\beta x}}{2\beta^3 EI}\left[P\cos\beta x - \beta M_0(\cos\beta x - \sin\beta x)\right] \tag{3.2}$$

Where $\beta = \sqrt[4]{\frac{k_0 b}{4EI}}$ and is referred to as the relative stiffness of the dowel on the concrete.

Friberg (*30*) applied the approach outlined above to a dowel with semi-infinite length embedded in concrete. To find the deflection of the dowel at the face of the concrete joint,

Friberg set $x = 0$ and $M_0 = \frac{Pz}{2}$ (i.e. the moment from the shear load applied at the center of the joint) in Equation 3.2, which becomes

$$y_0 = \frac{P}{4\beta^3 EI}(2 + \beta z) \tag{3.3}$$

Where,

$$\beta = \sqrt[4]{\frac{k_0 b}{4EI}} \tag{3.4}$$

k_0 = modulus of dowel support, pounds per square inch per inch (pci)

b = dowel bar width, in.

P = load transferred by the dowel, lbs

z = joint width, in.

E = modulus of elasticity of the dowel, psi

I = moment of inertia of the dowel cross section, in.^{4}

3.2 Relative Deflection

The Modified AASHTO T253 method was used to obtain y_0. For a given load, y_0 was used to solve β using Equation 3.3 and β was used to solve for k_0 using Equation 3.4. For the Modified AASHTO T253, y_0 is determined using the equation

$$\Delta = 2y_0 + z\frac{dy_0}{dx} + \frac{Pz^3}{12EI} + \delta \tag{3.5}$$

Where Δ is the relative displacement in inches between slabs at the joint and consists of the following components (see Figure 3.3):

- deflection at each joint face, y_0
- deflection due to the slope of the dowel, $\frac{zdy_0}{dx}$
- moment deflection, $\frac{Pz^3}{12EI}$
- shear deflection, δ

Where,

$$\delta = \frac{\lambda Pz}{AG}$$

λ = shear shape factor = 10/9 for round and elliptical cross sections and 6/5 for rectangular cross sections (*31*)

A = cross-sectional area of the dowel, in.^{2}

G = shear modulus of the dowel material, psi

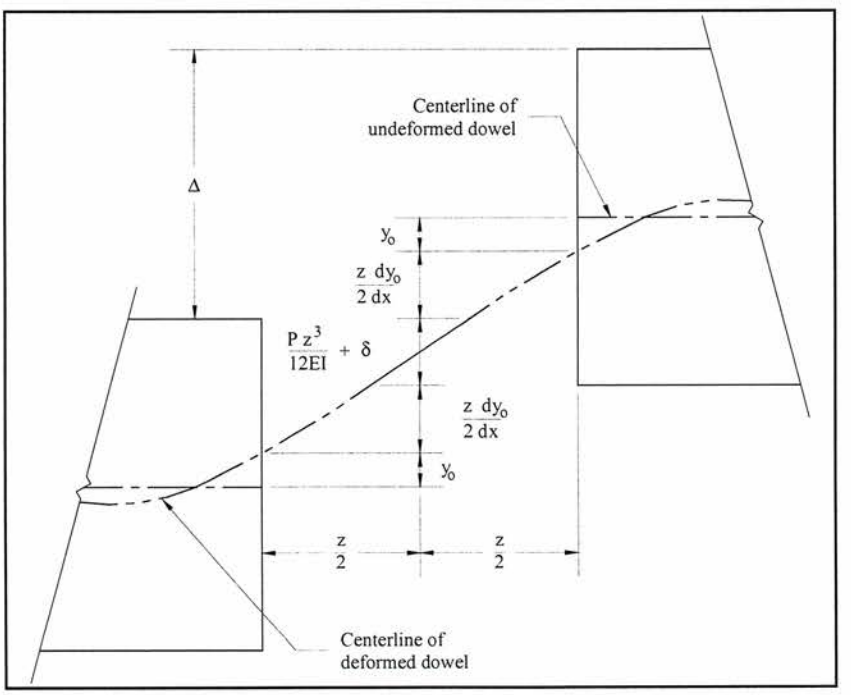

Figure 3.3. Relative deflection between slab sections

As an alternative to the shear shape factors of 10/9 and 6/5 (*31*), which are based on geometry, Cowper (*32*) developed a shear coefficient for Timoshenko's beam theory based on Poisson's ratio so that material properties factor in to shear deflection. Cowper's shear coefficients were slightly greater than the geometric coefficients but the geometric coefficients were used here for convenience and because the resulting changes to k_0 were insignificant. The deflections due to flexural effects in Equation 3.5 were assumed to be negligible due to small joint widths. (For example, even for joint widths of up to 1/2-inch, the moment deflection is on the order of hundred thousandths of an inch). Neglecting the moment deflection and slope deflection leaves

$$\Delta = 2y_0 + \delta$$

Or, solving for y_0,

$$y_0 = \frac{(\Delta - \delta)}{2} \tag{3.6}$$

Once the load and deflection data were obtained from testing, a spreadsheet was used to calculate y_0 and k_0 for each data point. To perform this calculation an initial value for k_0 was given so that β could be determined and applied to Equation 3.3. The Microsoft Excel Solver function was used to set Equation 3.3 equal to Equation 3.6 by changing k_0, thus giving the representative k_0 for a given data point.

3.3 Bearing Stress

Ultimately, the modulus of dowel support, k_0, is used to determine the bearing stress of the dowel on the concrete at the joint face. Since Timoshenko's model assumed that the intensity of the reaction continuously distributed at every section is proportional to the

deflection at a given section, then the bearing stress can be found by multiplying the modulus of dowel support by the deflection at the face of the joint:

$$\sigma_b = k_0 y_0 \tag{3.7}$$

The bearing stress must be kept at a minimum to prevent crushing of concrete above and below the dowel. Equation 3.8 shows an allowable bearing stress given by the American Concrete Institute's Committee 325 (*33*).

$$\sigma_a = \left(\frac{4-b}{3}\right) f_c^{'} \tag{3.8}$$

Where,

σ_a = allowable bearing stress, psi

b = dowel bar diameter for circles or major axis for ellipses, in.

$f_c^{'}$ = compressive strength of concrete, psi

Equation 3.8 provides a factor of safety of approximately three. The bearing stress calculated for a given data point load was compared to the allowable stress for a given dowel. The load at which the calculated bearing stress equaled the allowable bearing stress was recorded to compare the six dowel types.

Equation 3.8 applies to the highway dowels mentioned in this study and not the building slab dowels. Equation 3.8 was originally intended for round dowels but has been utilized here for both round and elliptical dowels less than three inches in width. Equation 3.8 is not used for the wide rectangular cross sections, which would provide negative values.

3.4 Strain Gages

Moment along a dowel bar can be found using measured strain values obtained with strain gages. Nine Modified AASHTO T253 specimens (18 dowel bars) were installed with 12 strain gages per dowel. Equation 3.9 (based on Equation 3.2) was used to find the deflected shape of the dowel (where $x = 0$ at the face of the slab joint).

$$y(x) = \frac{e^{-\beta x}}{2\beta^3 EI}\left[P\cos\beta x - \beta M_0(\cos\beta x - \sin\beta x)\right] \tag{3.9}$$

$$M(x) = -EI\frac{d^2y}{dx^2} = -\frac{e^{-\beta x}}{2\beta}\left[2(P - M_0\beta)\sin\beta x - 2M_0\beta\cos\beta x\right] \tag{3.10}$$

$$V(x) = -EI\frac{d^3y}{dx^3} = -\frac{e^{-\beta x}}{2}\left[2(P - M_0\beta)(\cos\beta x - \sin\beta x) + 2M_0\beta(2\sin\beta x + \cos\beta x)\right] \tag{3.11}$$

Where,

$$M_0 = \frac{Pz}{2}$$

The strain reading from the strain gages can be used to find moment by $\sigma = \frac{Mc}{I}$, where $\sigma = \varepsilon E$, therefore,

$$M(x) = \frac{\varepsilon EI}{c} \tag{3.12}$$

Where,

ε = strain reading from strain gage at x

σ = stress at x determined from strain gage reading at x, psi

c = half the vertical diameter of the dowel, in.

E = modulus of elasticity of the dowel bar material, psi

I = flexural moment of inertia for the dowel bar, in.^{4}

3.5 Dowel Embedment Length

Timoshenko's (Equation 3.2) and Friberg's (Equation 3.3) theories apply to a beam (dowel) of semi-infinite length. However, dowels are of measurable finite length. Albertson and others (2,3) have shown that the theory can be applied to dowels bars given that βL_e is greater than or equal to 2 (where L_e is the embedment length of the dowel within the slab). This requirement was developed by comparing the semi-infinite theory with a more complex finite theory. The two theories were determined to be nearly the same for values of βL_e greater than 2.

4. ANALYSIS AND RESULTS

4.1 Load Adjustments

The load applied to the center block of the Modified AASHTO T253 specimens was assumed to be distributed evenly between the two dowels. Analysis of load-deflection data for the test showed inconsistencies between the relative deflections measured on either joint. Many factors could have caused the inconsistencies, including the load frame, test specimens, and centeredness of the load application apparatus (the load actuator and spreader beam). Because of these inconsistencies the load was not necessarily distributed equally between dowels. Because of the unequal distribution the data was analyzed two ways:

1. Assuming load was distributed evenly between the two dowels (unadjusted loading)
2. Assuming load was distributed proportionally between the two dowels based on the relative deflection measurements (adjusted loading)

The difference in k_0 values determined using the unadjusted loads and the adjusted loads was usually within ten percent but as high as 45 percent in one extreme case. The outlier was due to dowel misalignment during specimen construction and concrete placement that produced unwanted eccentricities during loading.

4.2 Modulus of Dowel Support

4.2.1 Highway Dowels

Tables 4.1 and 4.2 show the average k_0 (see Section 3.1) value for the highway dowels tested broken down by dowel type, joint width, and load adjustment. The 0-inch joint width corresponds to a joint where one slab is cast against a previously placed slab (commonly referred to as a cold joint). Outlier data points—due to specimen seating during initial

loading and due to deflection reading errors—have been omitted from both Tables 4.1 and 4.2 and from the graphs in Appendix A.

Table 4.1. Average k_0 (pci) values—equal load distribution

		Joint Width		
Dowel Type	Dowel Size	0-inch*	1/8-inch	1/2-inch
Round Steel	1.5	2,770,000	1,280,000	610,000
Large Elliptical Steel	2.00 x 1.375	1,280,000	510,000	540,000
Small Elliptical Steel	1.66 x 1.13	3,410,000	520,000	510,000
Round Stainless Steel	1.5	3,590,000	710,000	790,000
Round GFRP	1.875	1,100,000	340,000	400,000
Elliptical GFRP	2.25 x 1.25	1,240,000	640,000	500,000

*Cold joint

Table 4.2. Average k_0 (pci) values—adjusted loads

		Joint Width		
Dowel Type	Dowel Size	0-inch*	1/8-inch	1/2-inch
Round Steel	1.5	2,980,000	1,220,000	620,000
Large Elliptical Steel	2.00 x 1.375	1,280,000	640,000	560,000
Small Elliptical Steel	1.66 x 1.13	3,690,000	530,000	560,000
Round Stainless Steel	1.5	3,840,000	790,000	810,000
Round GFRP	1.875	1,190,000	360,000	410,000
Elliptical GFRP	2.25 x 1.25	1,260,000	690,000	520,000

*Cold joint

Appendix A shows k_0 vs. load graphs for all highway dowel specimens tested.

4.2.2 Building Slab Dowels

Tables 4.3 and 4.4 show the average k_0 value (see Section 3.1) for the building slab dowels tested broken down by dowel type, joint width, and load adjustment. Appendix B shows k_0 versus load graphs for all building slab dowel specimens tested. Outlier data points have been removed from Tables 4.3 and 4.4 and Appendix B for the reasons described in Section 4.2.1.

Table 4.3. Average k_0 (pci) values—equal load distribution

Dowel Type	Dowel Size, in.	Without Sleeve	With Sleeve
Square Plate	4½ x 4½ x ¼	670,000	400,000
Diamond Plate	4½ x 4½ x ¼	370,000	220,000
Rectangular Plate	12 x 2 x ⅜	850,000	400,000
Round Bar	14 x ¾	2,850,000	650,000
Round Bar (12 inch)	14 x ¾	1,910,000	560,000

Table 4.4. Average k_0 (pci) values—adjusted loads

Dowel Type	Dowel Size, in.	Without Sleeve	With Sleeve
Square Plate	4½ x 4½ x ¼	620,000	270,000
Diamond Plate	4½ x 4½ x ¼	360,000	160,000
Rectangular Plate	12 x 2 x ⅜	810,000	370,000
Round Bar	14 x ¾	1,960,000	380,000
Round Bar (12 inch)	14 x ¾	1,980,000	550,000

Note that the k_0 values for the sleeved dowels are not true modulus of dowel support values. The k_0 values for the sleeved dowels have been computed for comparison purposes. The modulus of dowel support accounts for the dowel on the concrete foundation and not the effects of the sleeves and spaces between the dowels and the sleeves.

The sleeves reduced the computed k_0 values 40-55 percent for the rectangular cross section dowels and 70-80 percent for the circular cross section dowels. The reduction in k_0 values also corresponds to an increase in dowel deflection.

4.3 Effects of Joint Width

4.3.1 Highway Dowels

Neglecting the cold-joint specimens, Tables 4.1 and 4.2 show that joint width had some effect on the value of k_0. The values for the 0-inch joint are significantly greater than the 1/8-inch and 1/2-inch joints. This difference in k_0 can be attributed to the absence of a gap. The cold-joint specimens were affected by arching action taking place within the center block. The center block did not undergo an ideal vertical translation. Each end of the center block experienced a different downward deflection, causing a slight rotation within the block. The 1/2 and 1/8-inch gap specimens allowed enough clear space to avoid contact between the center block and the end blocks. The cold-jointed specimens resisted this rotation by developing normal forces between the center block and end blocks. These normal forces caused significant frictional forces between the blocks. The addition of these unknown frictional forces reduced the amount of shear force being transferred through the dowel bars. Thus, the measured loads were an exaggeration of the loads being transferred through the dowels. The exaggerated loading led to an inaccurate increase in the value of k_0. Because of the inaccuracies, all comparisons described herein for the highway dowels are based on 1/8-inch and 1/2-inch joints only.

The k_0 values calculated for the 1/8-inch and 1/2-inch joints were similar except for the 1.5-inch round epoxy coated steel dowels, which exhibited much greater k_0 values for the 1/8-inch specimens than the 1/2-inch specimens. The k_0 vs. load plots (in Appendix A) for the round steel specimens also had the largest data spreads. The data did not provide hard

evidence for significant differences in k_0 for 1/8 and 1/2-inch joint widths in terms of dowel material or shape.

There was a greater tendency for specimens with larger gaps to rotate about the dowel (i.e. for the unrestrained center block to twist while the end blocks remained restrained) during testing at higher loads and during handling of specimens after testing.

4.3.2 Building Slab Dowels

All building slab dowel specimens tested had 1/8-inch joints; therefore, no effects of joint width comparisons can be made for this set of tests.

4.4 Effects of Dowel Shape

4.4.1 Highway Dowels

Of the six highway dowel types tested, three had circular cross sections and three had elliptical cross sections. The theory behind using elliptically-shaped dowel bars is to provide a greater bearing area for the dowel on the concrete to reduce bearing stresses and more effectively transfer loads without crushing the concrete above and below the dowel. However, providing the greater bearing width of the dowel places the dowel in weak-axis flexural bending.

The elliptically-shaped dowel bars exhibited lower k_0 values than the circular dowels. The exception to this pattern is the 1.875-inch diameter GFRP dowel, which exhibited lower k_0 values than any other dowel tested. The reason for this discrepancy is more a matter of material properties rather than dowel shape as will be discussed in the next section.

The data show that both sizes of elliptical steel (2.00 x 1.375 & 1.66 x 1.13-inches) performed similarly in terms of k_0.

Although the elliptical shape provided smaller k_0 values they also had smaller allowable bearing stresses (according to Equation 3.8) since they are oriented in such a way that load is transferred by weak-axis bending. That is, increasing the theoretical bearing area of the dowel on the concrete by using an elliptical shape comes with the cost of using a larger dowel to provide the same flexural strength as an equivalent round dowel. However, determining rider comfort and analyzing fatigue effects while using smaller elliptical dowels is a possibility for future research.

4.4.2 Building Slab Dowels

Of the four building slab dowel types tested, three had rectangular cross sections and one had a circular cross section. The rectangular cross sections provide an increased bearing contact area between the dowel and concrete than the circular cross section, although the circular cross section is a more efficient use of material having greater rigidity with a smaller cross sectional area (but a greater length is needed for the circular dowel to satisfy the $\beta L_e \geq 2$ requirement than for the rectangular dowels).

The round dowel exhibited significantly higher k_0 values than the rectangular cross sections. The data for the rectangular cross sections show that the greater the cross sectional width, the smaller the k_0 value.

4.5 Effects of Dowel Material

4.5.1 Highway Dowels

The GFRP dowels produced lower k_0 values than the epoxy-coated steel dowels and the stainless steel dowels. This is expected since GFRP is a softer material than steel and because the GFRP dowels tested were of larger sizes than the steel, thus providing a greater

dowel-concrete bearing area to distribute the reaction. Steel has greater k_0 values for 1/8-inch joints than stainless steel, and stainless steel has greater k_0 values for 1/2-inch joints than steel because of the inconsistencies between 1/8-inch and 1/2-inch joints for the steel dowels. However, others (*11*) have demonstrated that steel exhibits a higher k_0 value than stainless steel.

The three steel dowel types were all epoxy-coated while the stainless steel dowel naturally was not. This soft (relative to the steel) coating around the perimeter of the dowels provides for more initial displacement at lower loads than the non-coated stainless steel dowel. The softness of the epoxy coating may explain why lower relative deflections were observed for stainless steel than for a similar sized epoxy-coated steel, even though steel has a slightly greater flexural rigidity than stainless steel (the moduli of elasticity for steel and stainless steel are 29×10^6 psi and 28×10^6 psi, respectively). The dowel stiffness and relative deflections will be discussed in the next two sections.

4.5.2 Building Slab Dowels

All building slab dowels were made of steel so no effects of material comparisons can be concluded for these dowels.

4.6 Effects of Dowel Flexural Rigidity

4.6.1 Highway Dowels

Table 4.5 shows the modulus of elasticity, the moment of inertia about the horizontal axis, and the dowel flexural rigidity, *EI*, for the six highway dowel types.

Table 4.5. Dowel properties

Dowel Type	Dowel Size, in.	Modulus of Elasticity, E, psi	Moment of Inertia, I, in.^{4}	Flexural Rigidity EI, lb-in.^{2}x10^6
Round Steel	1.5	29 x 10^6	0.2485	7.21
Large Elliptical Steel	2.00 x 1.375	29 x 10^6	0.2552	7.40
Small Elliptical Steel	1.66 x 1.13	29 x 10^6	0.1176	3.41
Stainless Steel	1.5	28 x 10^6	0.2485	6.96
Round GFRP	1.875	6.51 x 10^6	0.6067	3.95
Elliptical GFRP	2.25 x 1.25	8.66 x 10^6	0.2157	1.87

Table 4.6. Dowel flexural rigidity and k_0 comparison

Dowel Type	k_0*, pci	EI, lb-in.^{2}x10^6
Round GFRP	400,000	3.95
Elliptical GFRP	500,000	1.87
Small Elliptical Steel	510,000	3.41
Large Elliptical Steel	540,000	7.40
Round Steel	610,000	7.21
Stainless Steel	790,000	6.96

*For 1/2-inch joint, unadjusted loading

Table 4.6 suggests that as EI of the dowel bar increases, k_0 increases. The discrepancies in Table 4.6 were assumed to be caused by external factors. The first issue is the softness of the GFRP material compared to steel. The GFRP was more likely to experience small localized deformation at the location of the joint due to the high stresses caused by the concrete edge of the joint. The epoxy coating on the round steel bars is another example of softer materials undergoing localized deflections. This table is for 1/2-inch joint width in order to maximize flexural activity across the joint for comparison of stiffness.

4.6.2 Building Slab Dowels

Table 4.7 shows the modulus of elasticity, the moment of inertia about the horizontal axis, and the dowel flexural rigidity, EI, for the building slab dowels.

Table 4.7. Dowel properties

Dowel Type	Dowel Size	Modulus of Elasticity, E, psi	Moment of Inertia, I, in.^{4}	Dowel Flexural Rigidity, EI (x10^6)
Square Plate	4½ x 4½ x ¼	29 x 10^6	0.0059	0.170
Diamond Plate	4½ x 4½ x ¼	29 x 10^6	0.0083*	0.240
Rectangular Plate	12 x 2 x ⅜	29 x 10^6	0.0089	0.255
Round Bar	14 x ¾	29 x 10^6	0.0155	0.450
Round Bar (12 inch)	14 x ¾	29 x 10^6	0.0155	0.450

*Moment of inertia at center of joint (0.0081 in.^{4} at the face of the joint)

Table 4.8. Dowel stiffness and k_0 comparison

Dowel Type	k_0*, pci	EI
Diamond	370,000	0.240**
Square	670,000	0.170
Rectangle	850,000	0.255
Round	1,910,000	0.450
Round (12 inch)	2,850,000	0.450

*From unadjusted loading for non-sleeved specimens
**Using moment of inertia at center of joint—the flexural rigidity at the joint face is 0.236x10^6 and the average flexural rigidity along the diamond plate is 0.199x10^6

Table 4.8 shows that as flexural rigidity of the dowel bar increases, k_0 increases. Only the diamond plate did not follow the trend because the diamond plate has the only non-continuous cross section and the moment of inertia reported is for the cross sectional area at the center of the joint while the average moment of inertia along the length of the diamond plate is half of that. The moment of inertia for the diamond plate at the face of the joint is slightly less than at the center of the joint.

4.7 Dowel Deflection

4.7.1 Highway Dowels

Tables 4.9 through 4.12 show the average relative deflections, Δ (measured); shear deflections, δ (Equation 3.5); and displacements, y_0 (Equation 3.6), at the joint face for the

highway dowels. Tables are shown for both 1/8-inch and 1/2-inch joints and for a small (2 kip) and large (10 kip) load.

Table 4.9. Average deflections - 2 kip loading, 1/8-inch joint

Dowel Type	Average Δ, in.	Average δ, in	Average y_0, in.
Round GFRP	0.005794	0.000039	0.002877
Elliptical GFRP	0.005118	0.000037	0.002541
Large Elliptical Steel	0.006573	0.000012	0.003281
Small Elliptical Steel	0.006441	0.000017	0.003212
Round Steel	0.003534	0.000015	0.001760
Stainless Steel	0.004502	0.000015	0.002243

Table 4.10. Average deflections - 2 kip loading, 1/2-inch joint

Dowel Type	Average Δ, in.	Average δ, in.	Average y_0, in.
Round GFRP	0.006965	0.000162	0.003401
Elliptical GFRP	0.006340	0.000146	0.003097
Large Elliptical Steel	0.005274	0.000045	0.002615
Small Elliptical Steel	0.008616	0.000065	0.004276
Round Steel	0.004368	0.000055	0.002157
Stainless Steel	0.003314	0.000058	0.001628

Table 4.11. Average deflections - 10 kip loading, 1/8-inch joint

Dowel Type	Average Δ, in.	Average δ, in.	Average y_0, in.
Round GFRP	0.032065	0.000195	0.015935
Elliptical GFRP	0.019268	0.000182	0.009543
Large Elliptical Steel	0.016194	0.000057	0.008068
Small Elliptical Steel	0.022264	0.000084	0.011090
Round Steel	0.022447	0.000070	0.011188
Stainless Steel	0.018396	0.000073	0.009162

Table 4.12. Average deflections - 10 kip loading, 1/2-inch joint

Dowel Type	Average Δ, in.	Average δ, in.	Average y_0, in.
Round GFRP	0.028660	0.000773	0.013944
Elliptical GFRP	0.026095	0.000733	0.012681
Large Elliptical Steel	0.016064	0.000229	0.007918
Small Elliptical Steel	0.032607	0.000337	0.016135
Round Steel	0.022575	0.000267	0.011154
Stainless Steel	0.018402	0.000297	0.009052

Tables 4.9 through 4.12 show that the stainless steel and large elliptical steel dowels were better at limiting overall displacement. However, the additional flexural rigidity leads to greater bearing stresses between the dowel and concrete, especially for round dowels like the stainless steel dowels. Round FRP and small elliptical steel dowels did not perform as well as the others in limiting displacement because they have lower dowel flexural rigidity and narrower bearing area regions.

4.7.2 Building Slab Dowels

Tables 4.13 and 4.14 show the average relative deflections, Δ (measured); shear deflections, δ (Equation 3.5); and displacements, y_0 (Equation 3.6) at the joint face for each building slab dowel type. Tables are shown for both non-sleeved and sleeved dowels with 2000-pound loading.

Table 4.13. Average deflections (non-sleeved dowels)

Dowel Type	Average Δ, in.	Average δ, in.	Average y_0, in.
Square	0.004698	0.000024	0.002337
Diamond	0.005126	0.000017	0.002555
Rectangle	0.005855	0.000036	0.002910
Round	0.004336	0.000056	0.002140
Round (12 inch)	0.003942	0.000056	0.001945

Table 4.14. Average deflections (sleeved dowels)

Dowel Bar	Average Δ, in.	Average δ, in.	Average y_0, in.
Square	0.008817	0.000024	0.004396
Diamond	0.009824	0.000017	0.004904
Rectangle	0.017457	0.000036	0.008711
Round	0.014403	0.000056	0.007173
Round (12 inch)	0.014825	0.000056	0.007385

The round dowels without sleeves deflect the least due to their higher flexural rigidity than the other dowels, but the lower deflections come with the cost of having increased bearing stresses.

Of the rectangular cross sectional dowels, the rectangular dowel had greater deflections than the square or diamond dowels, which both displayed similar deflections.

Figures 4.1 and 4.2 show typical concrete failures that occurred due to dowel deflection during testing of the building slab dowels. The failure mode was concrete shear failure due to prying action of the dowel.

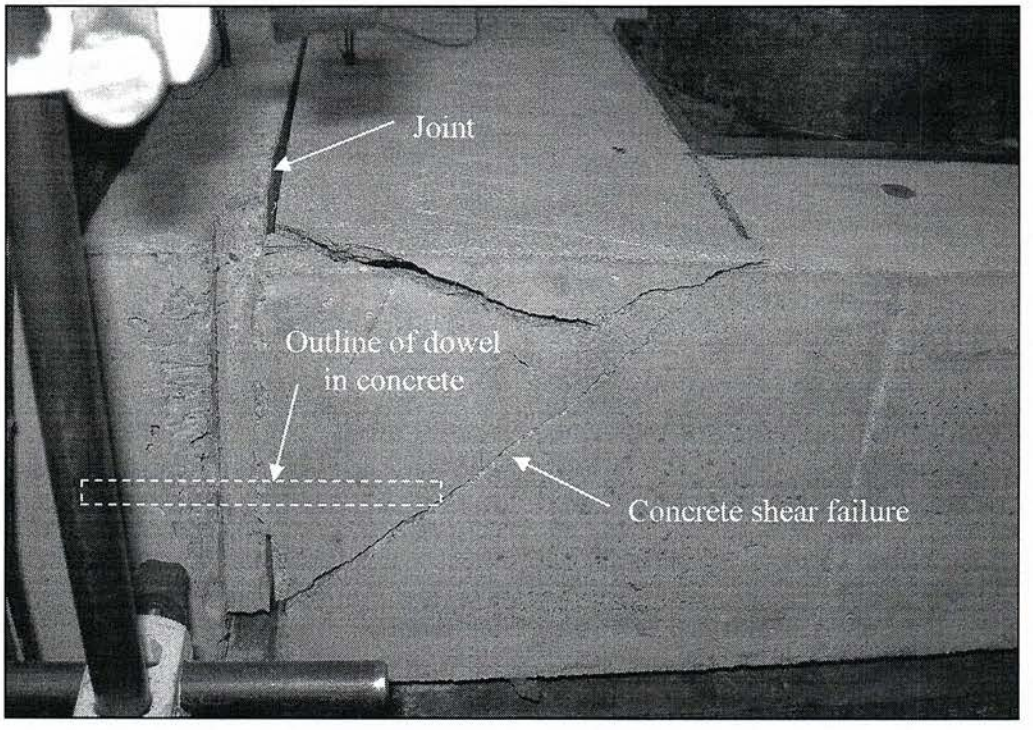

Figure 4.1. Typical concrete failure (square plate specimen)

Adding the sleeves to the dowel increases the relative deflection about 2-4 times more than without the sleeve. This increased deflection is due to the closing of void spaces in the sleeves surrounding the dowels and due to the compression of the sleeve between the dowel

and concrete while being loaded. The increased deflection was most noticeable for the round dowels in which the sleeves had the least tight fit of the four dowel types tested.

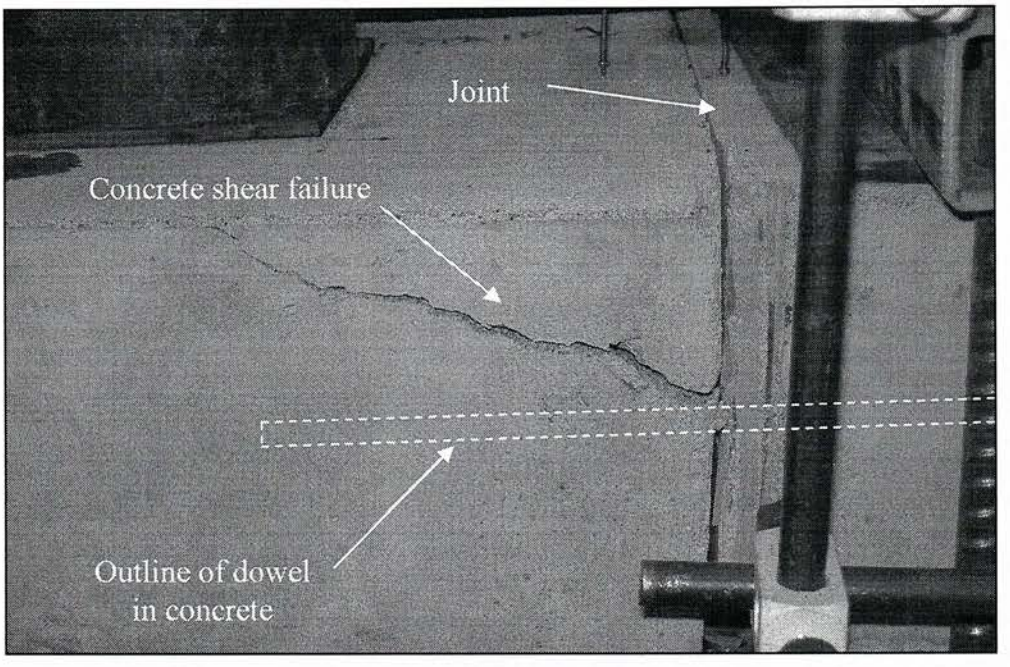

Figure 4.2. Typical concrete failure (rectangular plate specimen)

An additional factor involving dowel deflection is air voids in the concrete at the surface of the dowels. Figure 4.3 shows an extreme case of air voids for one of the diamond specimens. The presence of air voids only occurred for the rectangular cross section dowels and not the circular dowels. The flat surface of the bottom side of a dowel is a likely place for voids to occur. Care was taken during specimen construction to limit voids although in some cases more than 30 percent of a dowel footprint had void areas that were not in contact with concrete. However, since these voids would be expected in actual construction, the void areas were not taken into account for any of the calculations.

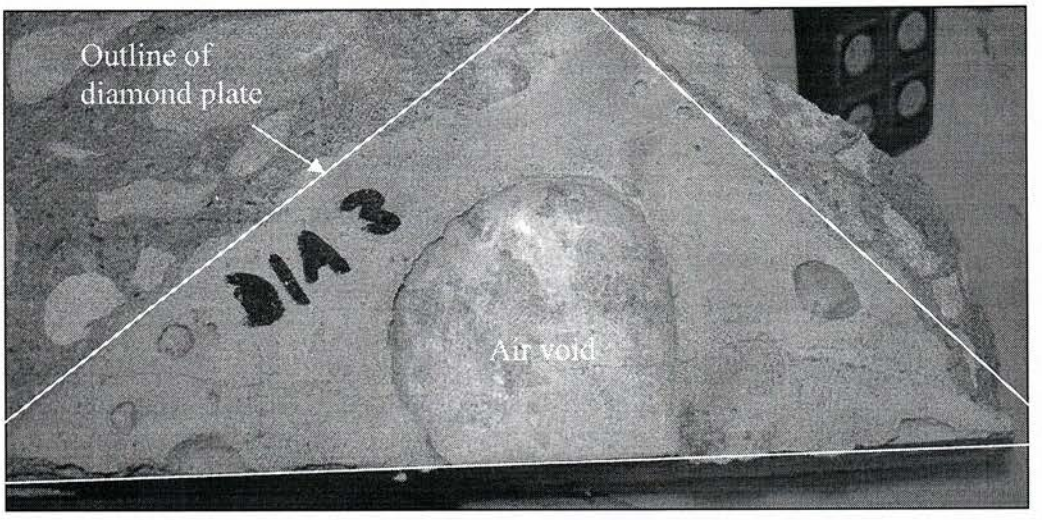

Figure 4.3. Air voids in concrete underneath one dowel

4.8 Bearing Stress

4.8.1 Highway Dowels

The bearing stress at the face of a joint is the product of k_0 and y_0. The allowable stresses (see Section 3.3) for each highway dowel bar type are presented in Table 4.15.

Table 4.15. Allowable stress and load at which the allowable stress is exceeded

Dowel Type	Allowable Stress*, psi	Load, lbs
Round Steel	4,583	6,000-8,500
Large Elliptical Steel	3,666	7,000-8,000
Small Elliptical Steel	4,290	6,500-8,500
Stainless Steel	4,583	6,000-8,000
Round GFRP	3,895	6,500-8,000
Elliptical GFRP	3,208	5,000-6,000

*Per ACI Committee 325 (*33*), determined from Equation 3.8, where $f_c^{'} = 5500$ psi

The last column in Table 4.15 shows the range of loads for each dowel type that the allowable bearing stress was reached during testing, that is, when σ_b (Equation 3.7) equals σ_a (Table 4.15).

4.8.2 Building Slab Dowels

The bearing stresses calculated before failure for each building slab dowel type are presented in Tables 4.16 and 4.17 along with the loads corresponding to the stresses.

Table 4.16. Dowel (no sleeve) bearing stresses and load before failure

Dowel Type	Bearing Stress Before Failure, psi	Corresponding Load, lbs
Square	3,500 - 3,600	5,200 - 5,400
Diamond	1,700 - 1,900	4,000 - 4,400
Rectangle	5,600 - 6,400	5,000 - 5,300
Round	11,000 - 15,500	4,200 - 4,700
Round (12 inch)	18,500 - 21,000	6,800 - 9,000

Table 4.17. Dowel (with sleeve) bearing stresses and load before failure

Dowel Type	Bearing Stress Before Failure, psi	Corresponding Load, lbs
Square	2,050 - 2,150	3,400 - 3,900
Diamond	1,350 - 2,000	4,000 - 5,200
Rectangle	2,500 - 4,400	3,400 - 4,200
Round	5,900 - 7,600	3,300 - 4,100
Round (12 inch)	12,500 - 16,000	6,700 - 8,300

Tables 4.16 and 4.17 show that the round dowels have the greatest bearing stresses. Diamond plates have the smallest bearing stresses. Just as k_0 decreases as dowel width increases and as flexural rigidity decreases, bearing stress also decreases.

All four dowel shapes reached similar loads before the specimens failed (note: the 12-inch deep specimens reached higher loads before failure because of the increased concrete volume surrounding the dowels). The sleeved dowel specimens reached failure at slightly lower loads than the non-sleeved dowels.

For design purposes, the loads shown in Tables 4.17 and 4.18 would need to be divided by an appropriate factor of safety, as deemed necessary by a jurisdictional authority.

4.9 Strain Gages

4.9.1 Highway Dowels

Nine of the highway dowel test specimens were equipped with strain gages. Both dowels in each specimen were installed with twelve strain gages each. Figure 4.4 shows the placement of the strain gages. Figure 4.5 shows two gaged dowels.

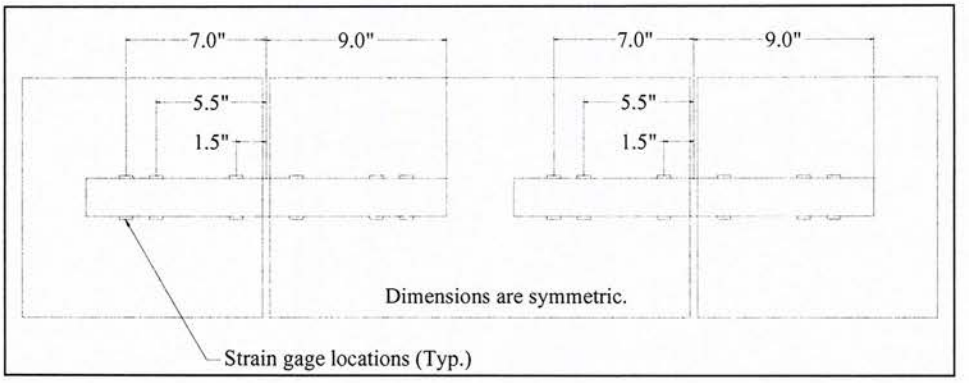

Figure 4.4. Strain gage placement

The following is a list of specimens with strain gages:

- 1.5-inch diameter steel with 0-inch joint
- 1.5-inch diameter steel with 1/2-inch joint
- Large elliptical steel with 1/2-inch joint
- Small elliptical steel with 1/2-inch joint
- 1.5-inch diameter stainless steel with 1/8-inch joint
- 1.875-inch diameter FRP with 0-inch joint
- 1.875-inch diameter FRP with 1/8-inch joint
- Elliptical FRP with 1/8-inch joint

(Note: there was also one small elliptical steel with 0-inch joint specimen that had strain gages installed but provided unusable data.)

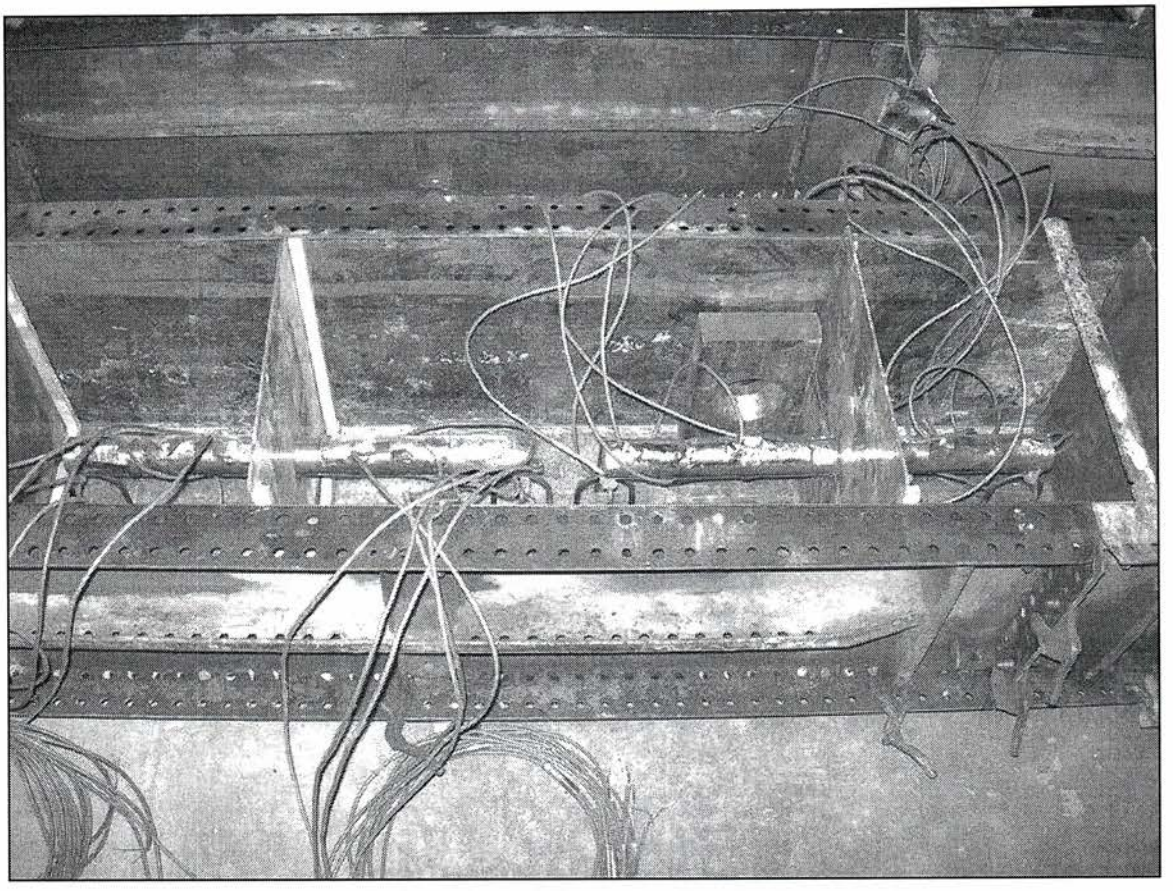

Figure 4.5. Two stainless steel dowels with strain gages set in concrete forms

The strain gages were wired into the same data acquisition system as the DCDTs so that load, deflections, and strains were read simultaneously. The strain readings were used to determine the moment using Equation 3.12. These moments can be plotted and compared to the theoretical moments based on Equation 3.10.

The strain gage moment plots are created assuming zero moments at the ends of the dowels and a moment, M_0, at the face of the joint. Figures 4.6 and 4.7 show plots of strain-gage-measured moment and theoretical moment along a 1.5-inch diameter epoxy-coated steel dowel specimen with 1/2-inch joints. The distance along the dowel (abscissa) is measured from the face of the joint. Both the measured and the theoretical plots are determined using the measured k_0 value for each specimen.

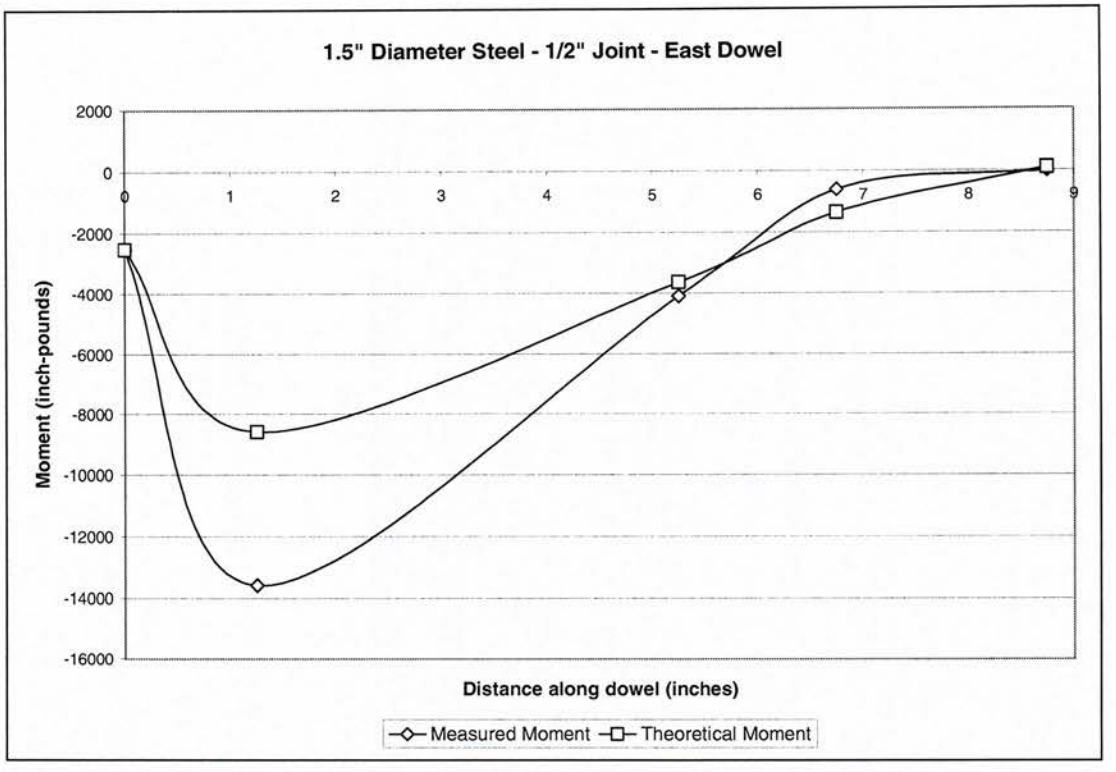

Figure 4.6. Moment diagram, 1.5-inch diameter steel, 1/2-inch joint, east dowel

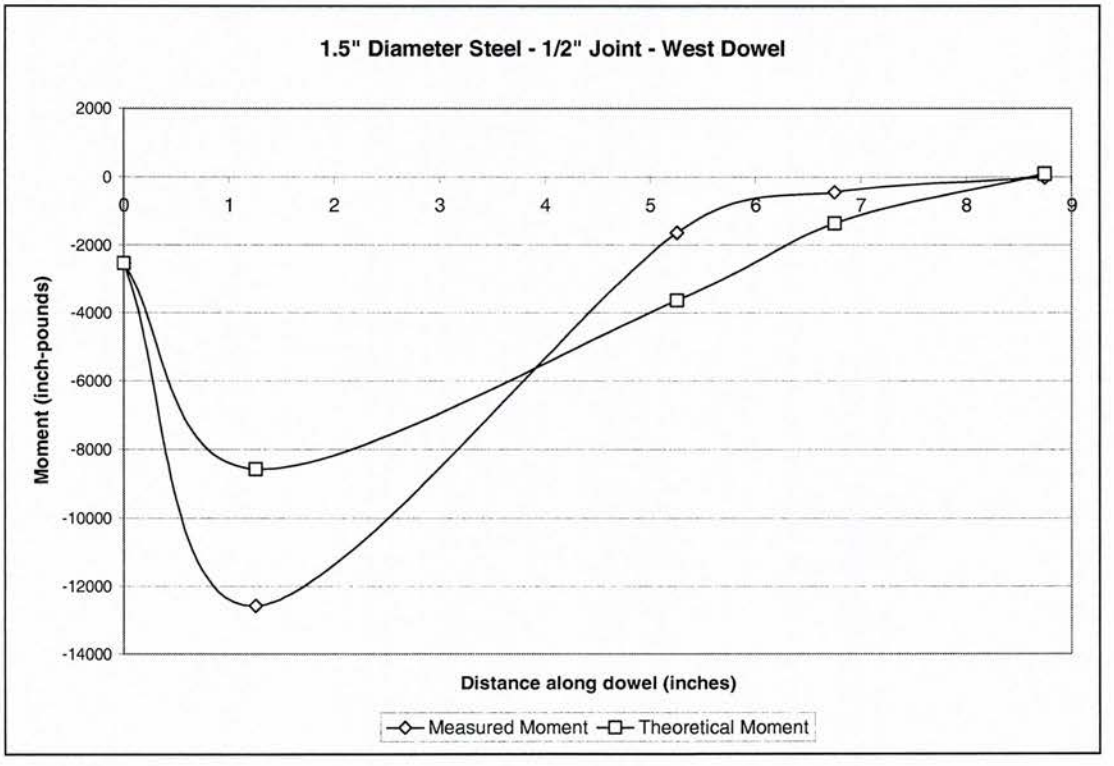

Figure 4.7. Moment diagram, 1.5-inch diameter steel, 1/2-inch joint, west dowel

Figure 4.8 shows a dowel displacement diagram based on Equation 3.9 for the 1.5-inch diameter steel specimen with 1/2-inch joint.

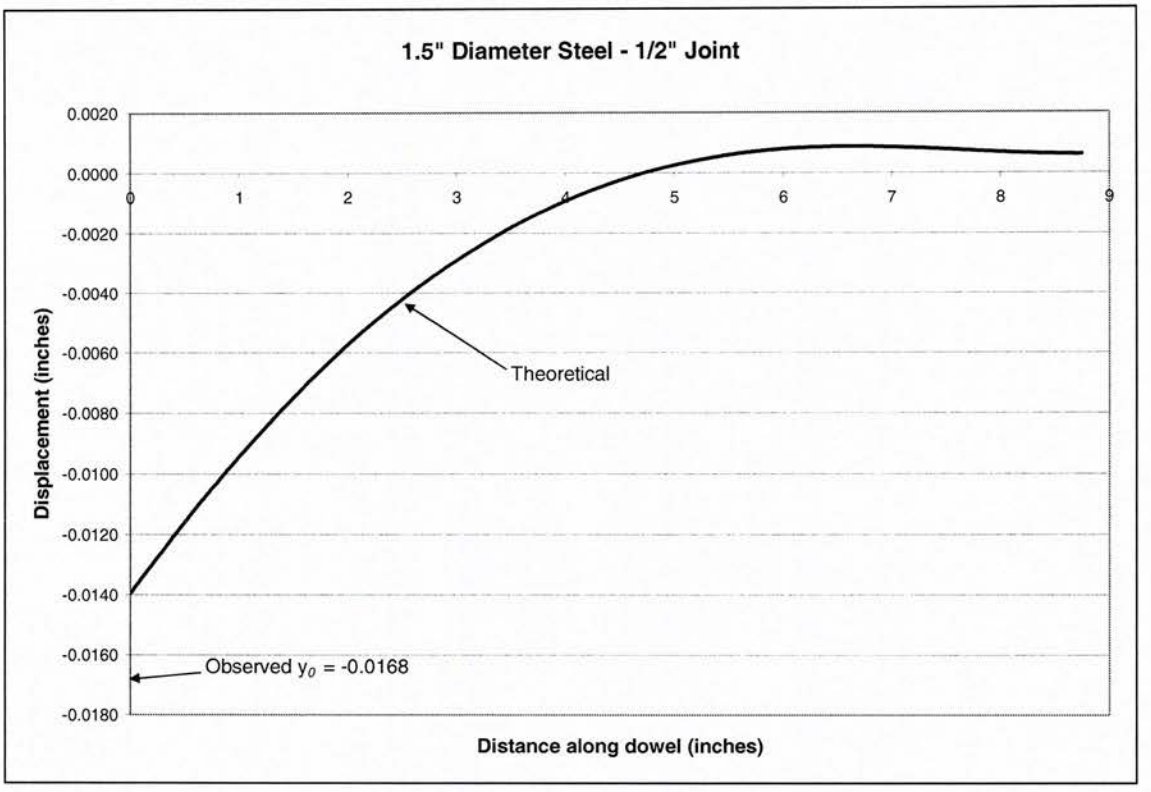

Figure 4.8. Dowel displacement diagram, 1.5-inch diameter steel, 1/2-inch joint

Appendix C contains representative moment diagrams for all the strain-gage equipped specimens. The moment diagrams are for various arbitrary loads that occur within the linear region of the load-deflection plot. Typically, 10-kip loads were used to maximize moment action in the dowel for the strain gage readings.

The strain gage readings for the different dowels show that the actual moment diagram follows a similar shape as the theoretical moment diagram. The following observations were also made:

- The moments observed from the gages 1.5 inches from the center of the dowel were less than the theoretical moments for 11 of the 16 dowels.

- Data from the gages furthest from the center of the dowel (7 inches) usually exhibited values close to zero and were closer to zero than the theoretical value for 10 of 16 dowels.
- Reviewing the moment diagrams for each specimen does not show any pattern for or against the theoretical moments (i.e. the actual moment diagrams are not collectively similar to each other while being different from the theoretical).

There are many factors that could influence the slight discrepancies between the observed and theoretical moments. The moments in the dowel at the face of the joint and the end of the dowel are assumed to be M_0 and zero, respectively, when developing the moment diagram using the strain gages. These moment value assumptions are based on the assumption that an inflection point occurs at the center of the dowel (at center of the joint). The strain gage data from gages closest to either side of the joint show that the moments are not symmetrical about the center of the dowel. Thus, the value M_0 at the face of the joint is incorrect. Finite element analysis has also provided evidence that the assumption that the inflection point is located at the center of the joint is incorrect (*10*). Thus far, the Iosipescu test (*3*) is the only method for testing dowels that produces an inflection point at the center of the joint.

Since the moments at opposite faces of a joint are not equal then y_0 at either face is not likely equal either. But for the Modified AASHTO T253 this inequality is not a major concern because y_0 is determined from the relative deflection, which takes into account two y_0 terms that are essentially averaged to find a representative y_0 value used to determine k_0.

The theoretical y_0 for the 1.5-inch diameter steel dowel with 1/2-inch joints shown in Figures 4.6 and 4.7 is 0.014 inch. The observed y_0 determined from the relative deflection

and averaged for the two dowels was 0.017 inch. Table 4.16 shows the observed and theoretical y_0 values for each of the strain gage specimens (typically for a 10 kip load).

Table 4.16. Observed and theoretical y_0 values

Dowel Type	Joint Width, in.	Observed y_0, in.	Theoretical* y_0, in.
Round Steel	0	0.004	0.004
Round Steel	1/2	0.014	0.017
Large Elliptical Steel	1/2	0.006	0.008
Small Elliptical Steel	1/2	0.020	0.027
Round Steel	1/8	0.005	0.006
Round GFRP	0	0.006	0.006
Round GFRP	1/8	0.022	0.023
Elliptical GFRP	1/8	0.015	0.010

*Equation 3.9

The observed y_0 values were similar to the theoretical y_0 values. The largest differences occurred for the small elliptical steel and elliptical GFRP specimens, which both exhibited significantly unsymmetrical loading.

Appendix D shows the theoretical displacement diagrams for the eight strain gage specimens with the observed joint face displacement.

4.9.2 Building Slab Dowels

None of the building slab dowels specimens included strain gages.

4.10 Dowel Embedment Length

The dowel embedment length requirement that $\beta L_e \geq 2$ was satisfied for all highway and building slab dowels tested. This requirement is necessary when assuming a semi-infinite length, which is required for the theory presented in Chapter 3.

5. SUMMARY, CONCLUSIONS, AND RECOMMENDATIONS

5.1 Summary

The AASHTO T253 method of determining modulus of dowel support and evaluating dowels has been in use for several years. Many modifications have been made to the test to provide better results and recommendations have been made for more sweeping changes (*20*). Though not exact, the Modified AASHTO T253 is a useful tool to evaluate dowel bars. This study focuses on the results obtained from the Modified AASHTO T253 as follows:

- 54 full scale highway dowel tests including:
    - Six different dowels types
    - Circular and elliptical sections
    - Steel (epoxy-coated), stainless steel, and GFRP materials
    - 1/2-inch, 1/8-inch, and 0-inch joint widths
    - Eight tests with strain gages used to show dowel behavior
- 30 full scale building slab dowel tests including:
    - Four different dowel types
    - Circular and rectangular sections
    - Six normal size specimens and 24 small size specimens
    - Dowels with and without sleeves

Altogether, these tests evaluated 28 different configurations of dowel type, joint width, specimen size, and whether sleeved or not.

In addition to determining the modulus of dowel support for each dowel, the effects of joint width, dowel shape, dowel material, dowel flexural rigidity were also observed. Dowel deflections and bearing stresses were also compared.

5.2 Highway Dowel Conclusions

The calculations and evaluation of the six highway dowel types showed that none of the specimens failed (dowel yield or concrete failure) before the ACI Committee 325 (*33*) allowable stress was achieved. All six dowels can transfer loads of at least 5000 pounds without exceeding the allowable stresses. Previous research (*20*) has shown that 5000 pounds is more load than a dowel will experience for a wheel load distributed to several dowels in a highway joint. Thus, all six dowel bars will perform adequately in highway use, depending upon the repeated (or fatigue) load requirements and the effects of repeated loading on oblonging of the dowel hole.

The elliptical shape did help reduce bearing stresses although wider bars in general tend to reduce bearing stresses. Consequently, elliptical dowels that reduce bearing stresses lead to increased dowel deflection. However, all deflections measured were well within the required magnitude to maintain rider comfort on highways. The benefit of lower bearing stresses implies a lower likelihood of the oblonging of a dowel hole under repeated loading.

Corrosion resistance is a main concern for testing alternative material such as stainless steel and GFRP. Neither stainless steel nor GFRP corrode, but GFRP may expand due to prolonged moisture exposure. More long term testing is needed for GFRP. Stainless steel is much more expensive than steel and GFRP (*26*). GFRP is currently more expensive than

steel, but this may change as steel prices increase, technology is improved, and benefits of mass production are achieved for GFRP manufacturing.

All six highway dowels tested are adequate for load transfer. Cost and environment are criteria that should be considered when choosing among these six dowel types.

5.3 Building Slab Dowel Conclusions

Four building slab dowel types were tested, each with and without a dowel sleeve. The modulus of dowel support and several other parameters were determined. The results show that dowels with rectangular cross sections and large widths are effective in reducing bearing stresses while dowels with round cross sections are effective in limiting the total deflection.

Adding sleeves to the dowels (half of the building slab dowels tested had sleeves) resulted in increased deflections, reduced k_0 values (although a true k_0 value cannot be measured for the sleeved dowels by the theory used in this study), reduced bearing stresses, and reduced capacity. The deflection increases were significant, but the reduction in bearing stresses and capacity as compared to the non-sleeved dowels was not as significant. The reason the deflection increases were so significant is because the dowels have some play within the sleeve before the dowel/sleeve mechanism deflects into the surrounding concrete.

The test results show that specimen depth limited capacity. For the round dowel, the 6-inch deep specimens failed at half the load the 12-inch specimens failed at. However, a 6-inch slab depth is more common for a building slab.

All the building slab dowel types tested were able to transfer a load of at least 3000 pounds between adjacent slabs, without any factor of safety. An appropriate factor of safety

should be applied, as deemed necessary by a jurisdictional authority. Slab thickness, dowel spacing, and dowel cost should all be considered when selecting among these four dowels.

5.4 Behavioral Conclusions

The following behavioral conclusions can be made from the tests:

- As flexural rigidity increases, k_0 increases and bearing stresses increase
- As dowel width increases, k_0 decreases and bearing stresses decrease
- Larger deflections correspond to lower k_0 values and lower bearing stresses
- Adding sleeves to dowels reduces bearing stresses
- Adding sleeves to dowels increases deflection
- Different joint widths do not provide definitive changes to k_0

5.5 General Conclusions

The purpose of studying the elliptical dowels and GFRP dowels is to determine whether they are a viable alternative to round steel dowels typically found in highway joints. The results of this study show that elliptically-shaped dowels do reduce bearing stresses at the dowel-concrete interface. The study also shows that GFRP dowels have load transfer capacities nearly as large as the steel and stainless steel dowels studied. However, the deflections measured for the elliptical dowels and GFRP dowels were greater than for round steel dowels. But the deflections measured for all dowels were well within the recommended maximum deflection (*27*) to ensure "rider comfort" for vehicles traversing the joint. The laboratory investigation suggests that there is merit in using elliptical dowels and GFRP dowels as an alternative to round steel dowels; however, testing of long-term fatigue

characteristics and environmental effects on the elliptical dowels and GFRP dowels should be performed.

5.6 Recommendations for Future Research

Continued research on the parametric effects of dowel-concrete behavior is needed. As new dowels are introduced and as more effective test methods are developed (*20*), more testing will be needed to help determine the most efficient dowel for a specific need. Future research needs include:

- Effects of wider joints, such as those used for contraction, e.g. 1-inch or more
- Effects of repeated loading (fatigue testing) on the oblonging of dowel holes, especially for alternative dowels such as elliptically-shaped dowels and GFRP dowels
- Effects of repeated loading on dowel sleeves
- Long-term evaluation of FRP in pavement structures
    - Effects of repeated loading
    - Effects of environment

APPENDIX A. HIGHWAY DOWEL MODULUS OF DOWEL SUPPORT VS. LOAD DIAGRAMS

Figures A.1 through A.36 show k_0 vs. load plots for all 18 modified AASHTO T253 series of specimens where k_0 is determined as described in Chapter 3. There are three specimens for each series (54 specimens total) and two dowels per specimen for a total of six plots per figure. Each series has two plots: one with unadjusted loading and one with adjusted loading (see Section 4.1). The dowels are broken down by specimen number and specimen orientation (east or west).

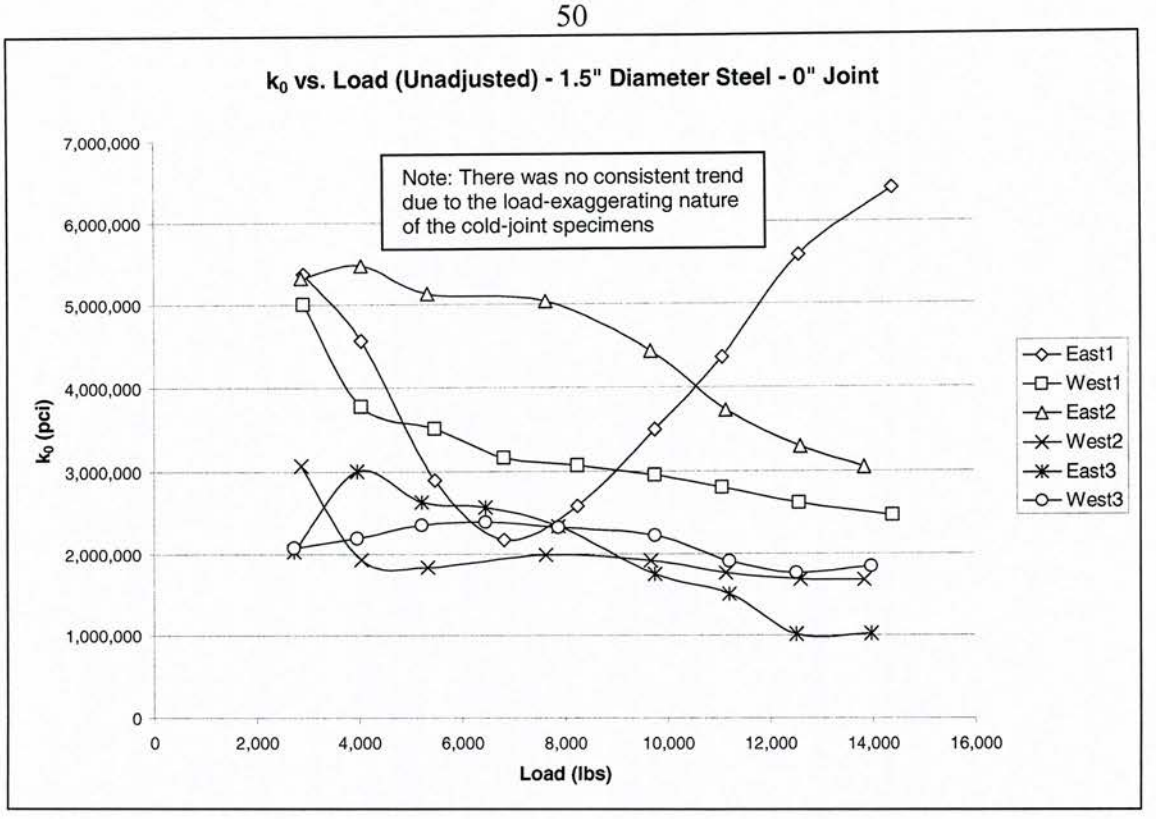

Figure A.1. k_0 plots, round steel, 0-inch joint, unadjusted loads

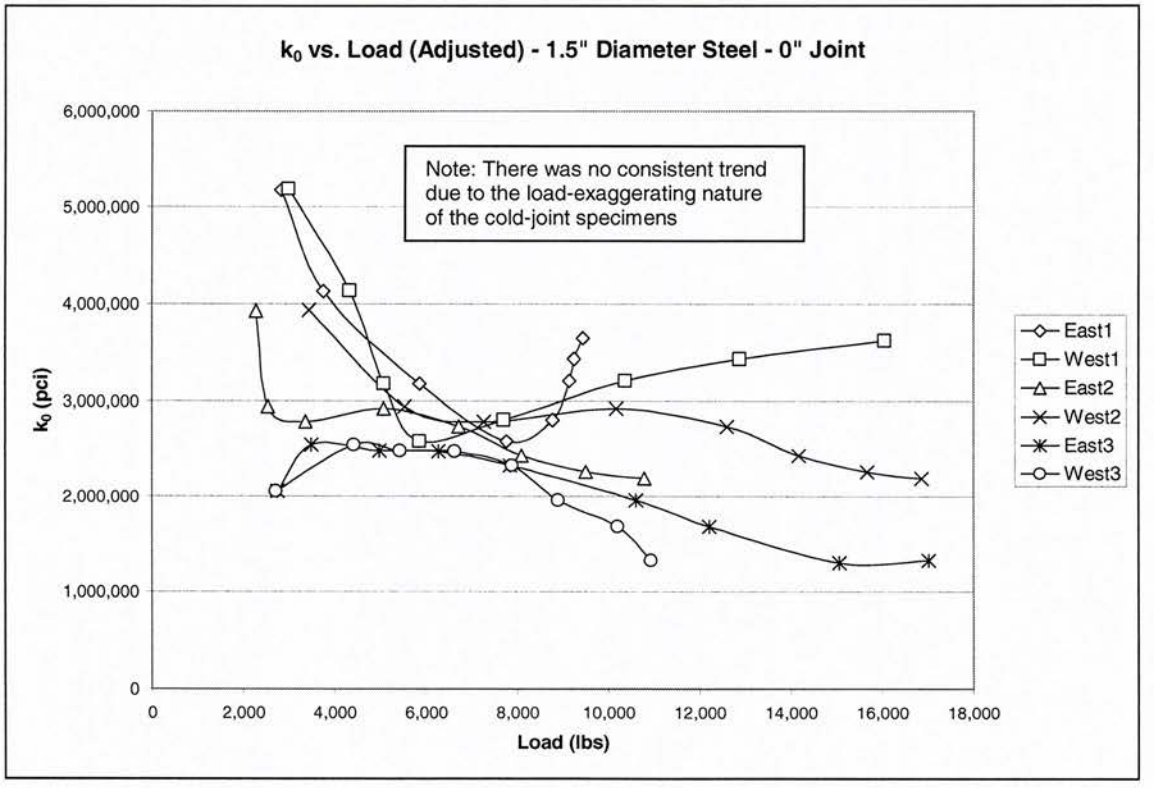

Figure A.2. k_0 plots, round steel, 0-inch joint, adjusted loads

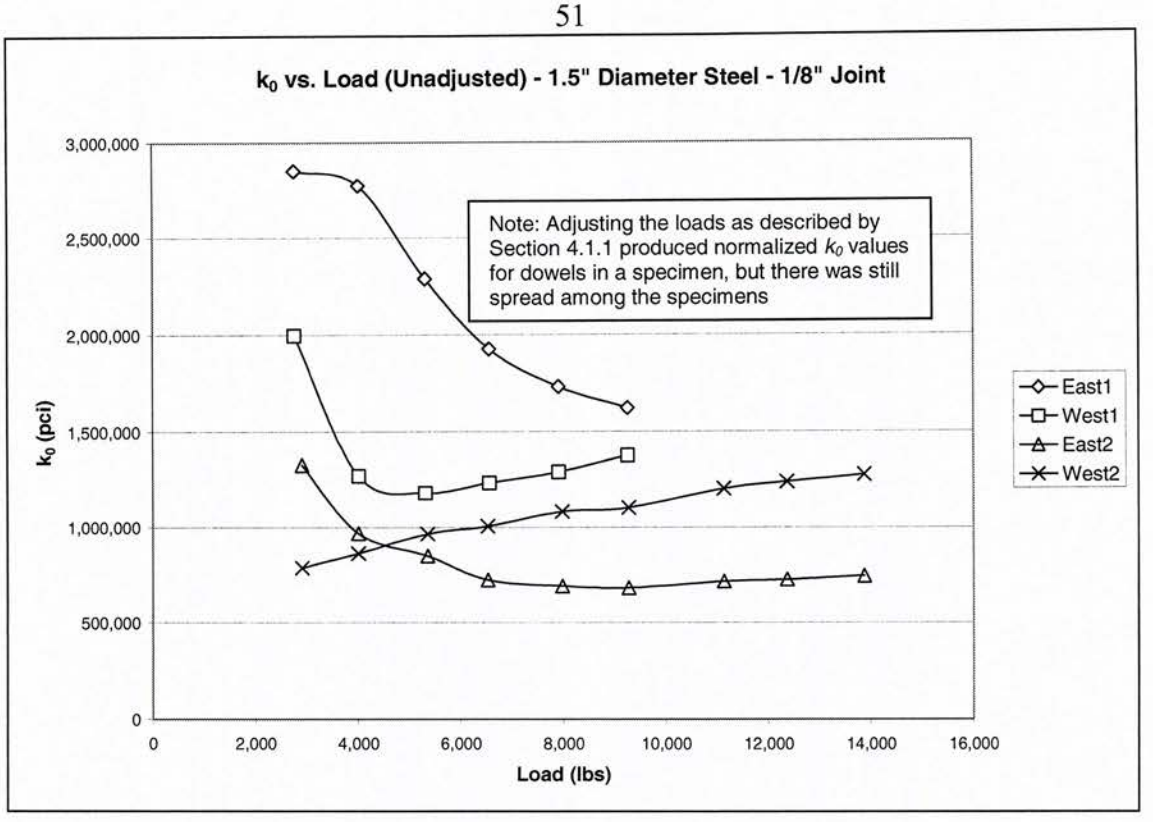

Figure A.3. k_0 plots, round steel, 1/8-inch joint, unadjusted loads

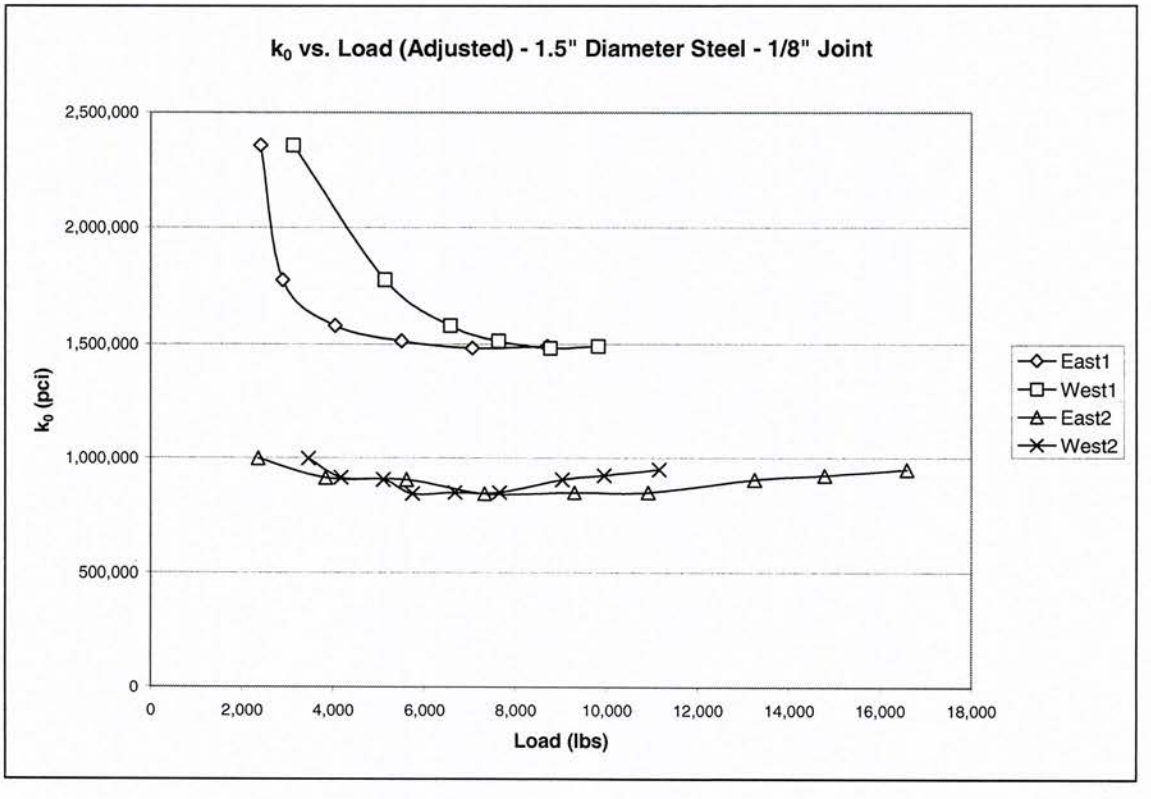

Figure A.4. k_0 plots, round steel, 1/8-inch joint, adjusted loads

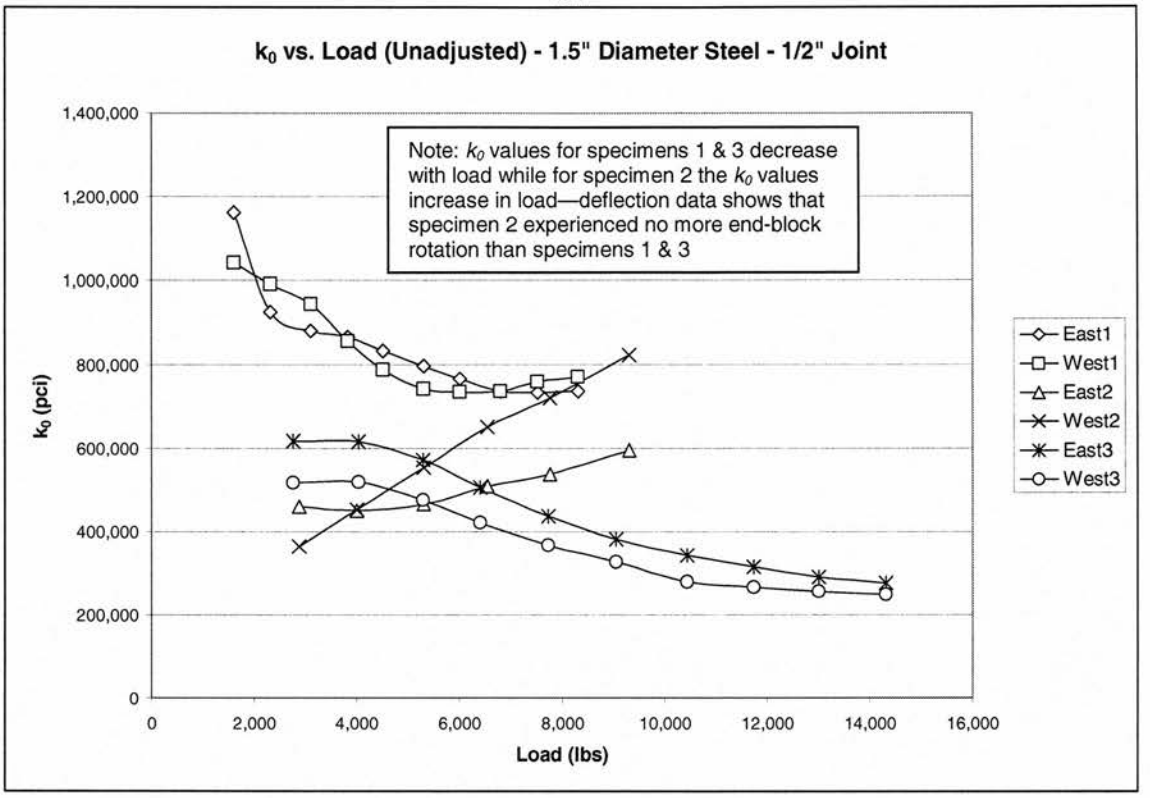

Figure A.5. k_0 plots, round steel, 1/2-inch joint, unadjusted loads

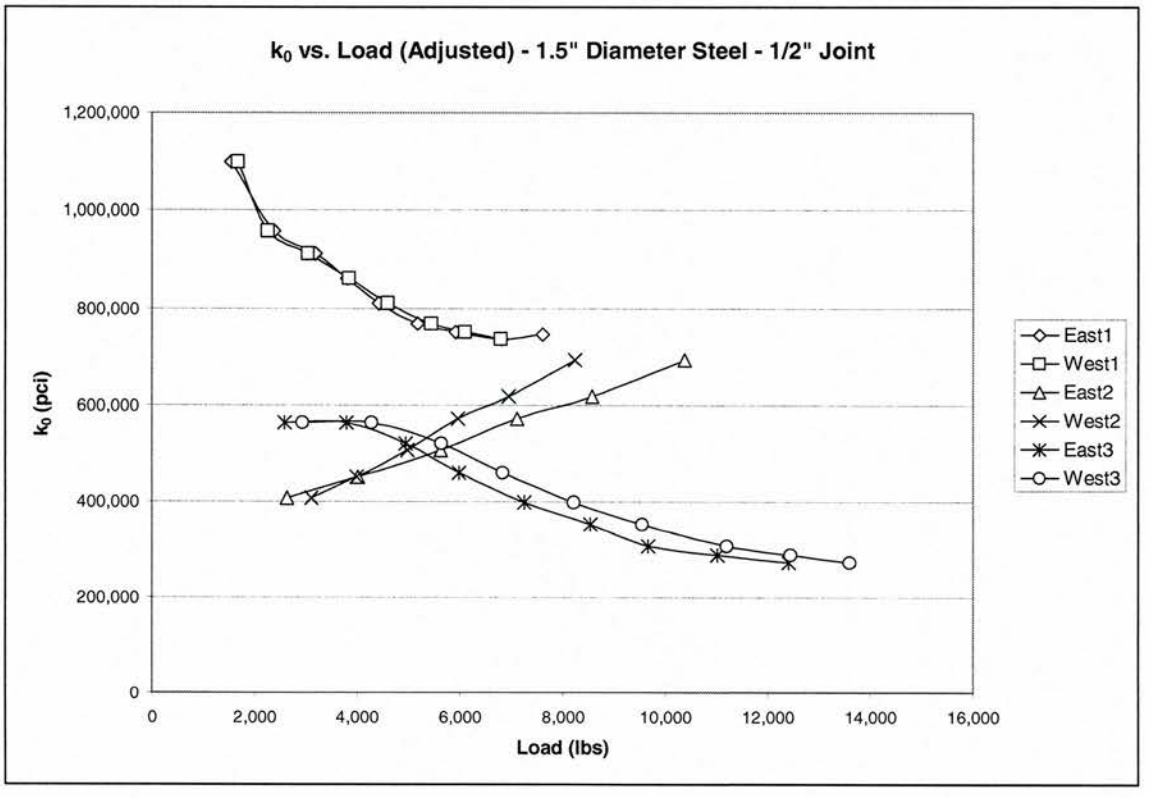

Figure A.6. k_0 plots, round steel, 1/2-inch joint, adjusted loads

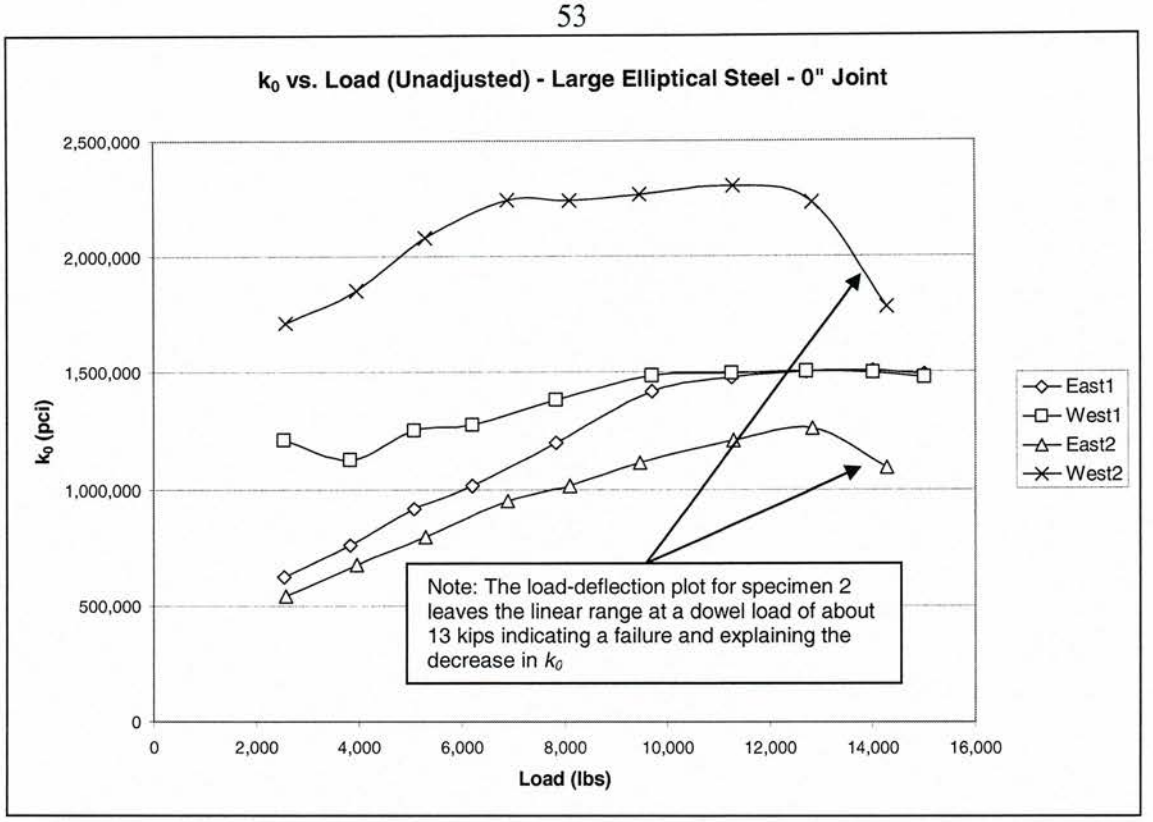

Figure A.7. k_0 plots, large elliptical steel, 0-inch joint, unadjusted loads

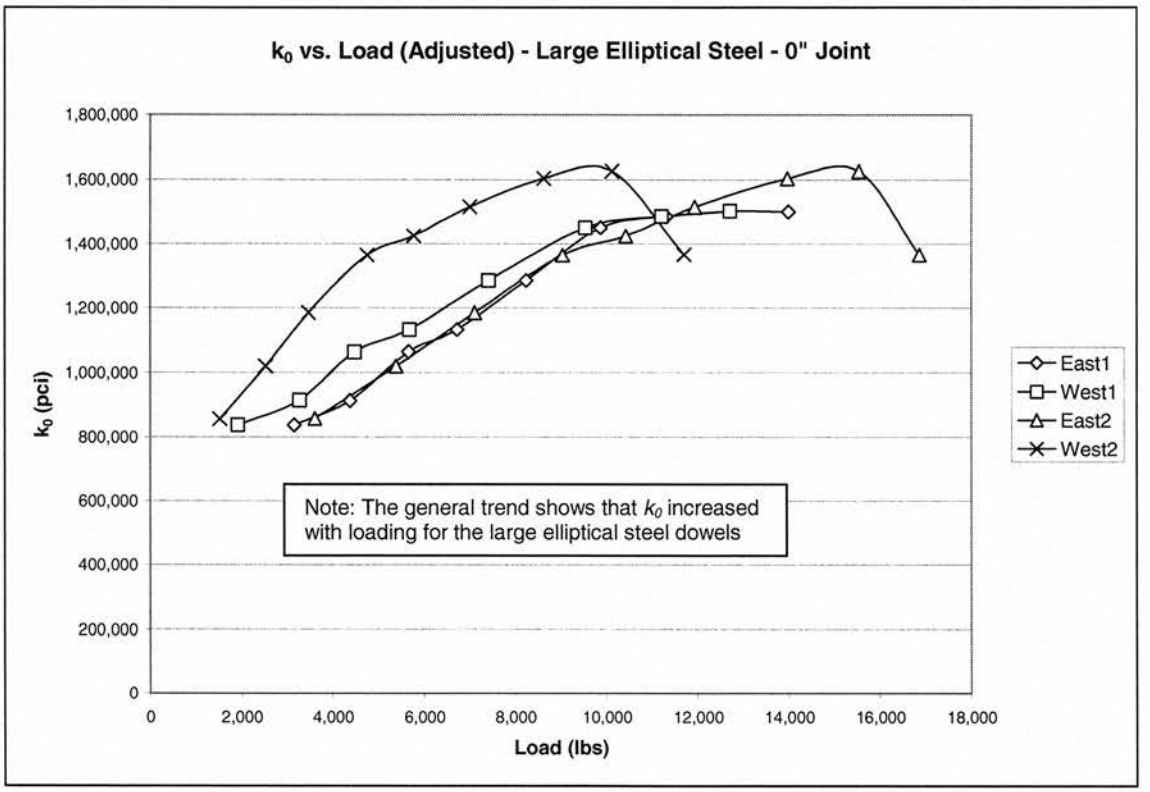

Figure A.8. k_0 plots, large elliptical steel, 0-inch joint, adjusted loads

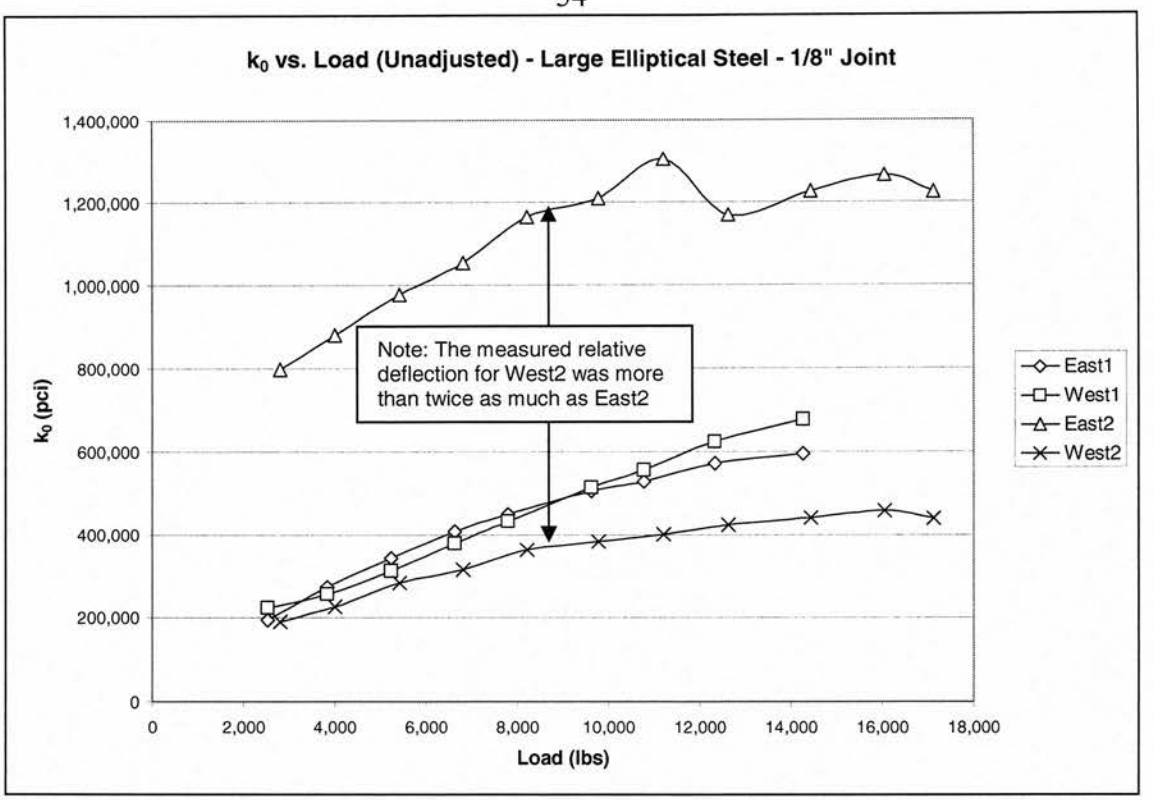

Figure A.9. k_0 plots, large elliptical steel, 1/8-inch joint, unadjusted loads

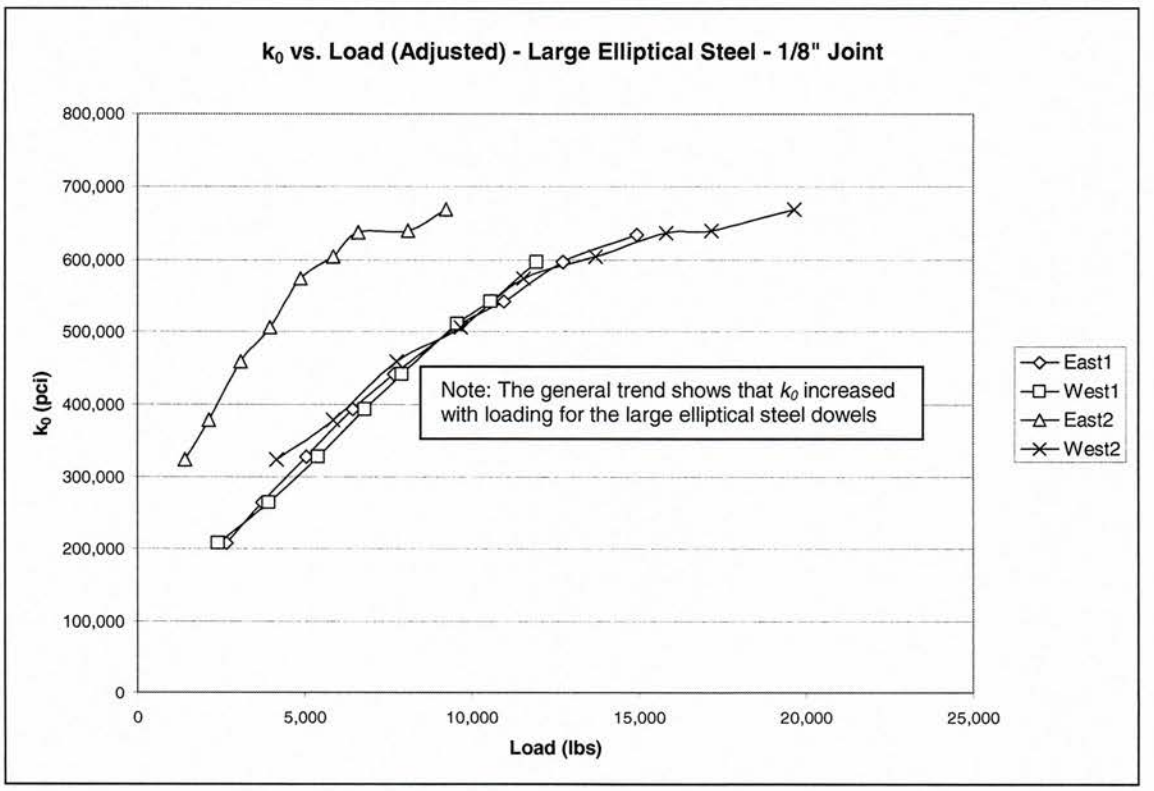

Figure A.10. k_0 plots, large elliptical steel, 1/8-inch joint, adjusted loads

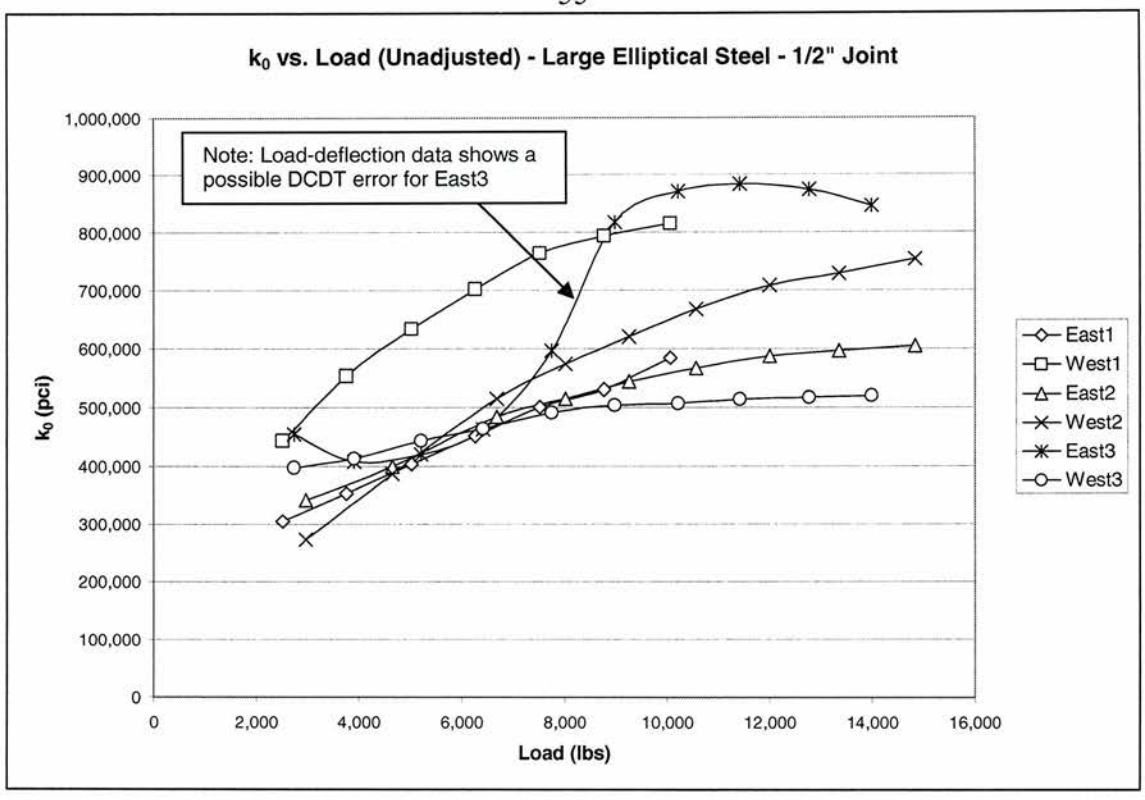

Figure A.11. k_0 plots, large elliptical steel, 1/2-inch joint, unadjusted loads

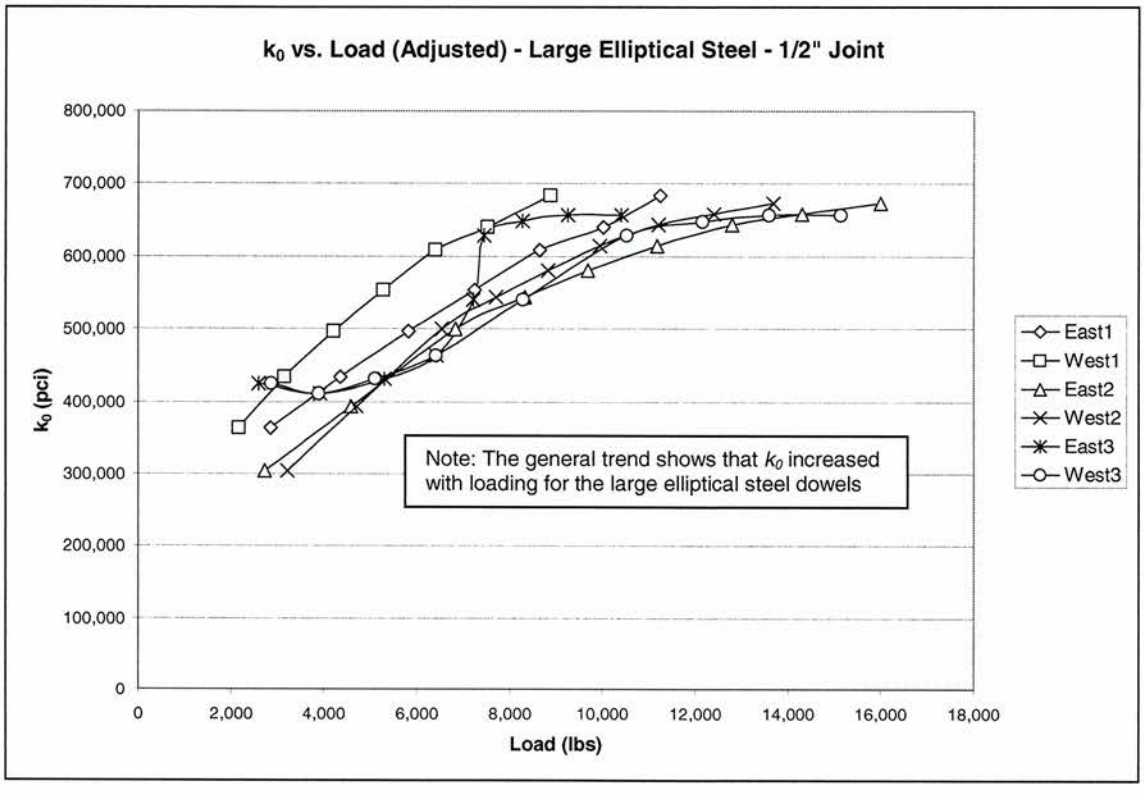

Figure A.12. k_0 plots, large elliptical steel, 1/2-inch joint, adjusted loads

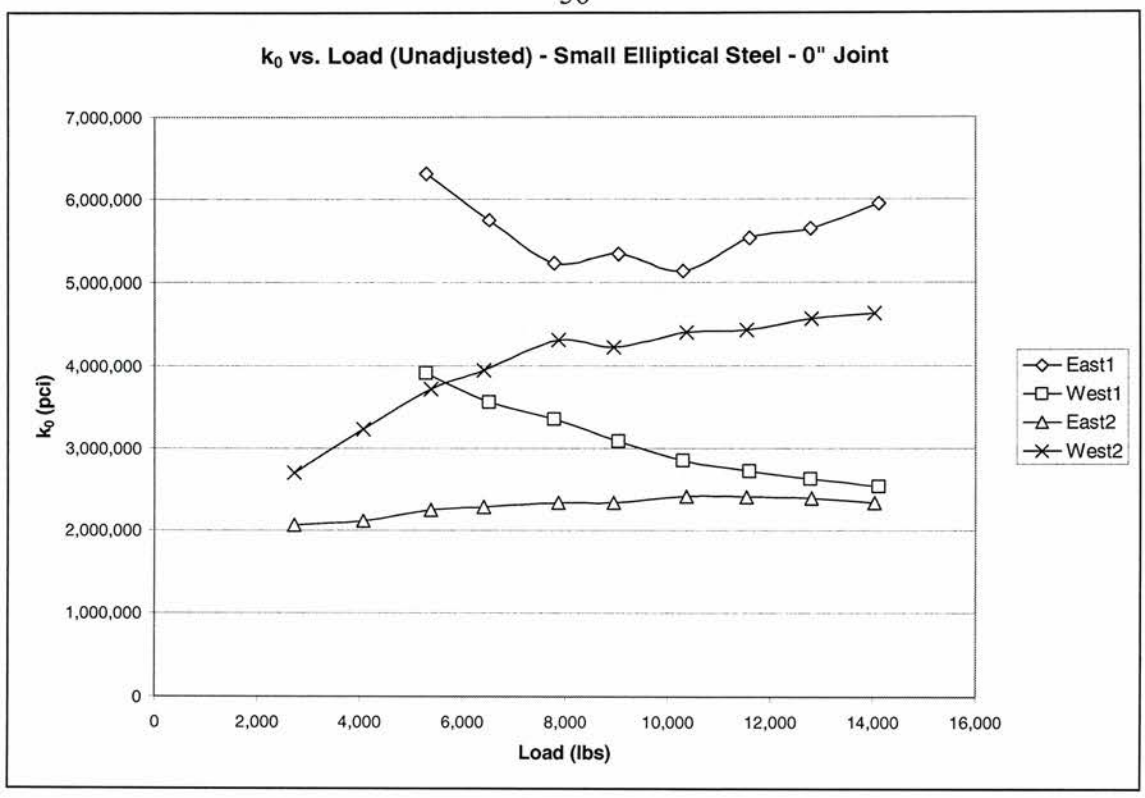

Figure A.13. k_0 plots, small elliptical steel, 0-inch joint, unadjusted loads

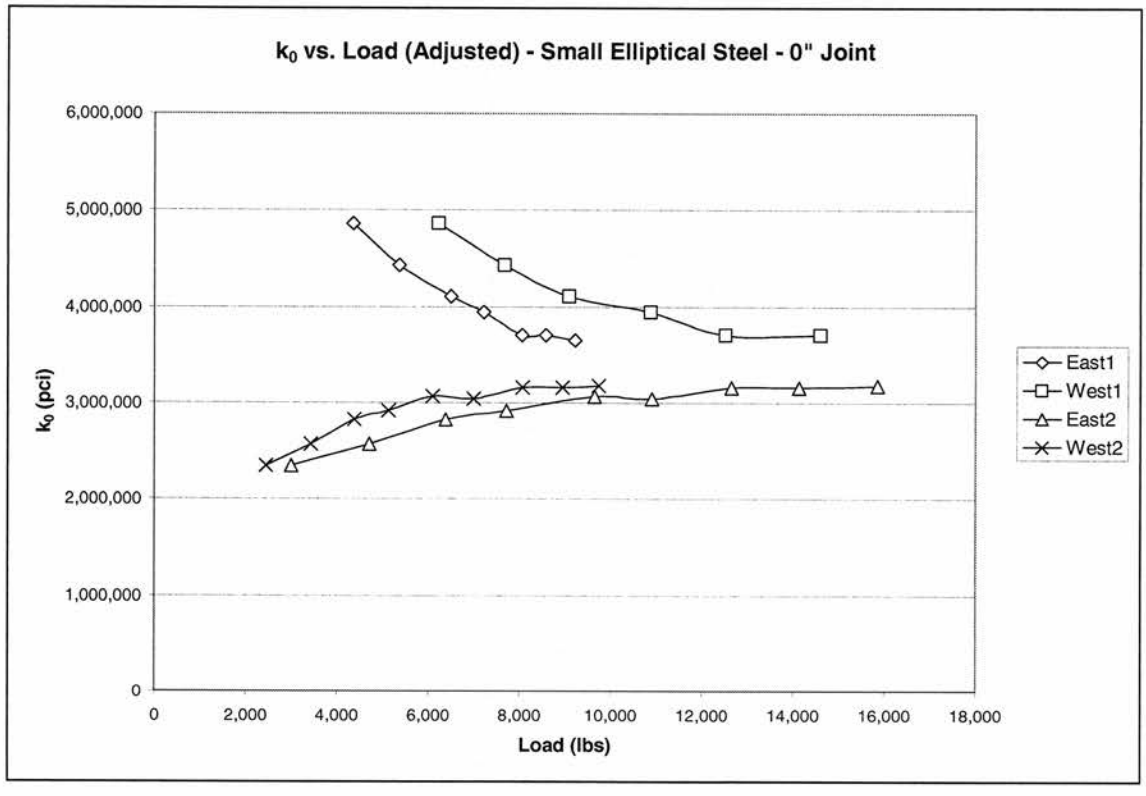

Figure A.14. k_0 plots, small elliptical steel, 0-inch joint, adjusted loads

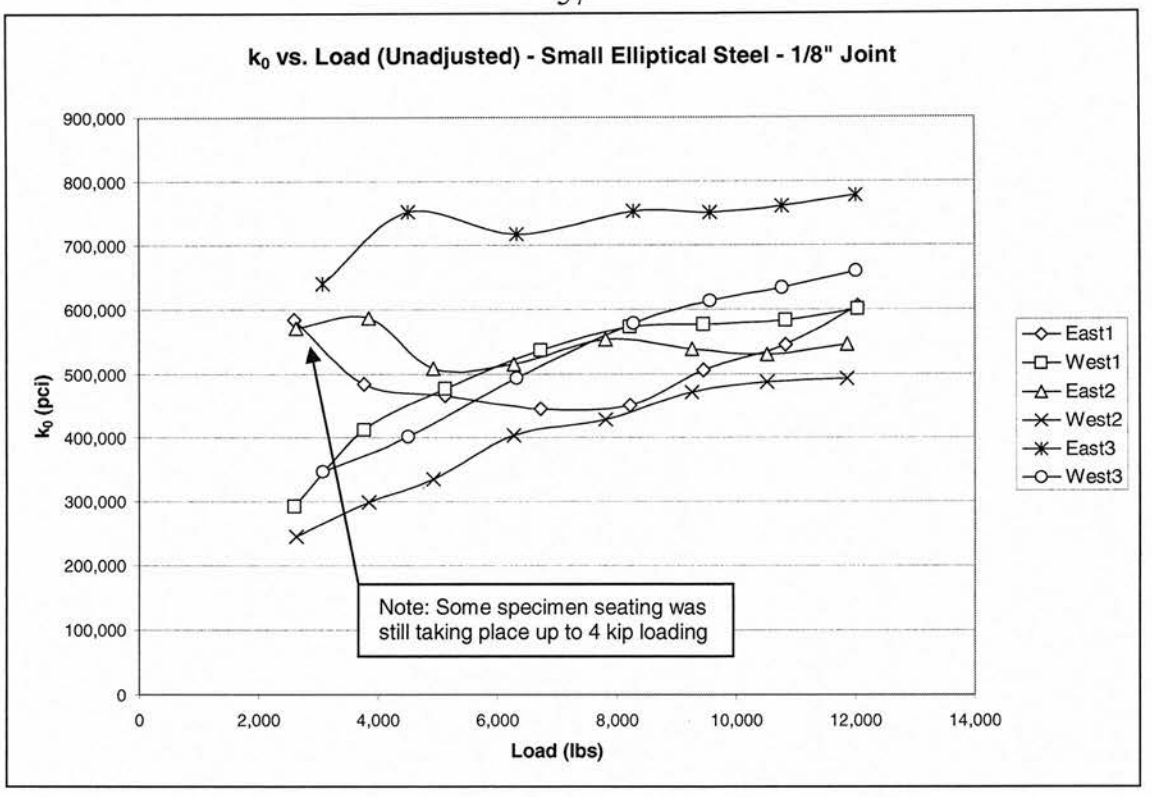

Figure A.15. k_0 plots, small elliptical steel, 1/8-inch joint, unadjusted loads

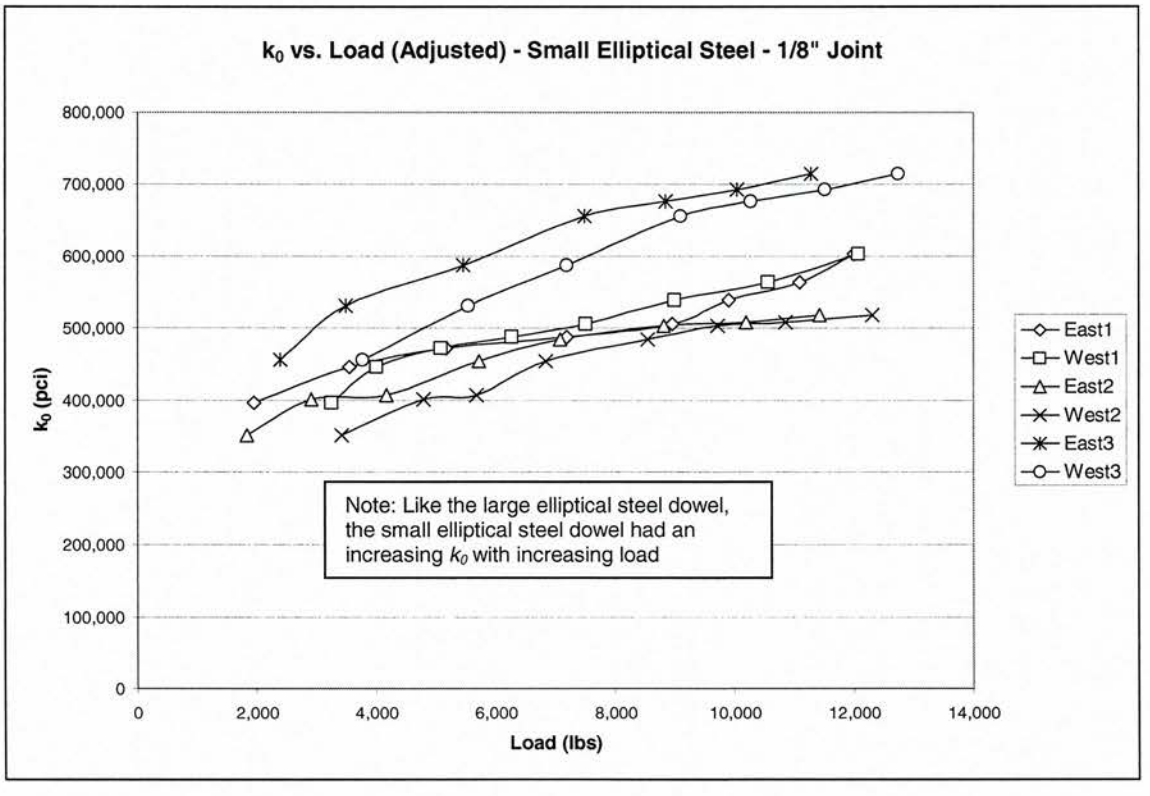

Figure A.16. k_0 plots, small elliptical steel, 1/8-inch joint, adjusted loads

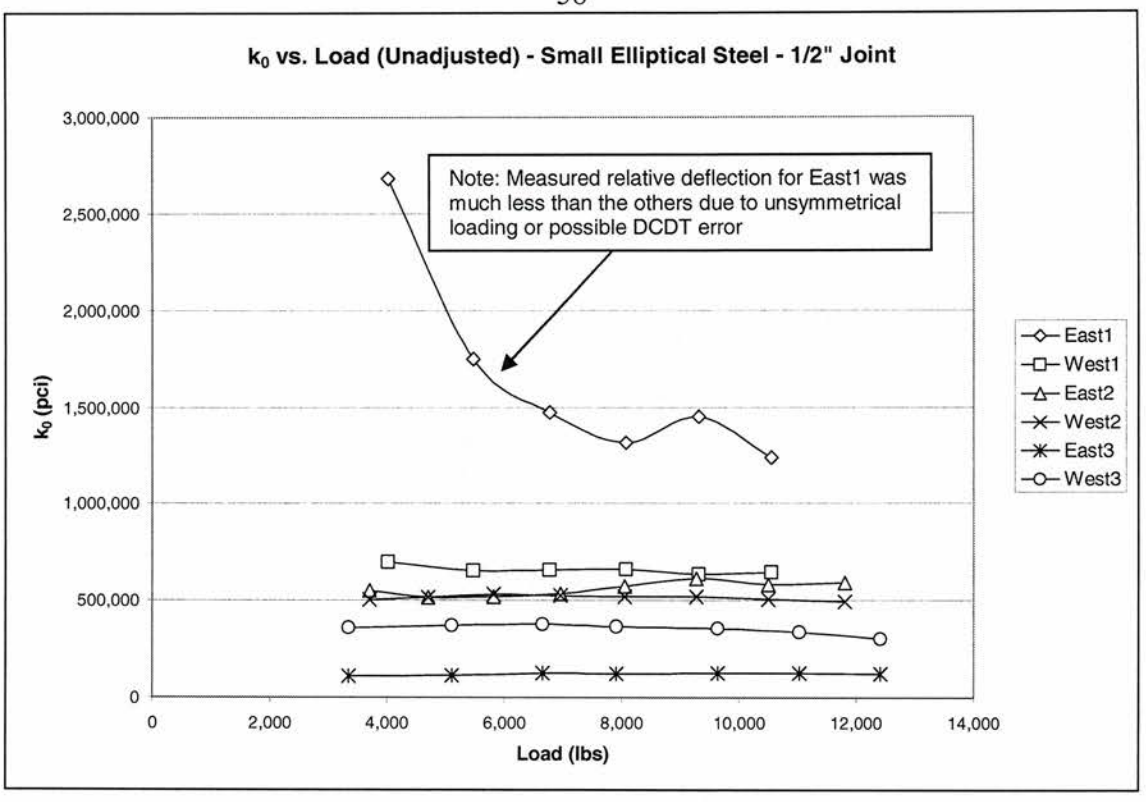

Figure A.17. k_0 plots, small elliptical steel, 1/2-inch joint, unadjusted loads

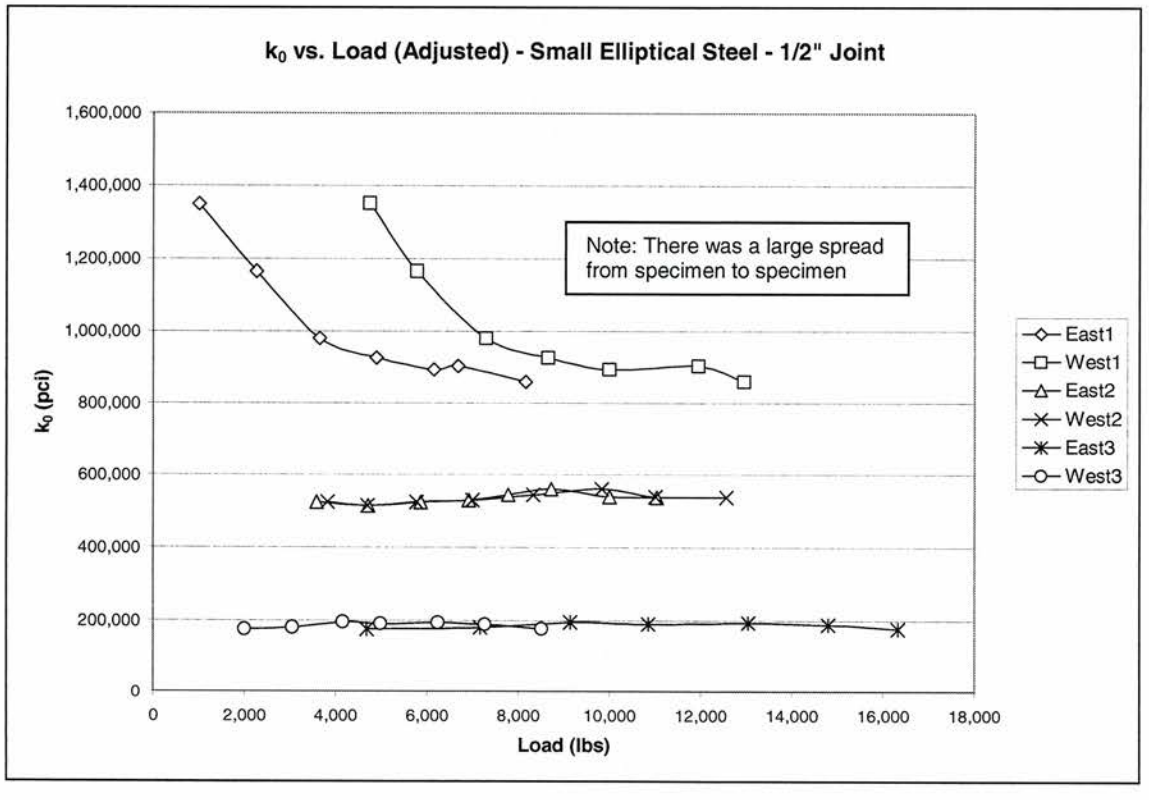

Figure A.18. k_0 plots, small elliptical steel, 1/2-inch joint, adjusted loads

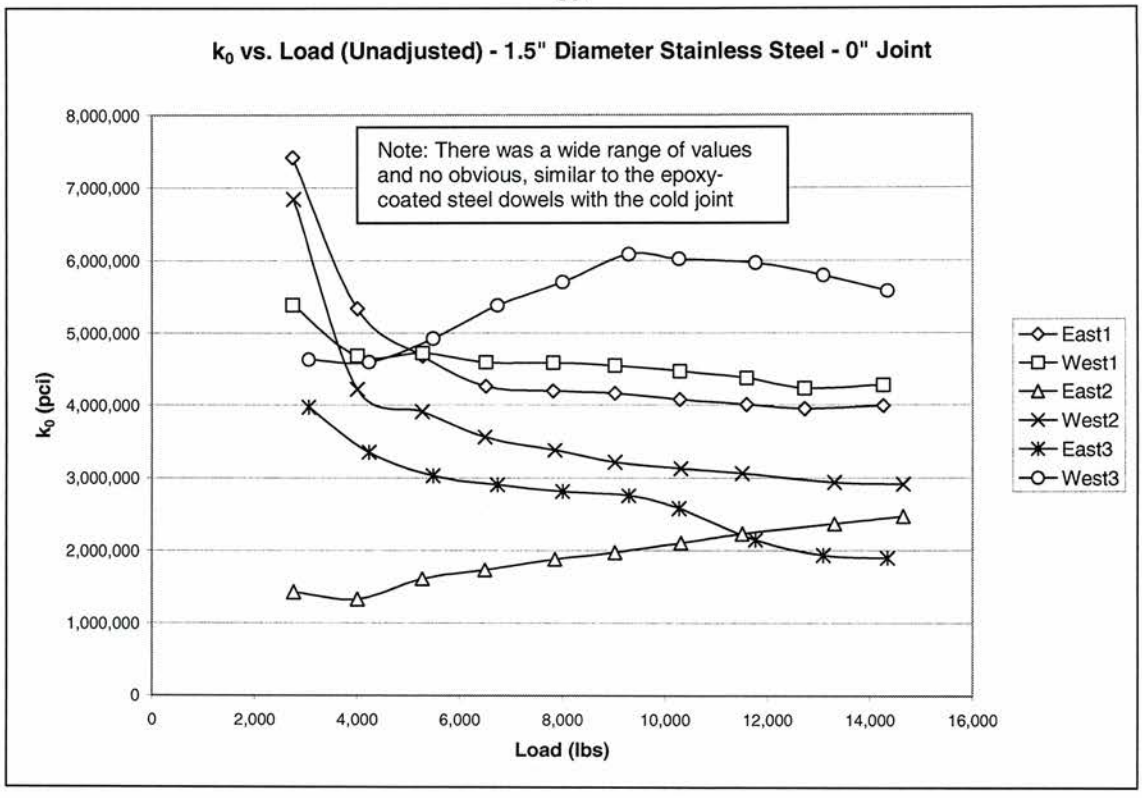

Figure A.19. k_0 plots, round stainless steel, 0-inch joint, unadjusted loads

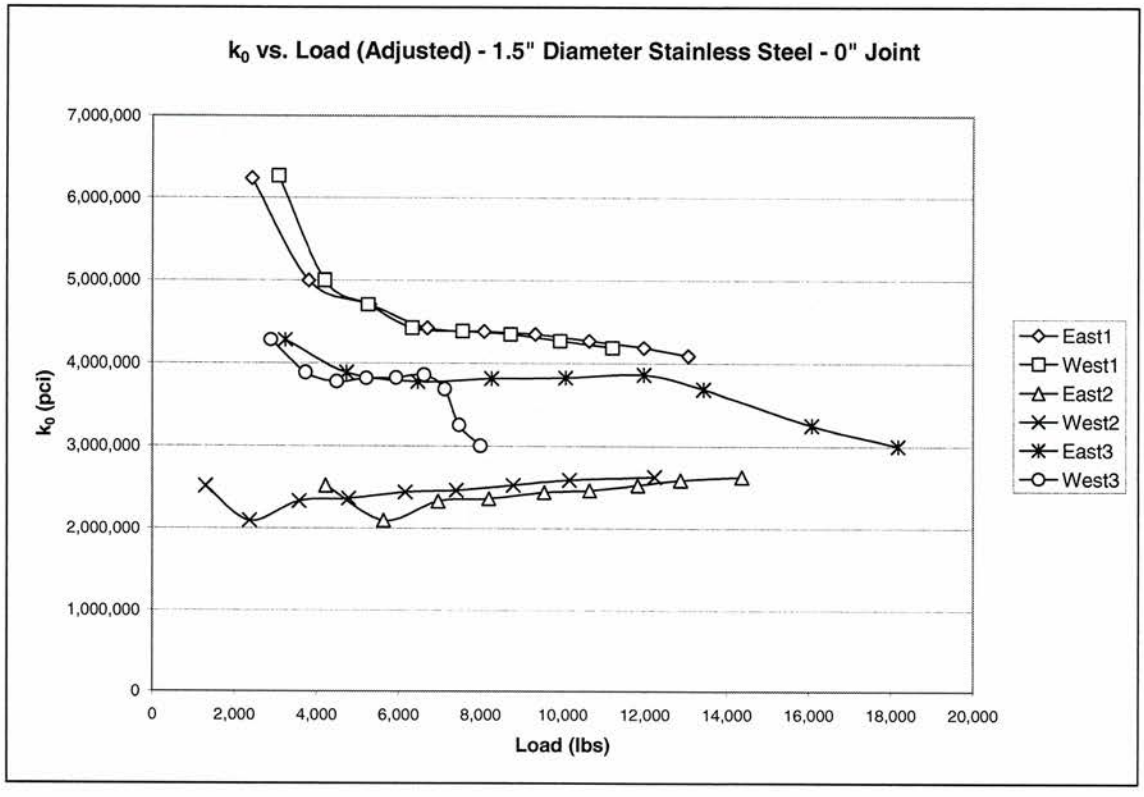

Figure A.20. k_0 plots, round stainless steel, 0-inch joint, adjusted loads

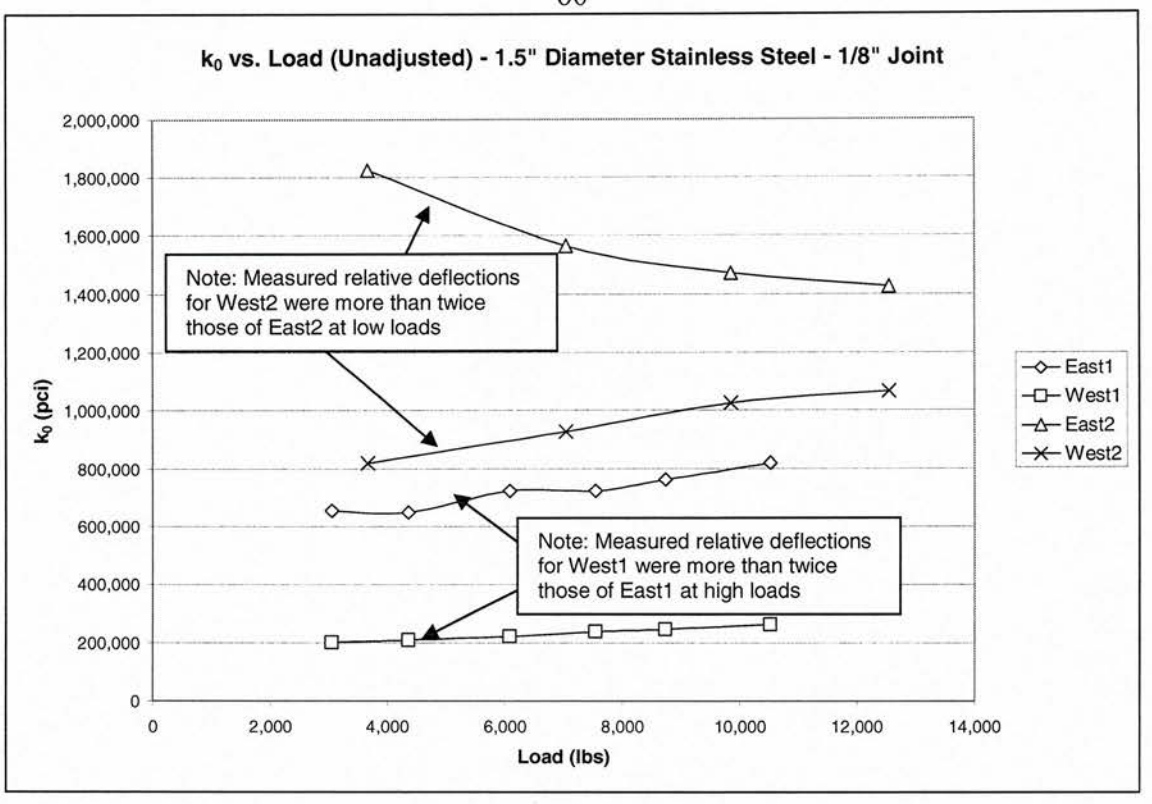

Figure A.21. k_0 plots, round stainless steel, 1/8-inch joint, unadjusted loads

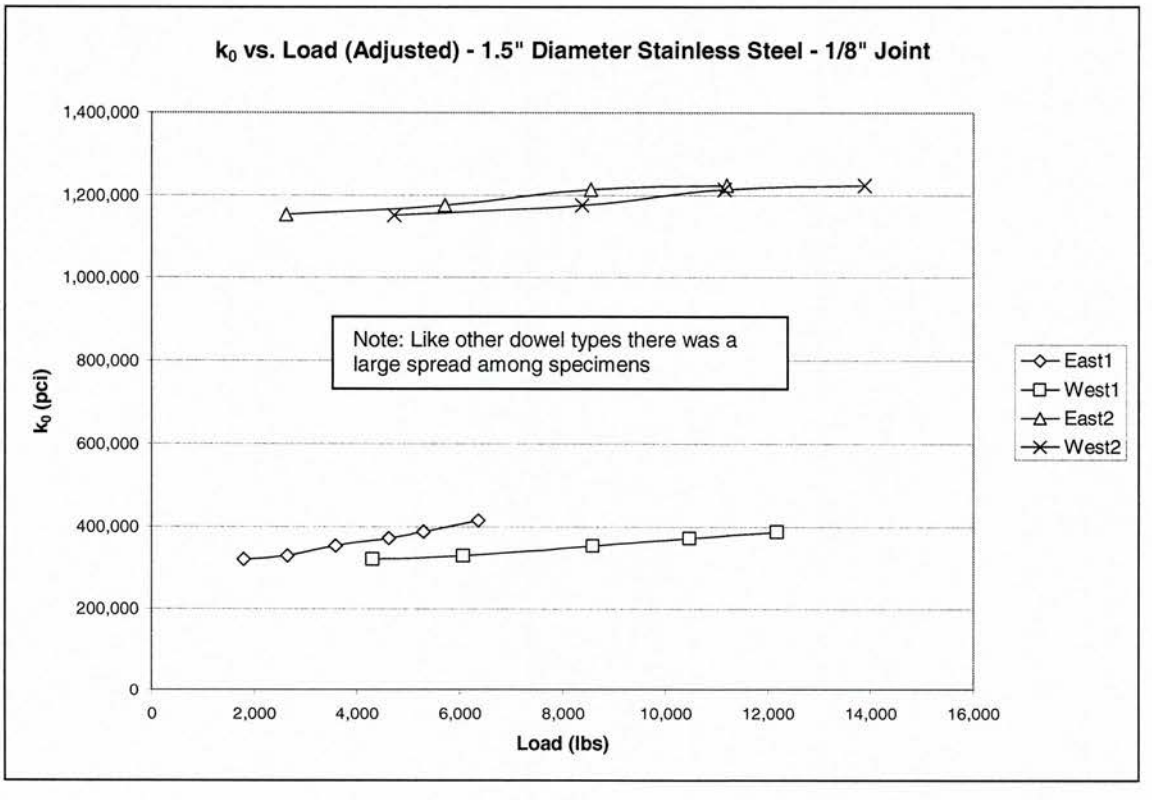

Figure A.22. k_0 plots, round stainless steel, 1/8-inch joint, adjusted loads

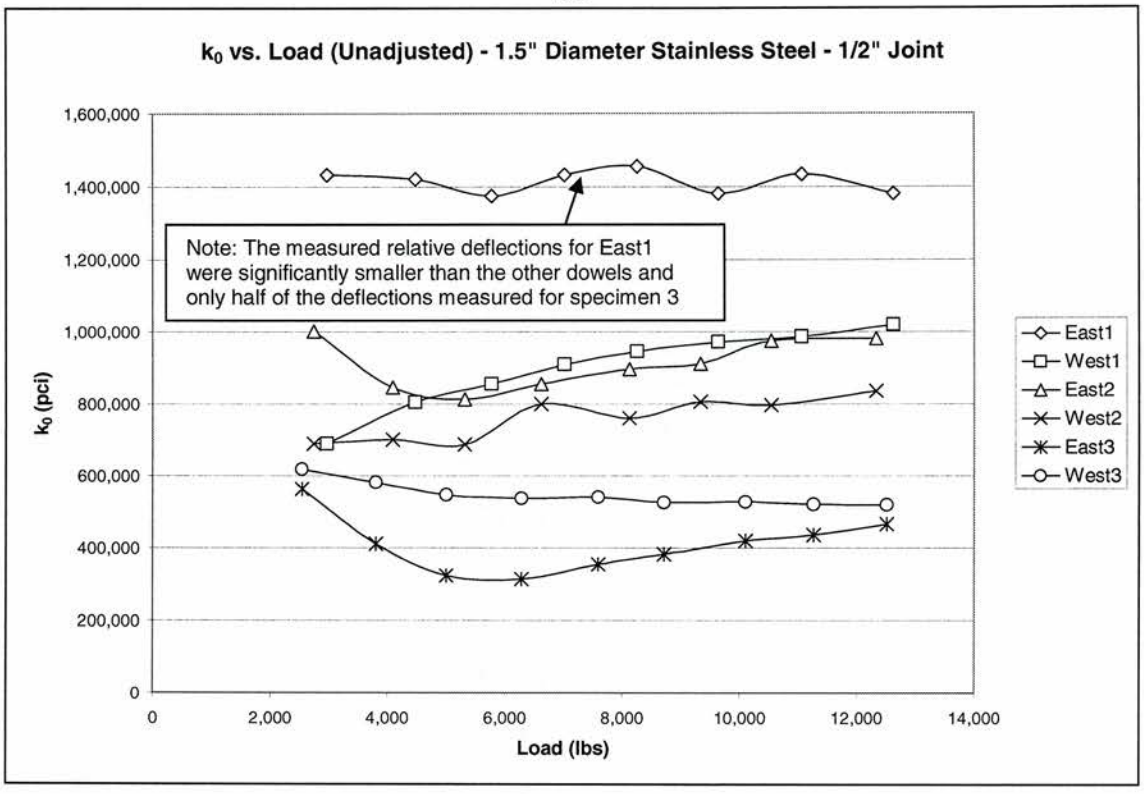

Figure A.23. k_0 plots, round stainless steel, 1/2-inch joint, unadjusted loads

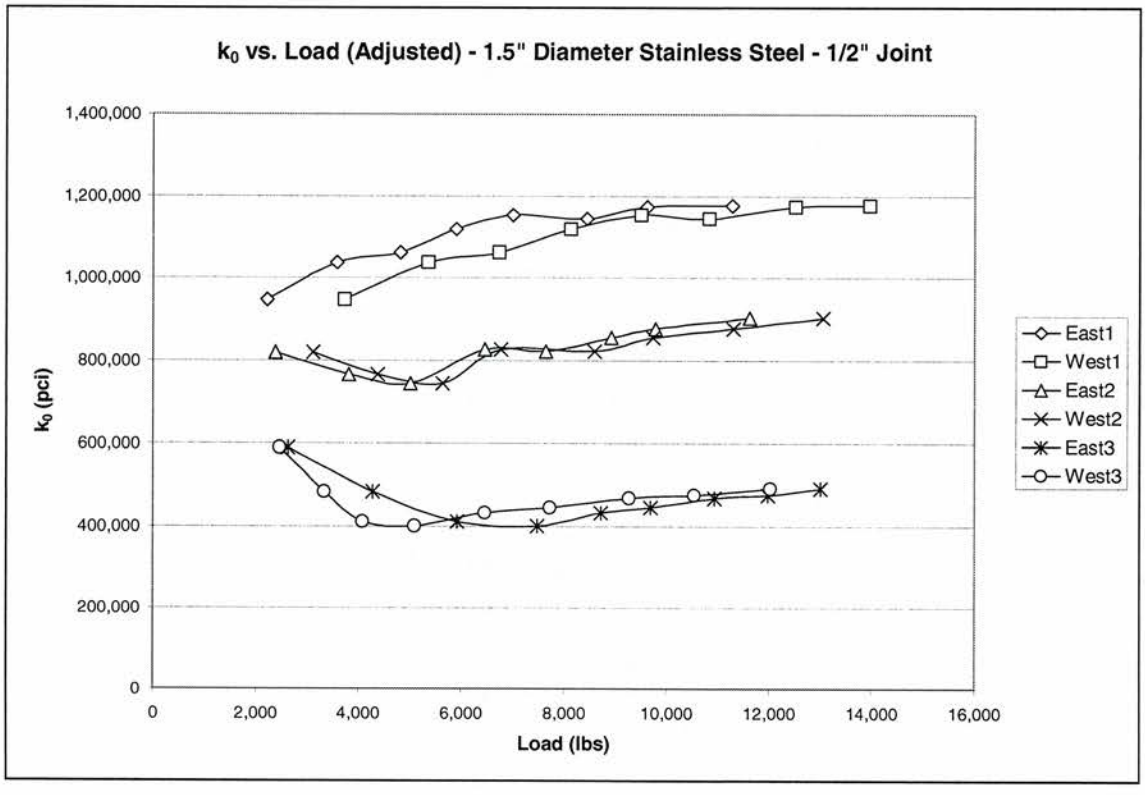

Figure A.24. k_0 plots, round stainless steel, 1/2-inch joint, adjusted loads

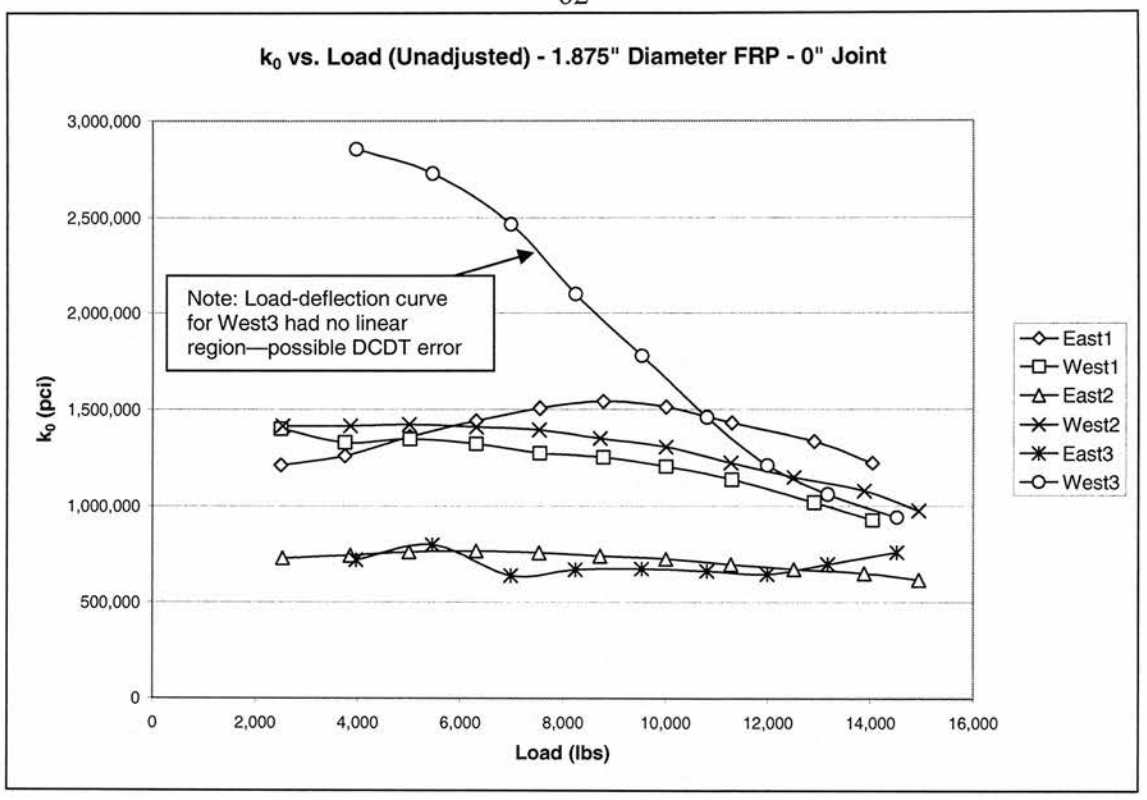

Figure A.25. k_0 plots, round GFRP, 0-inch joint, unadjusted loads

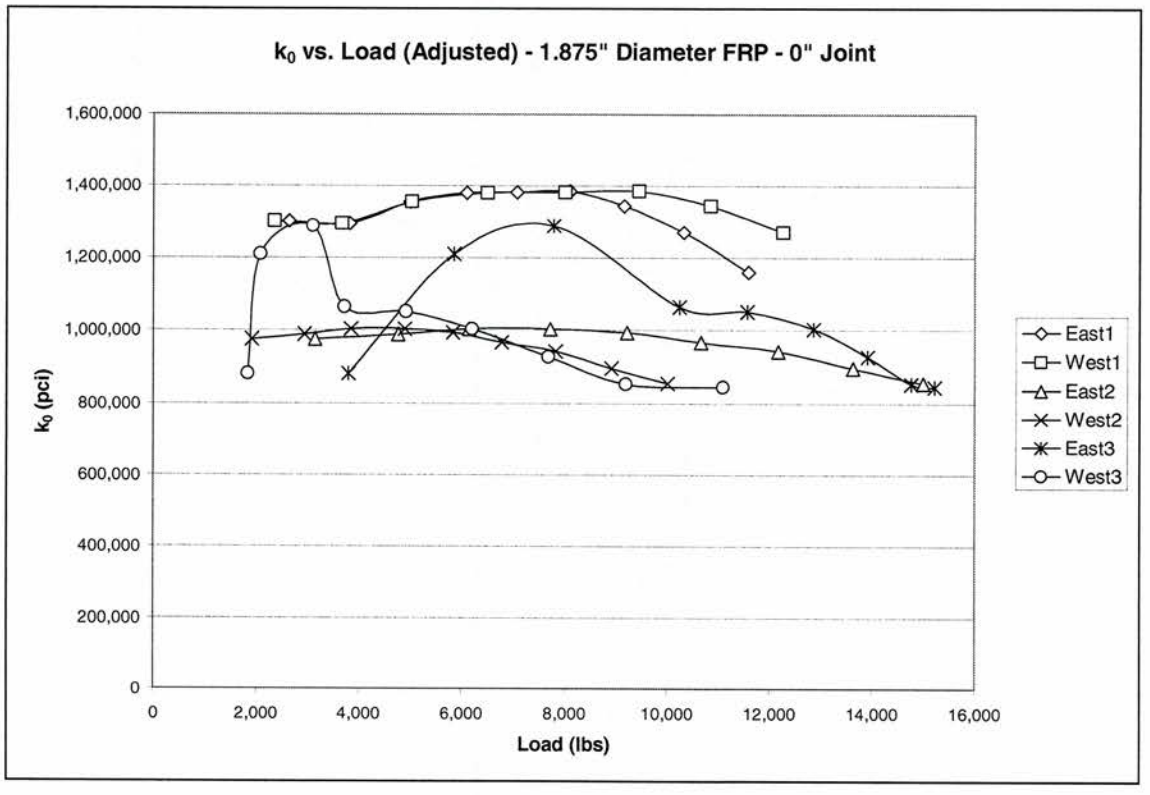

Figure A.26. k_0 plots, round GFRP, 0-inch joint, adjusted loads

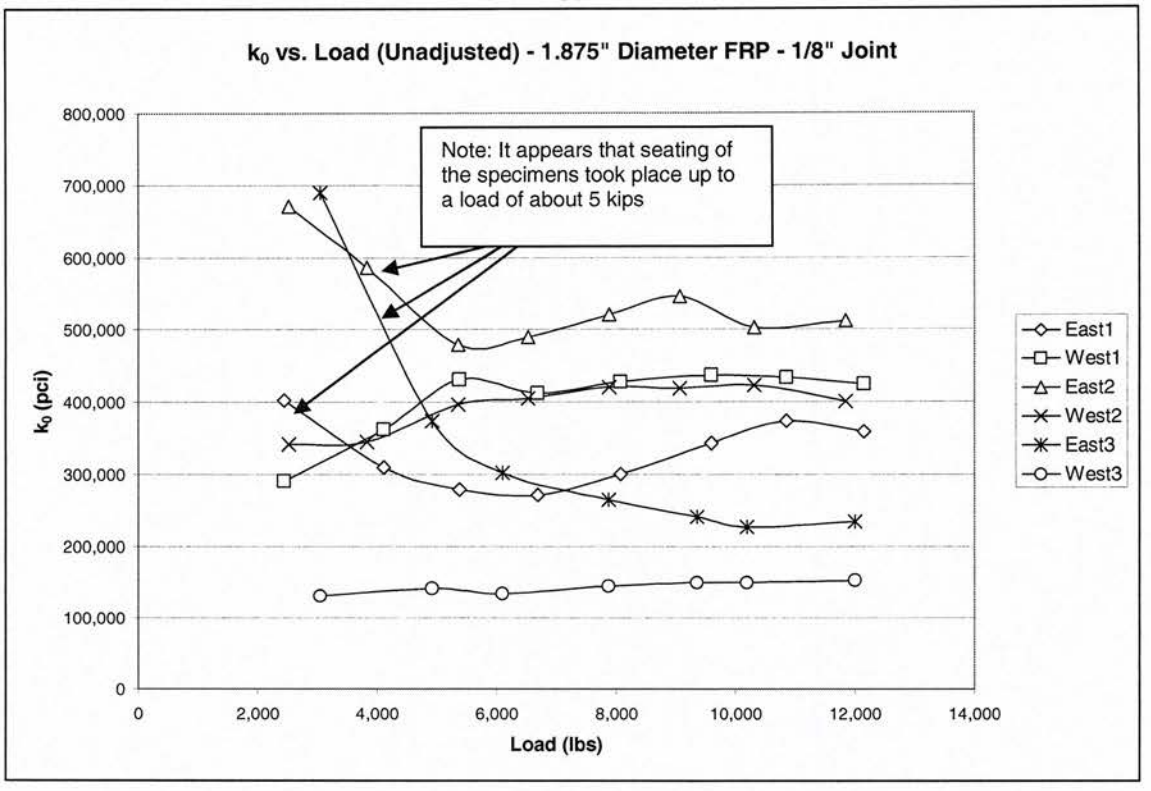

Figure A.27. k_0 plots, round GFRP, 1/8-inch joint, unadjusted loads

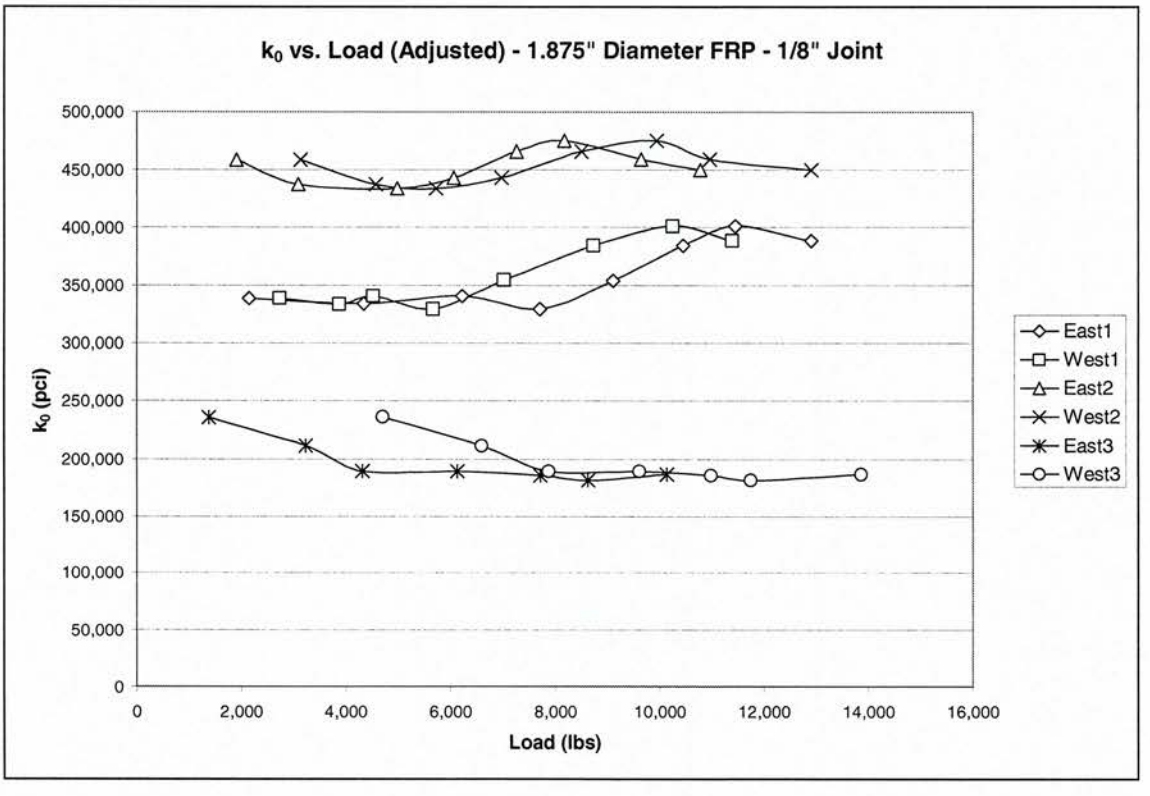

Figure A.28. k_0 plots, round GFRP, 1/8-inch joint, adjusted loads

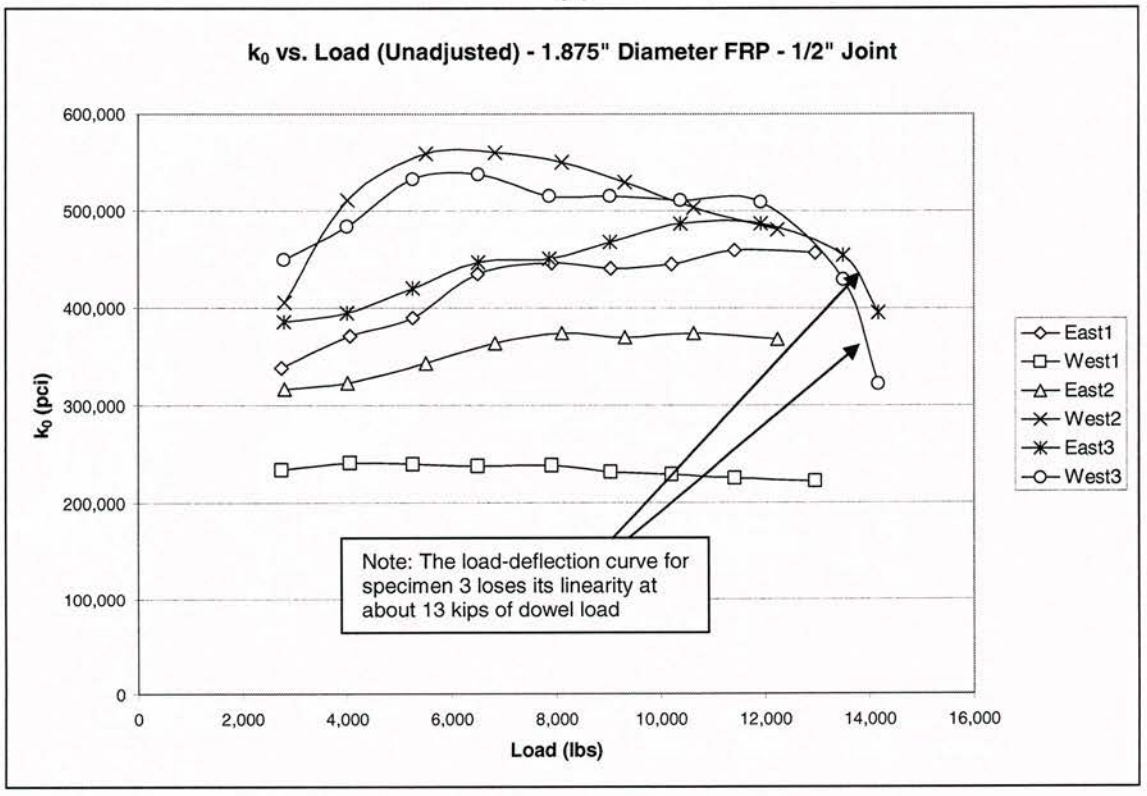

Figure A.29. k_0 plots, round GFRP, 1/2-inch joint, unadjusted loads

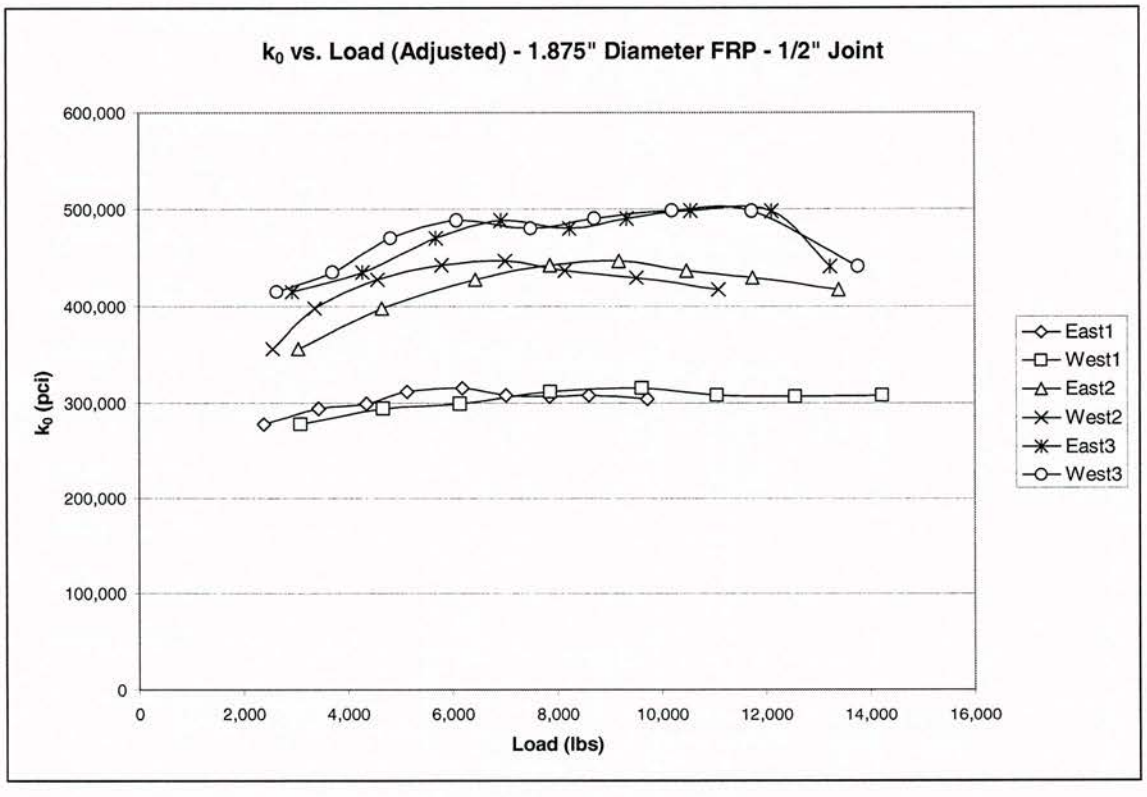

Figure A.30. k_0 plots, round GFRP, 1/2-inch joint, adjusted loads

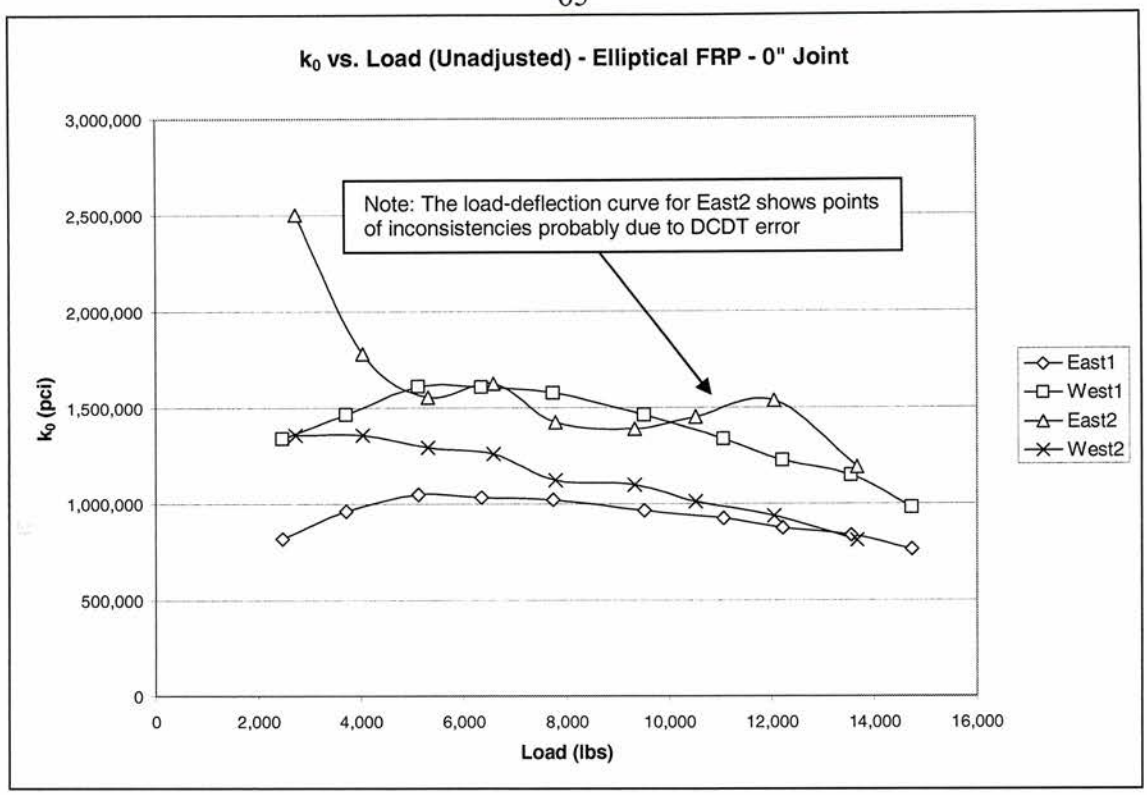

Figure A.31. k_0 plots, elliptical GFRP, 0-inch joint, unadjusted loads

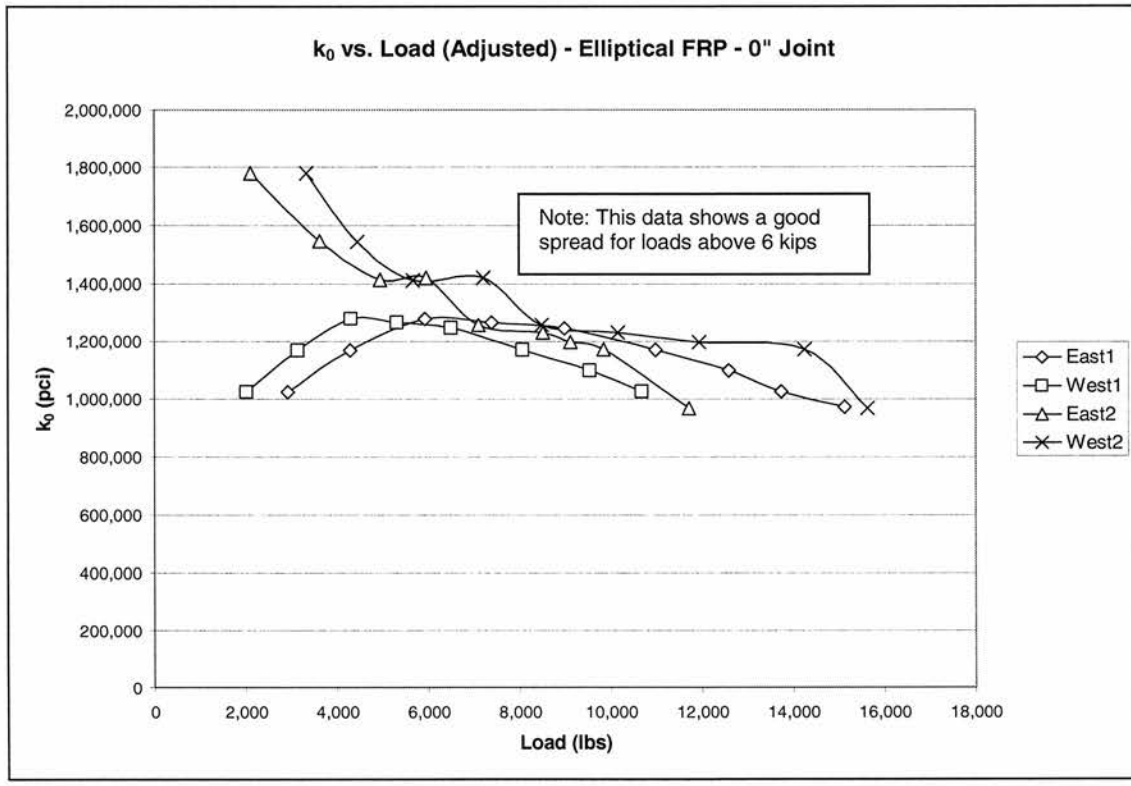

Figure A.32. k_0 plots, elliptical GFRP, 0-inch joint, adjusted loads

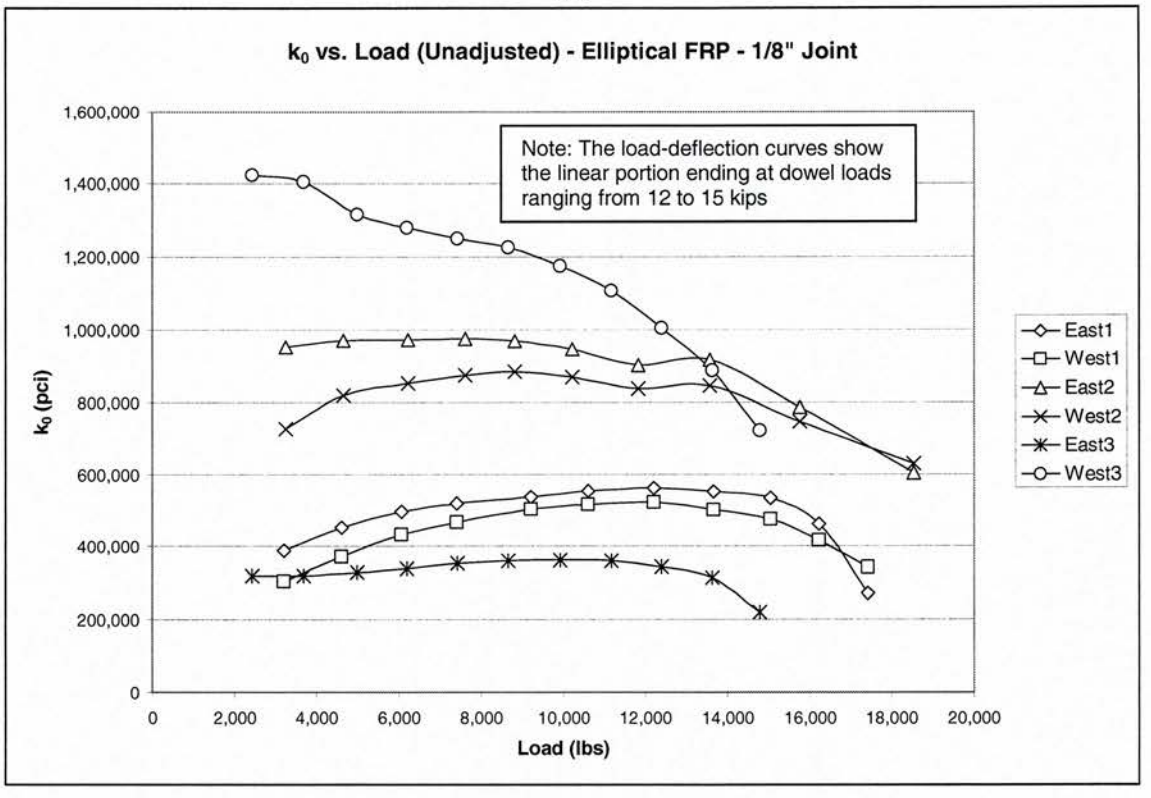

Figure A.33. k_0 plots, elliptical GFRP, 1/8-inch joint, unadjusted loads

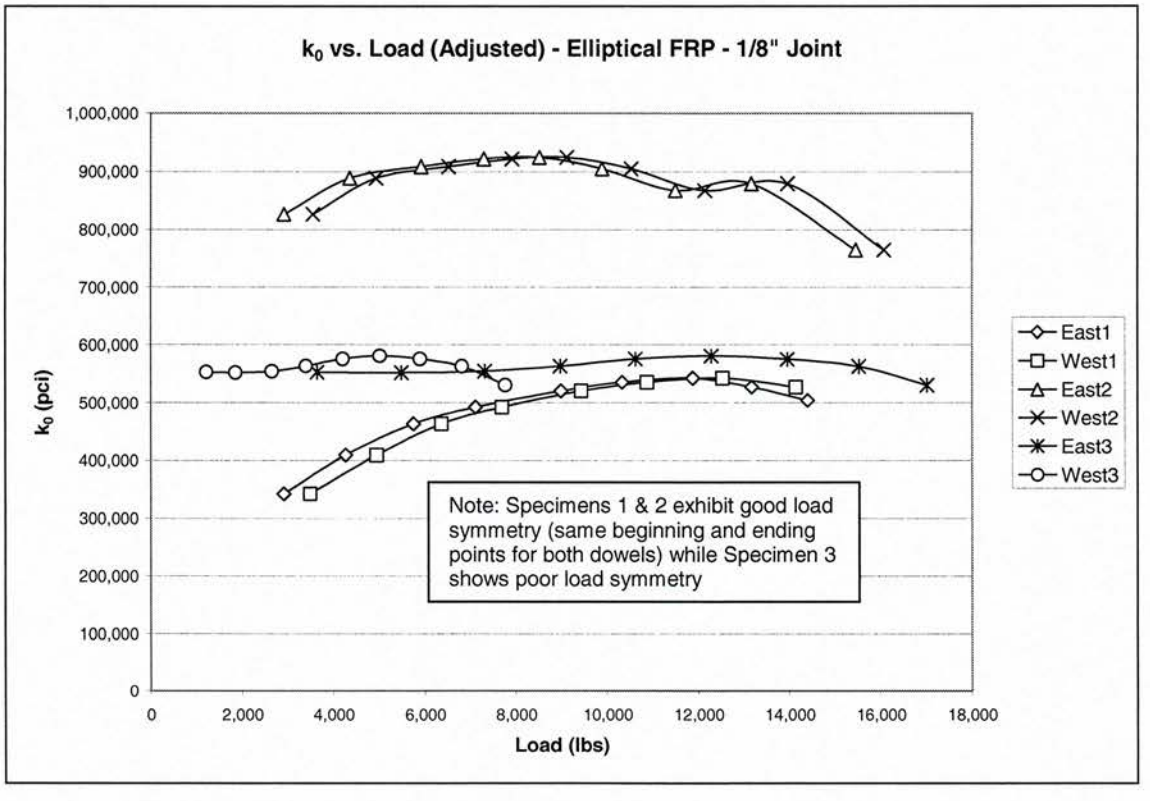

Figure A.34. k_0 plots, elliptical GFRP, 1/8-inch joint, adjusted loads

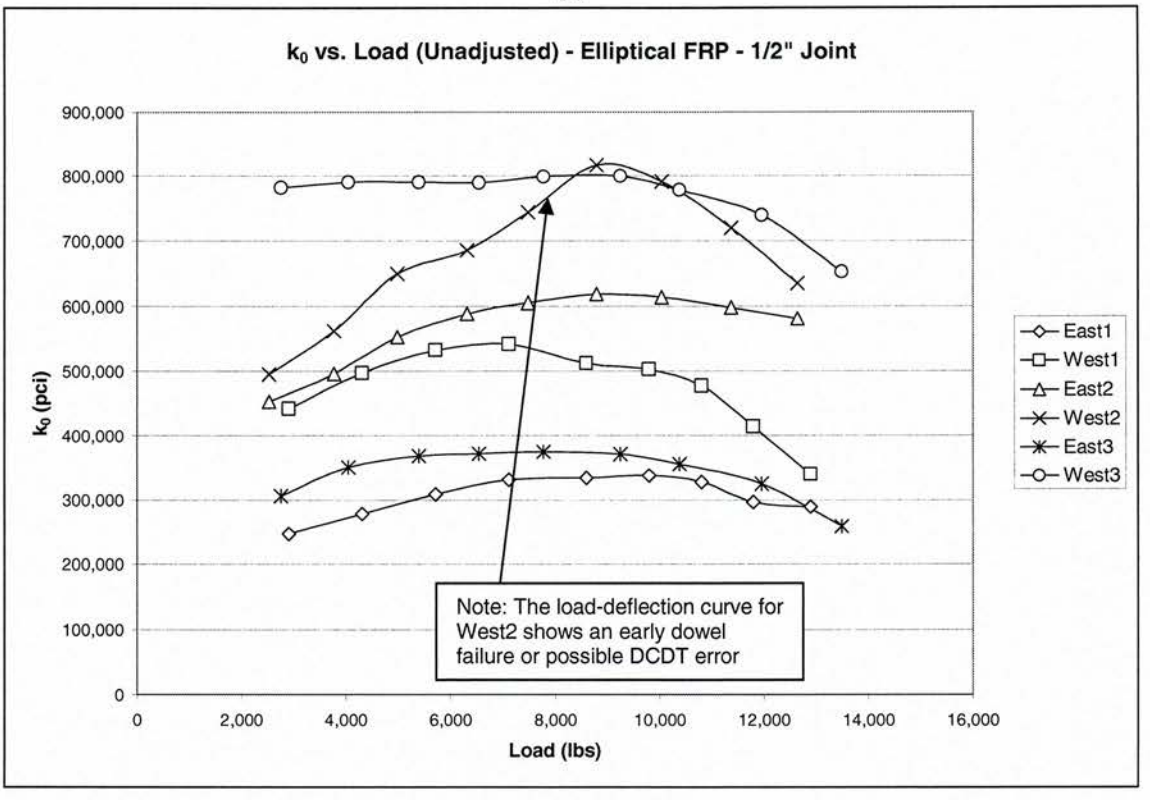

Figure A.35. k_0 plots, elliptical GFRP, 1/2-inch joint, unadjusted loads

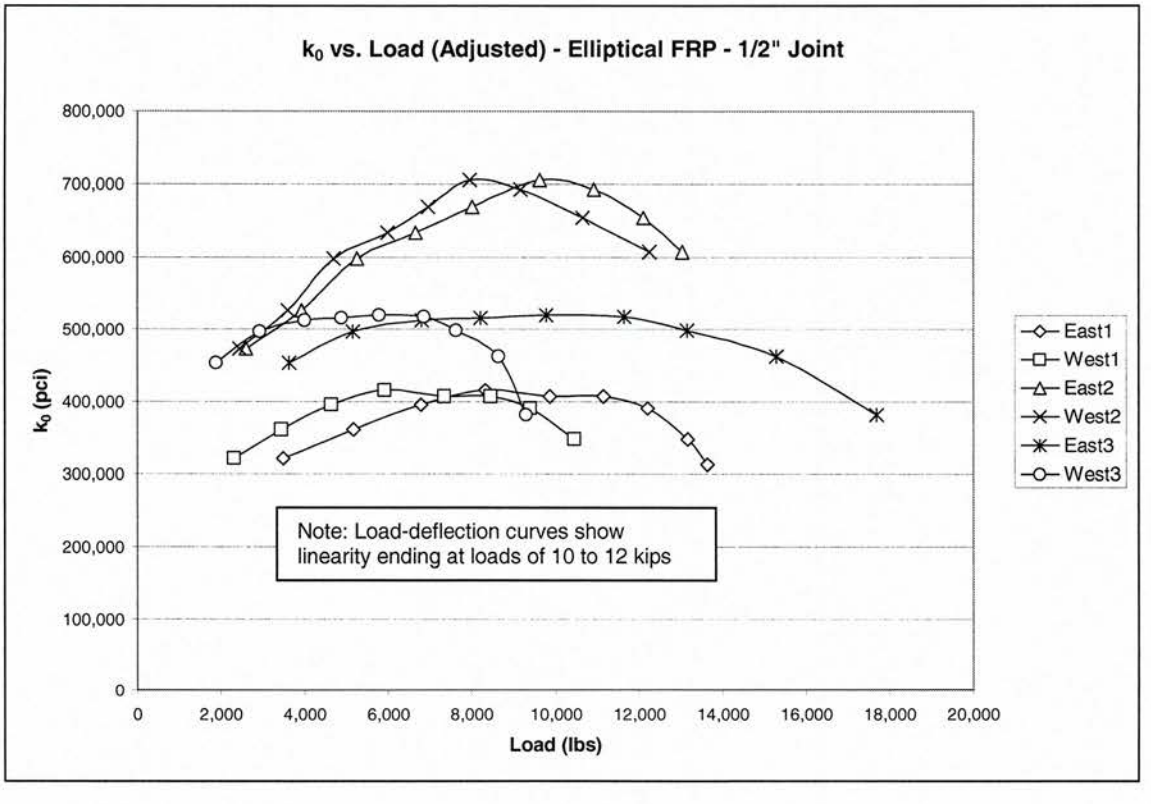

Figure A.36. k_0 plots, elliptical GFRP, 1/2-inch joint, adjusted loads

APPENDIX B. BUILDING SLAB DOWEL MODULUS OF DOWEL SUPPORT VS. LOAD DIAGRAMS

Figures B.1 through B.20 show k_0 vs. load plots for all 10 building slab dowel series of specimens where k_0 is determined as described in Chapter 3. There are three specimens for each series (30 specimens total) and two dowels per specimen for a total of six plots per figure. Each series has two plots: one with unadjusted loading and one with adjusted loading (see Section 4.1). The dowels are broken down by specimen number and specimen orientation (east or west).

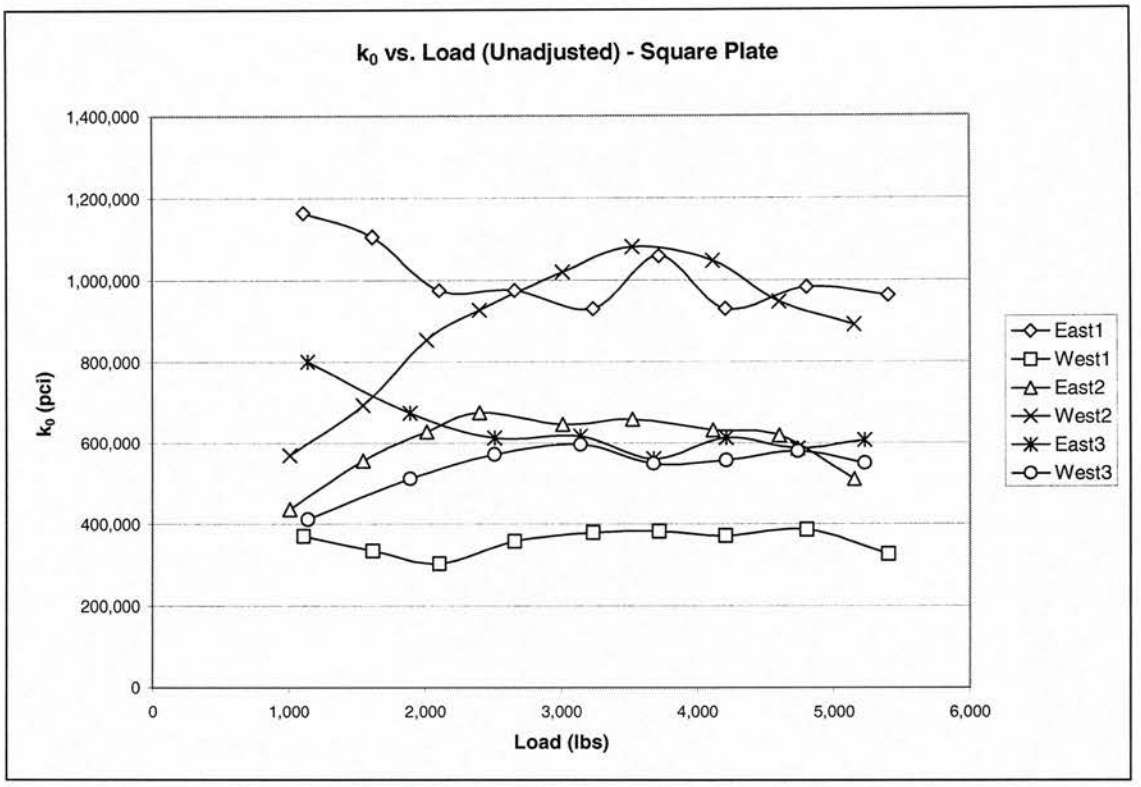

Figure B.1. k_0 plots, square plate, unadjusted loads

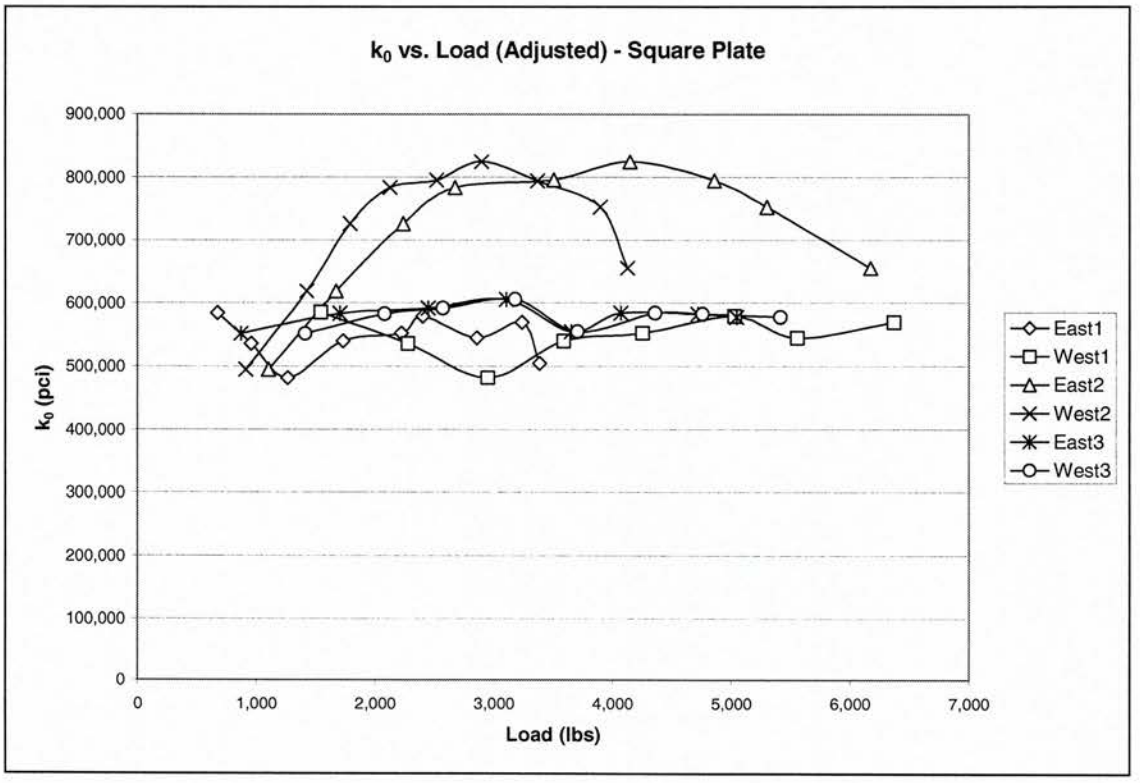

Figure B.2. k_0 plots, square plate, adjusted loads

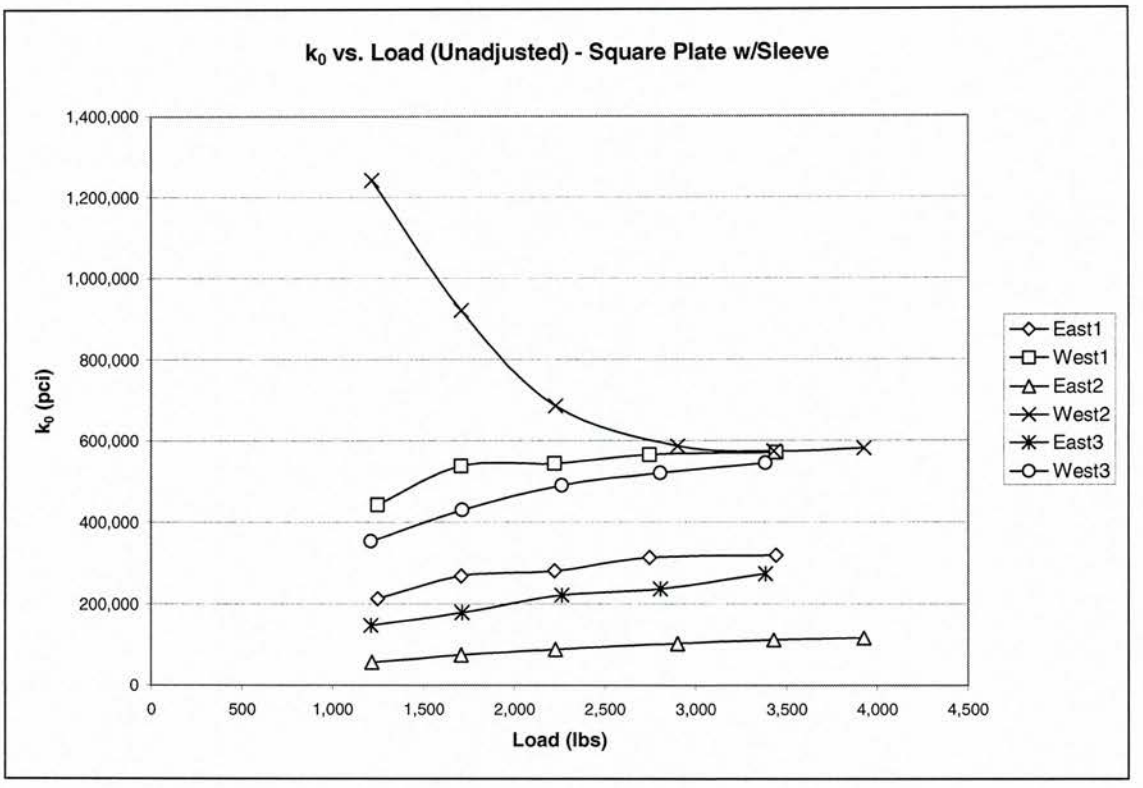

Figure B.3. k_0 plots, square plate w/sleeve, unadjusted loads

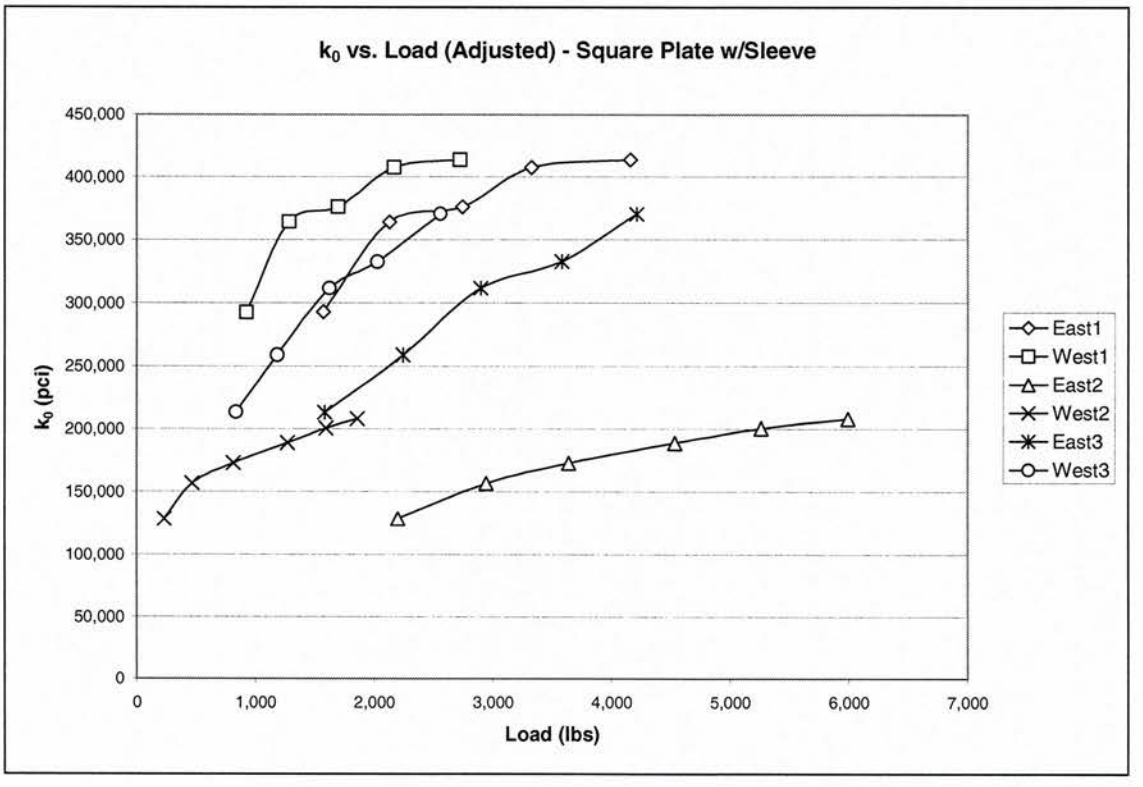

Figure B.4. k_0 plots, square plate w/sleeve, adjusted loads

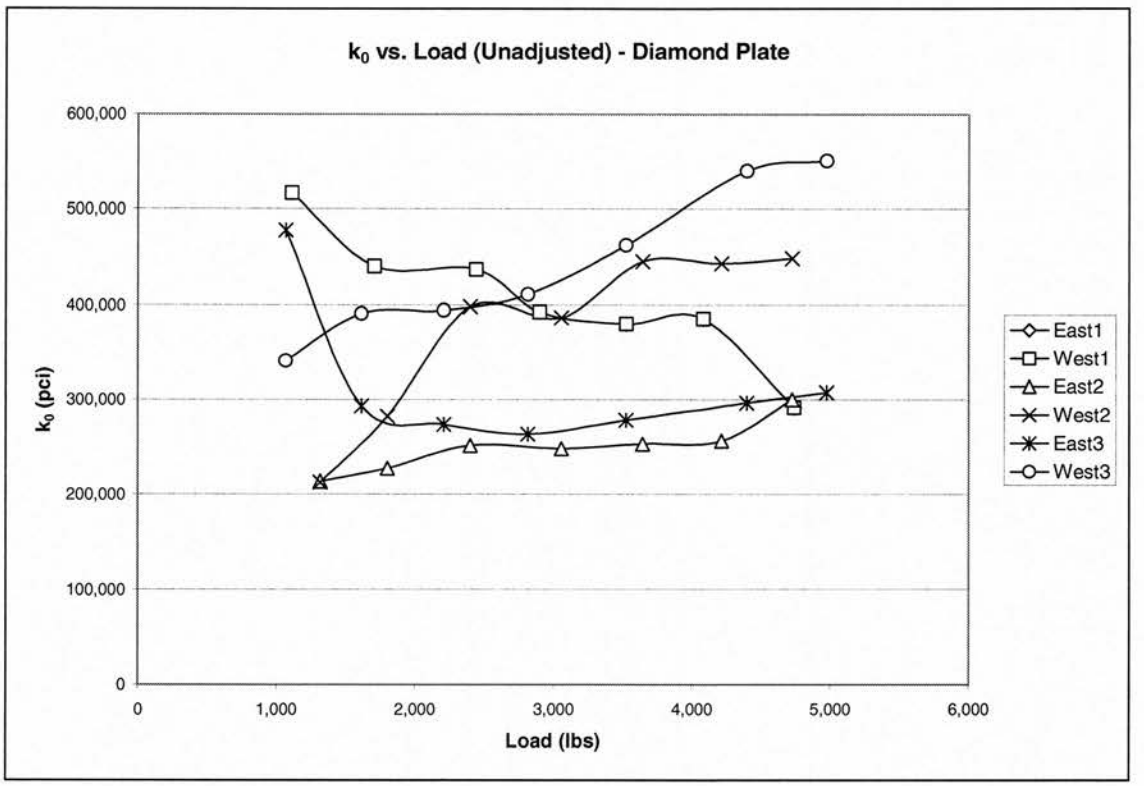

Figure B.5. k_0 plots, diamond plate, unadjusted loads

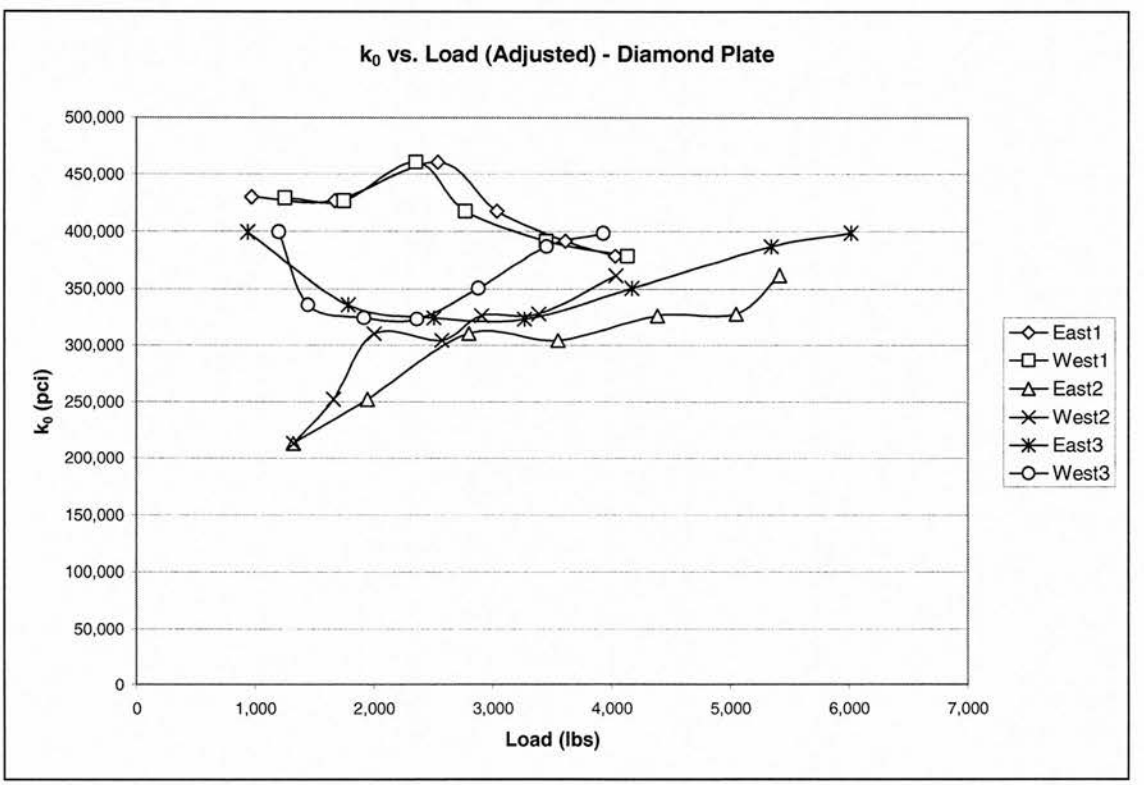

Figure B.6. k_0 plots, diamond plate, adjusted loads

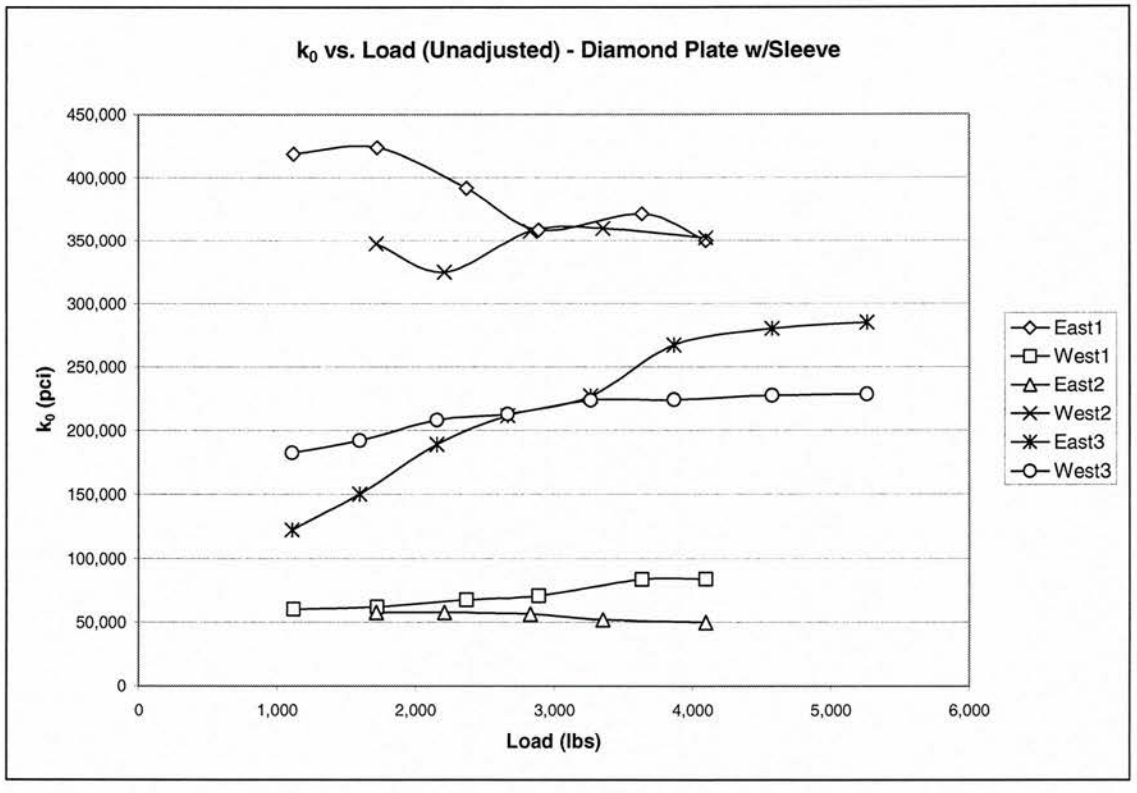

Figure B.7. k_0 plots, diamond plate w/sleeve, unadjusted loads

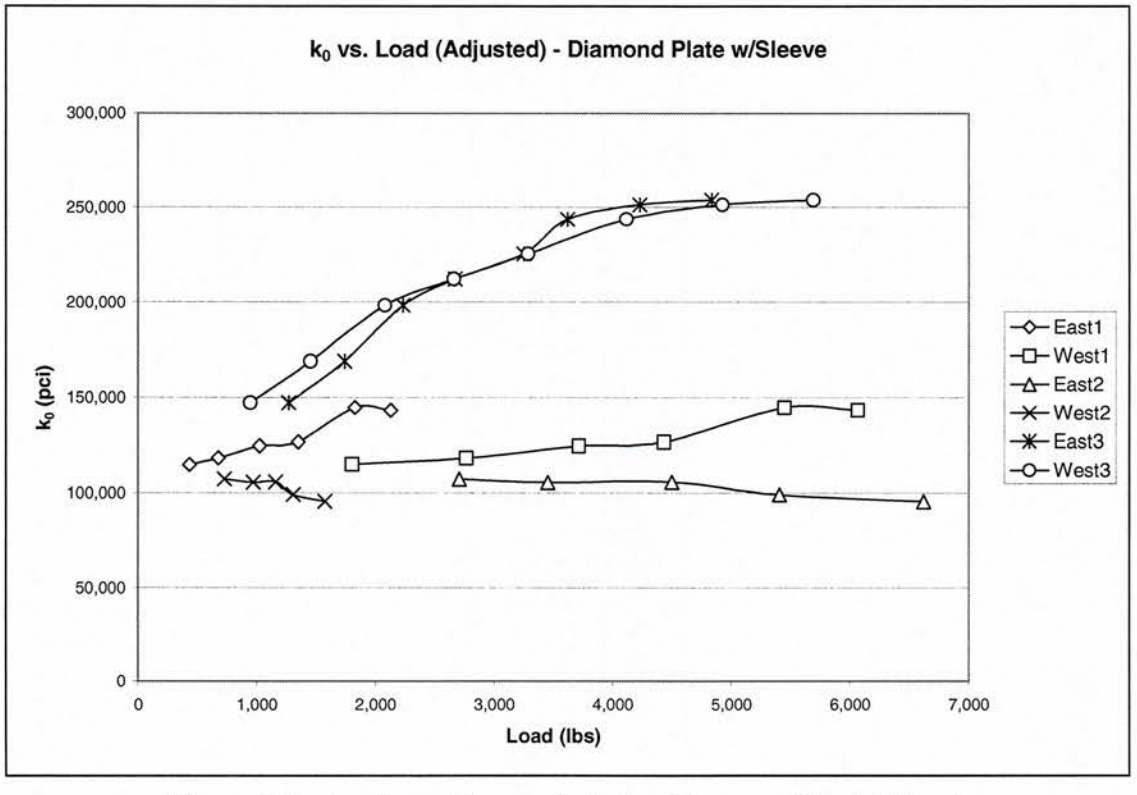

Figure B.8. k_0 plots, diamond plate w/sleeve, adjusted loads

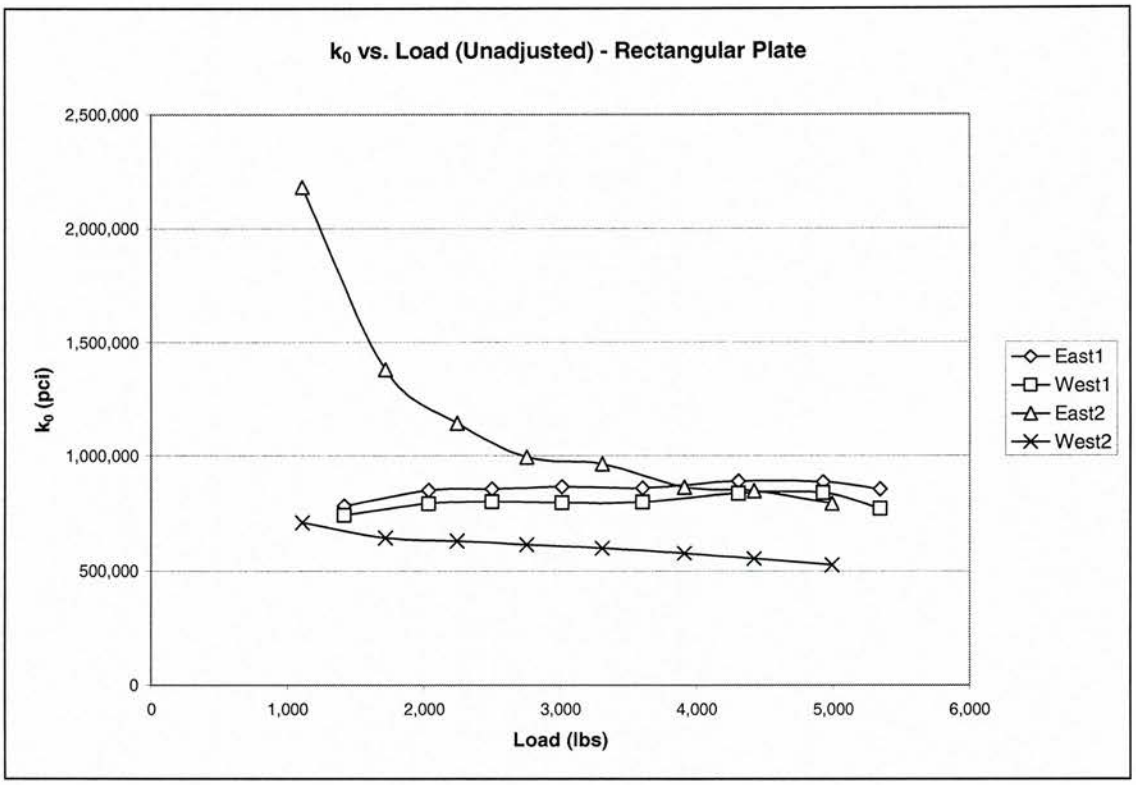

Figure B.9. k_0 plots, rectangular plate, unadjusted loads

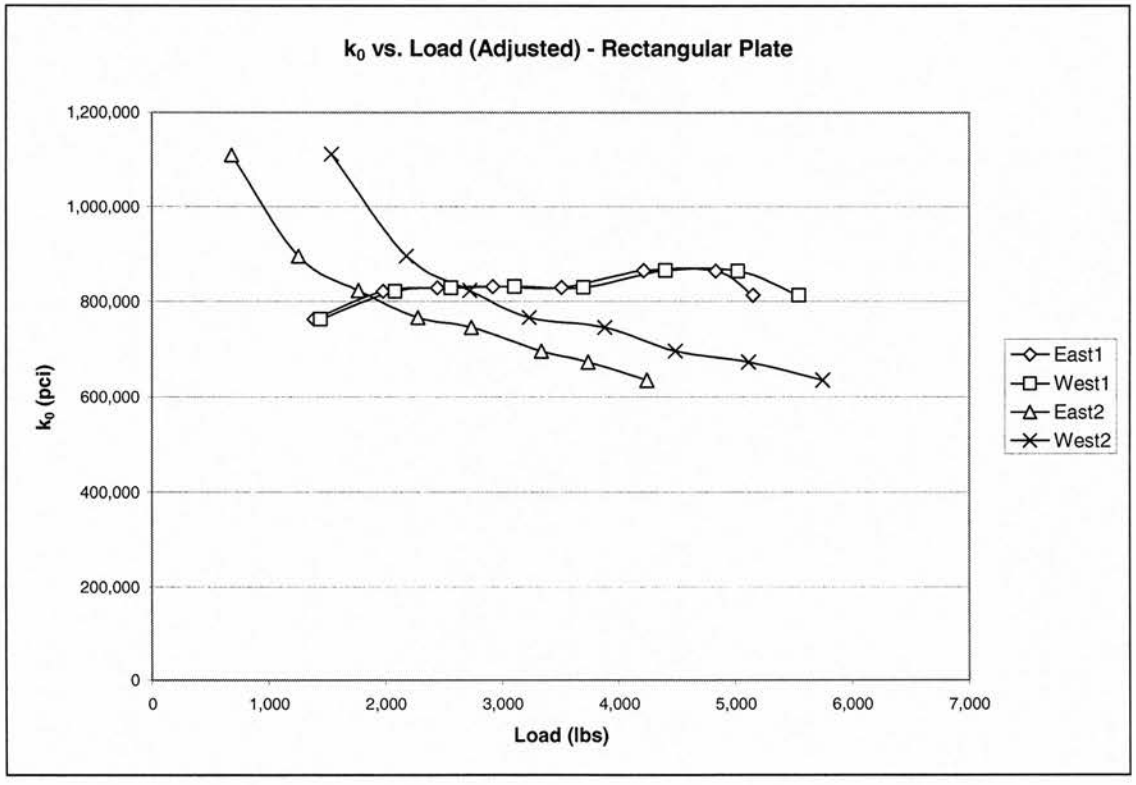

Figure B.10. k_0 plots, rectangular plate, adjusted loads

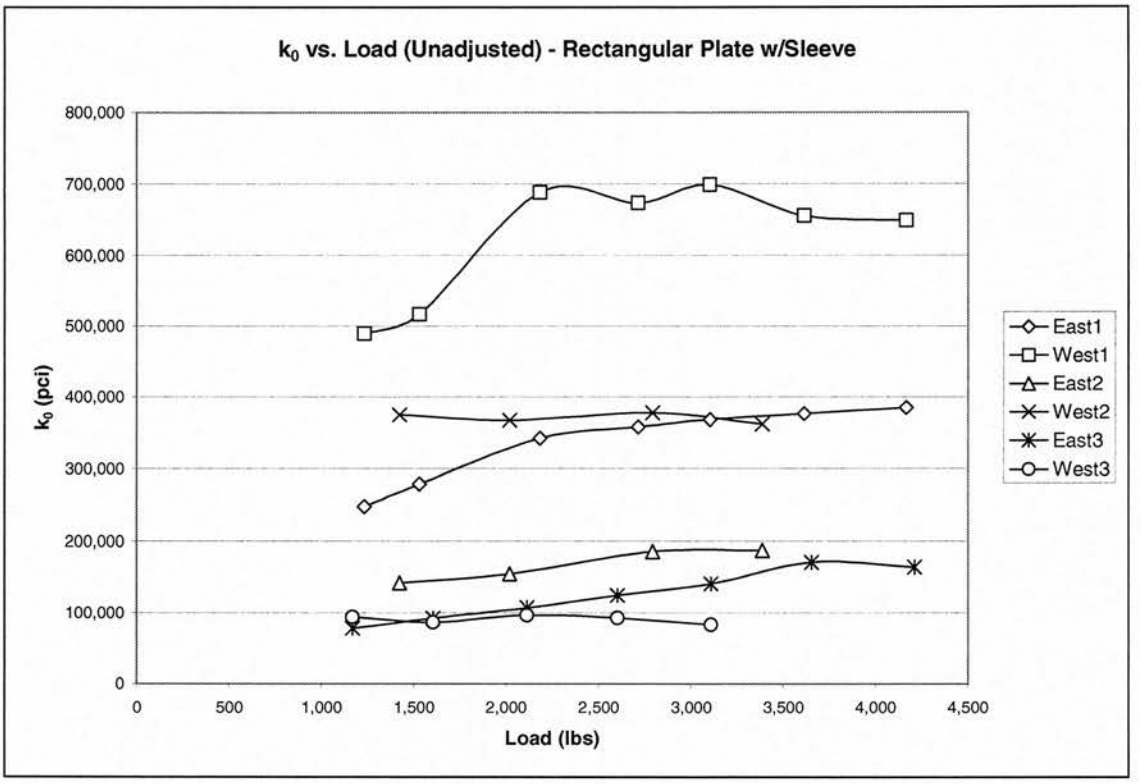

Figure B.11. k_0 plots, rectangular plate w/sleeve, unadjusted loads

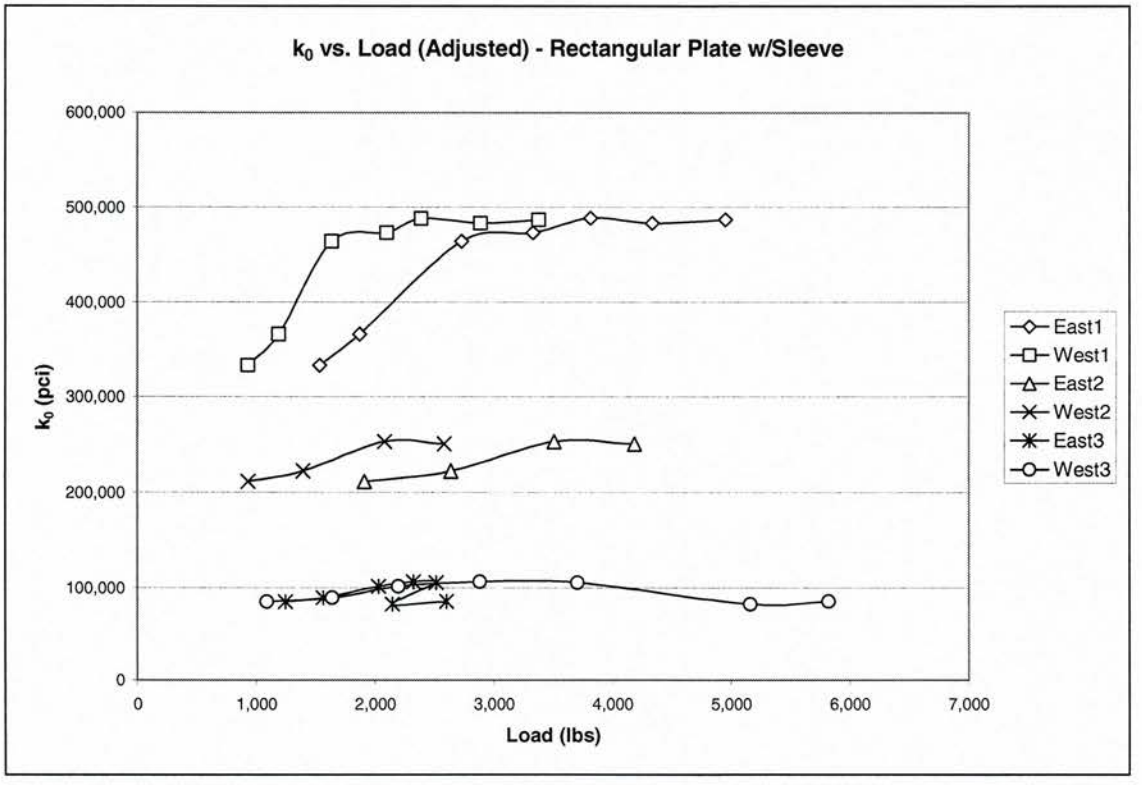

Figure B.12. k_0 plots, rectangular plate w/sleeve, adjusted loads

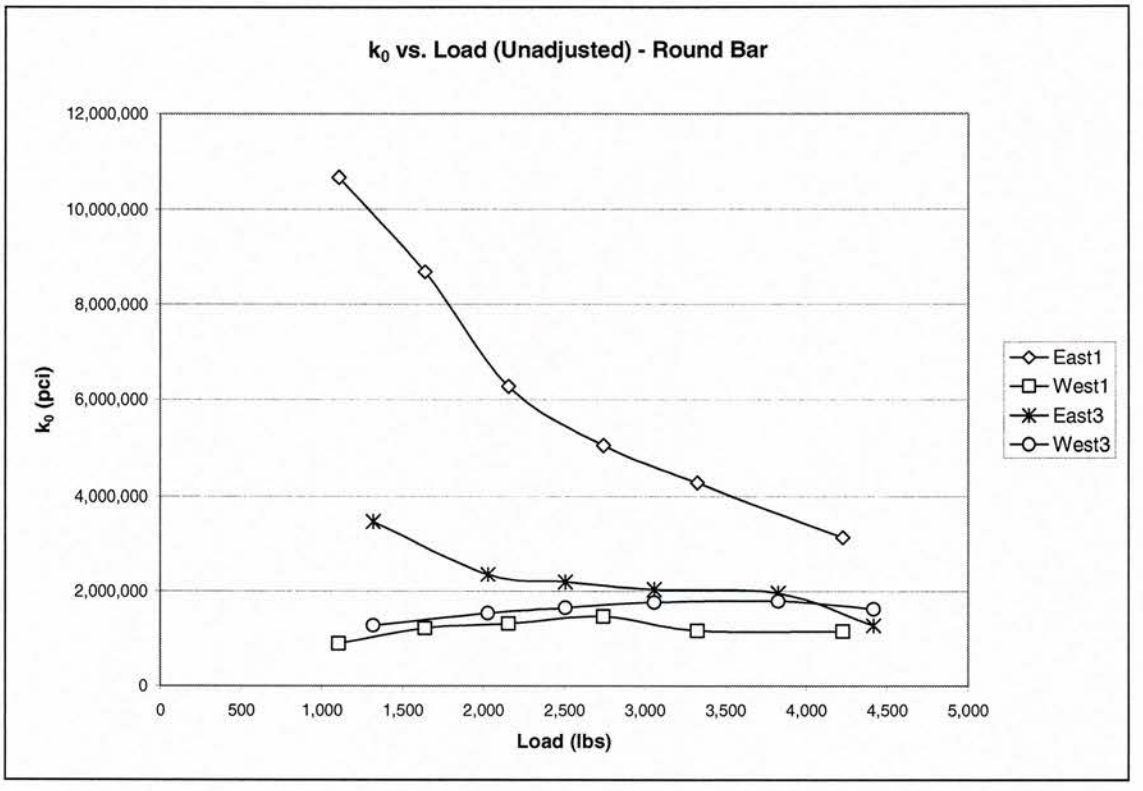

Figure B.13. k_0 plots, round bar, unadjusted loads

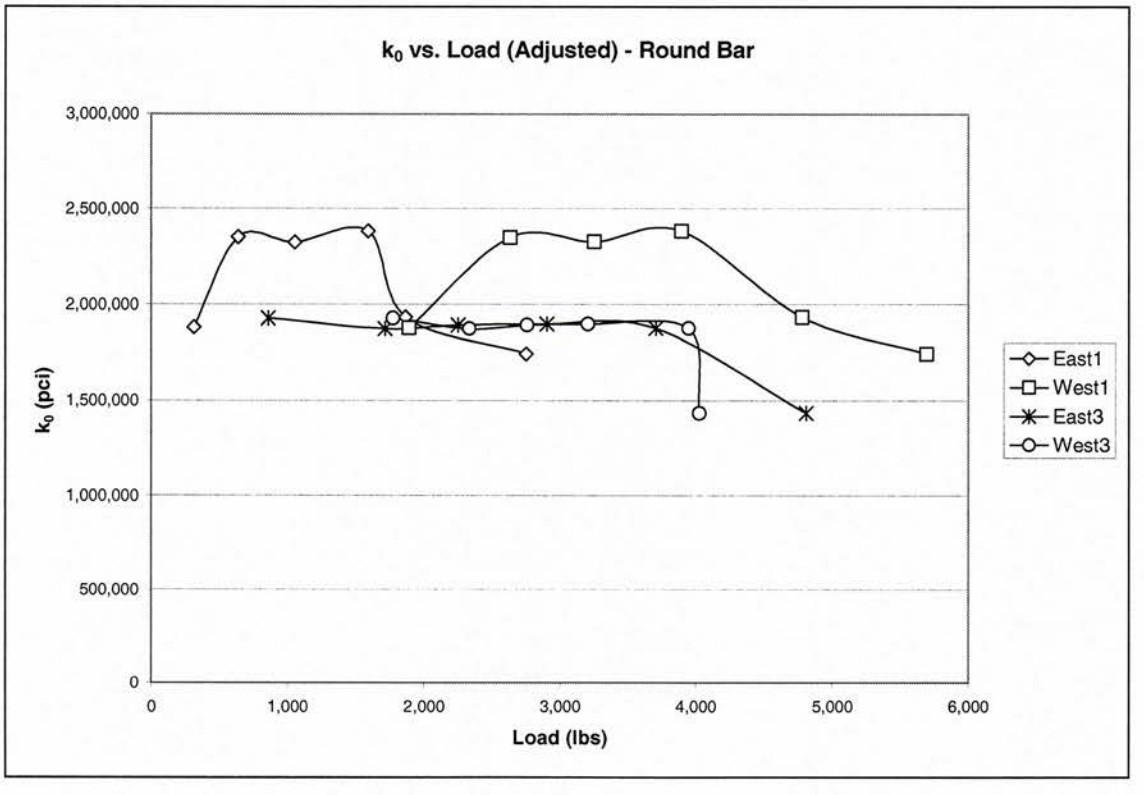

Figure B.14. k_0 plots, round bar, adjusted loads

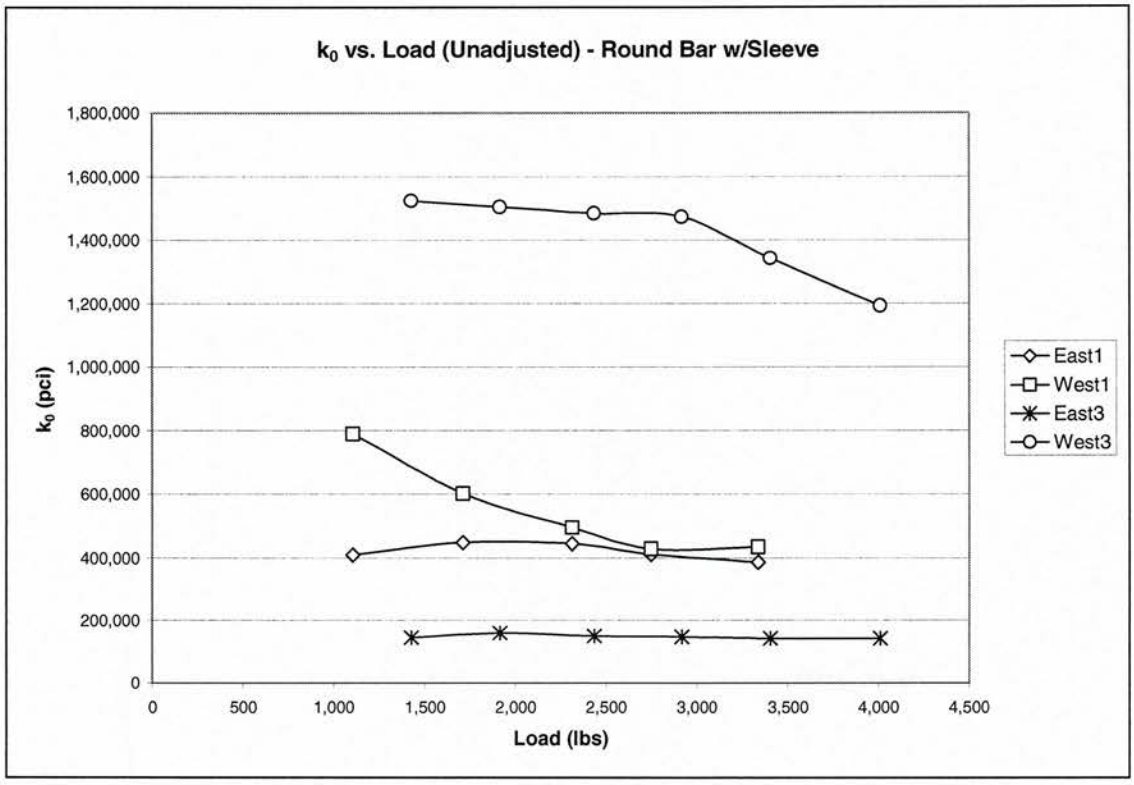

Figure B.15. k_0 plots, round bar w/sleeve, unadjusted loads

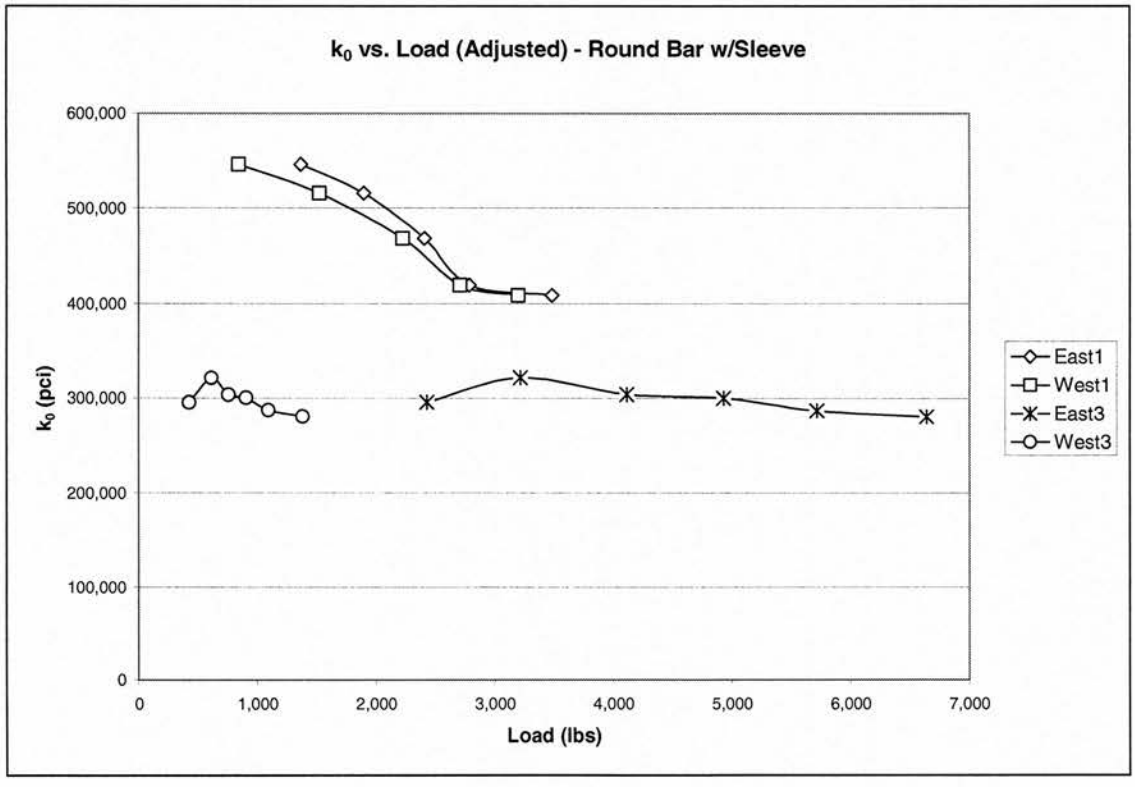

Figure B.16. k_0 plots, round bar w/sleeve, adjusted loads

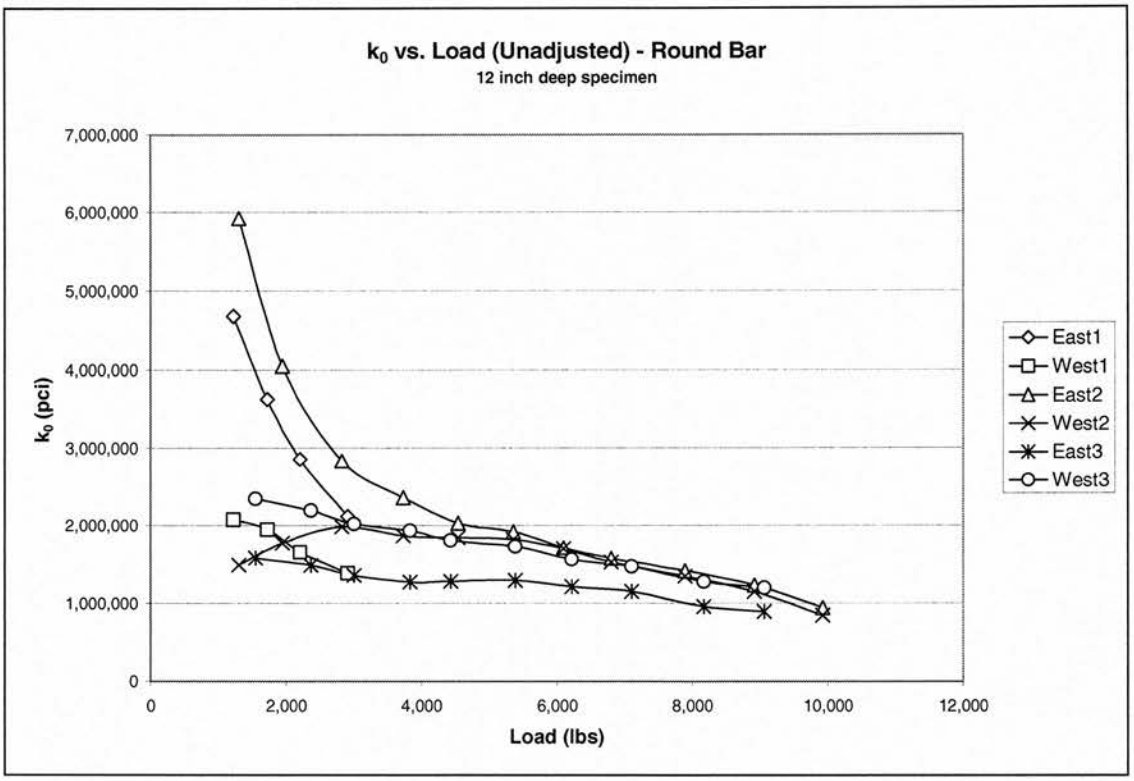

Figure B.17. k_0 plots, round bar (12-inch deep specimen), unadjusted loads

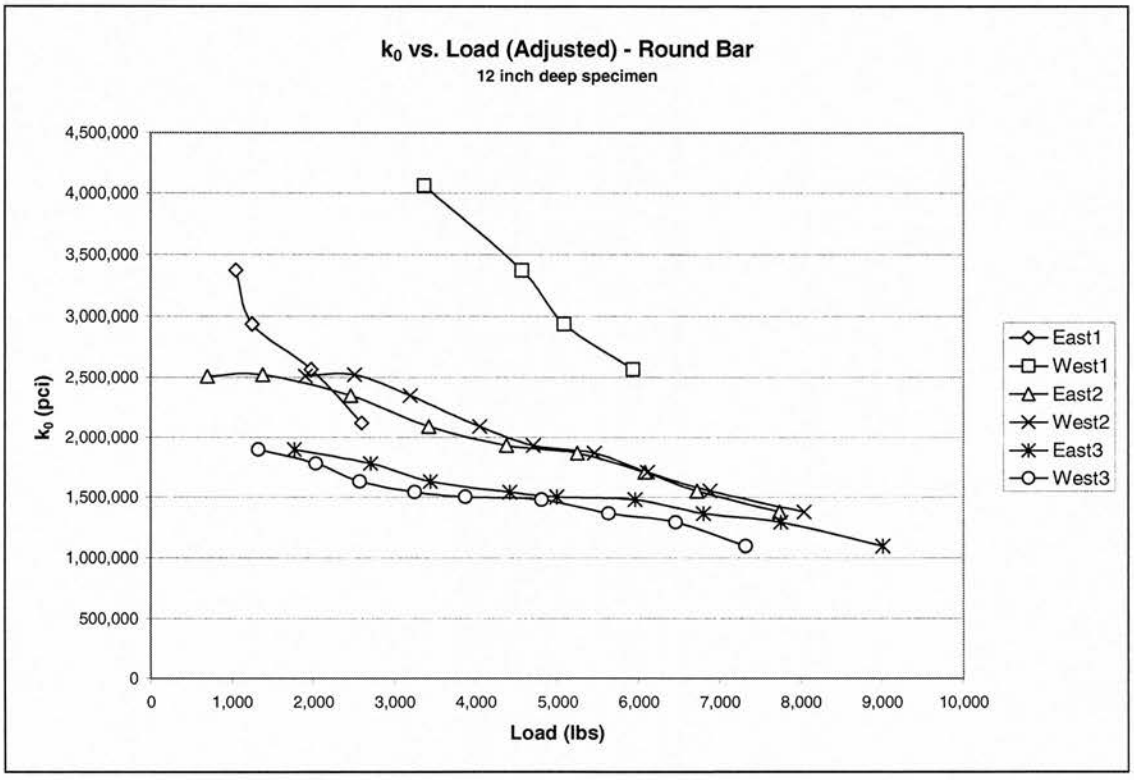

Figure B.18. k_0 plots, round bar (12-inch deep specimen), adjusted loads

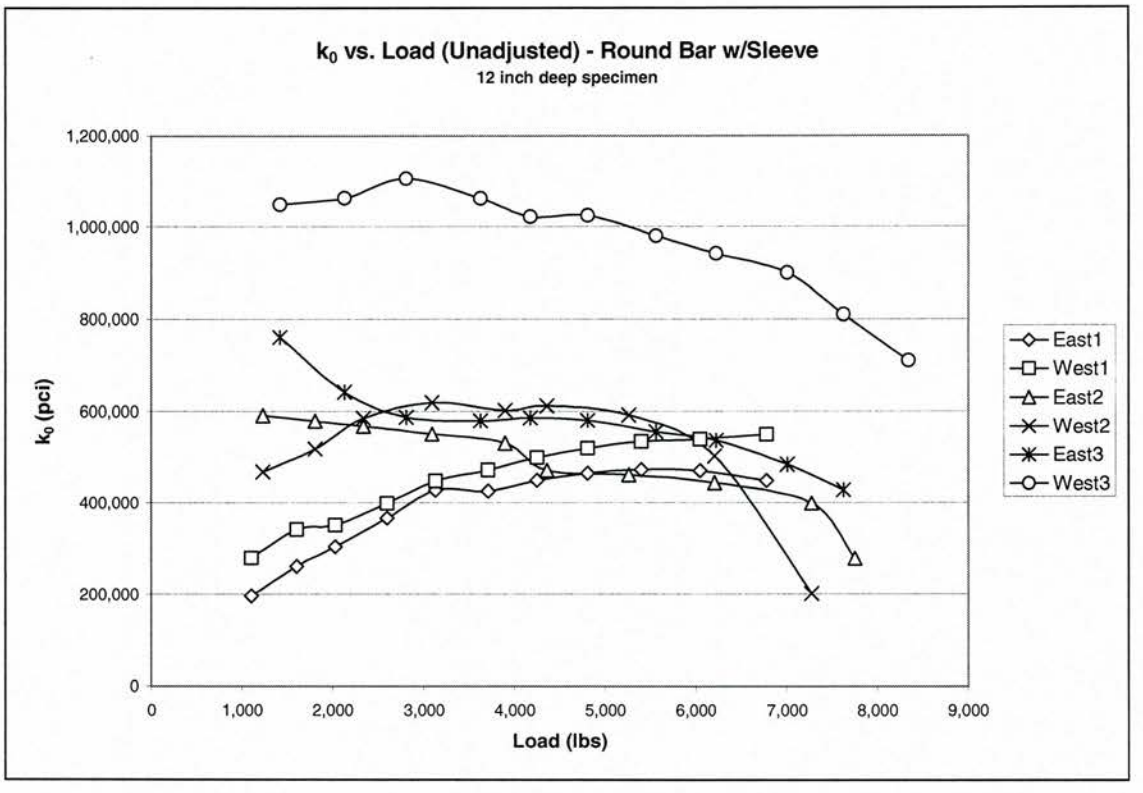

Figure B.19. k_0 plots, round bar w/sleeve (12-inch deep specimen), unadjusted loads

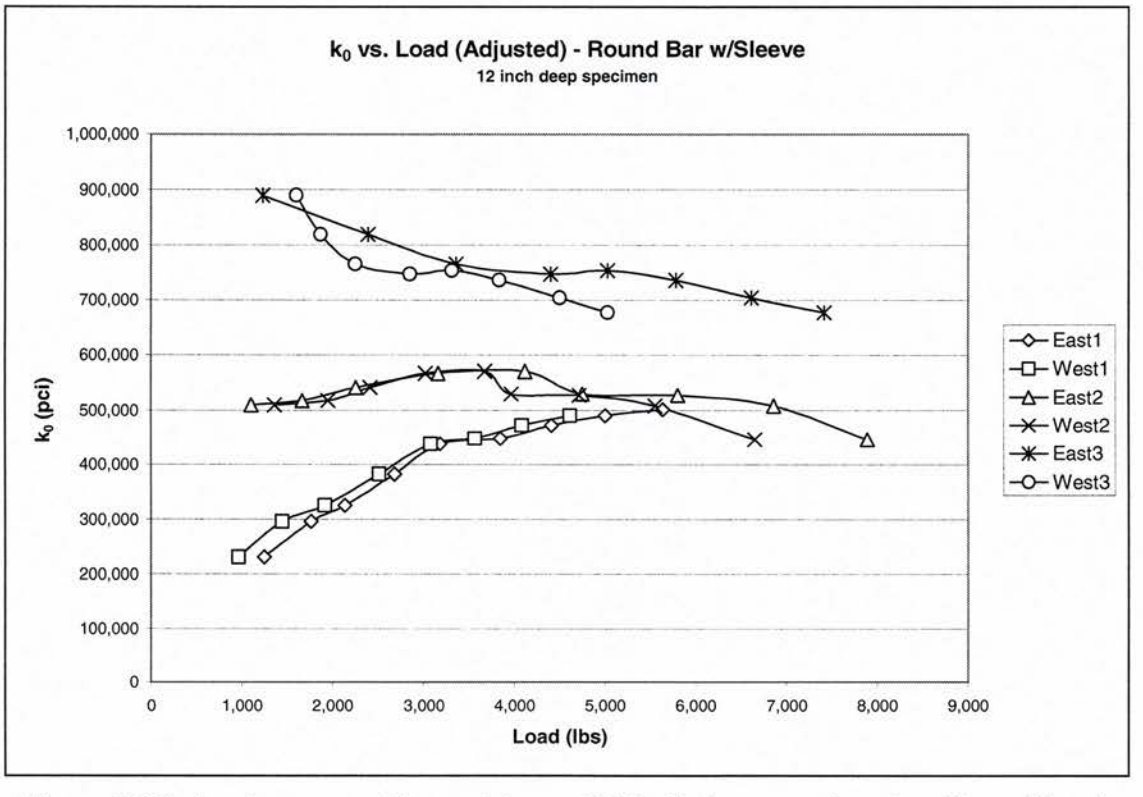

Figure B.20. k_0 plots, round bar w/sleeve (12-inch deep specimen), adjusted loads

APPENDIX C. HIGHWAY DOWEL MOMENT DIAGRAMS: THEORETICAL AND STRAIN-GAGE MEASURED

Figures C.1 through C.16 show moments along the length of the dowel. Each figure contains two moment graphs: the measured moment and the theoretical moment. The measured moment is the moment calculated from the strain gages (see Section 3.4) where the magnitude of the strains at the top and bottom of the dowel at a point are averaged and the average strain is used to calculate the moment. The theoretical moment is the moment from Timoshenko's theory (*23*) shown in Equation 3.10. All the moment curves' signs (positive or negative moment) have been adjusted to show uniformity among the figures.

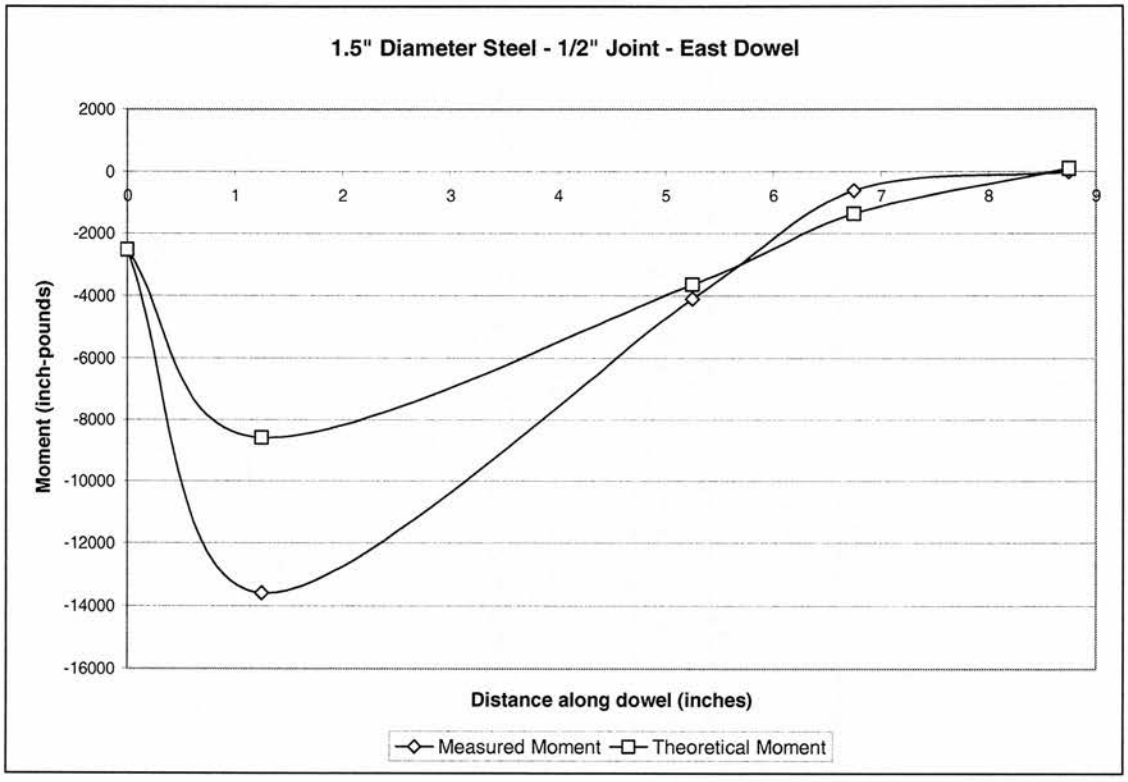

Figure C.1. Theoretical and measured moments, round steel specimen, east dowel, 1/2-inch joint

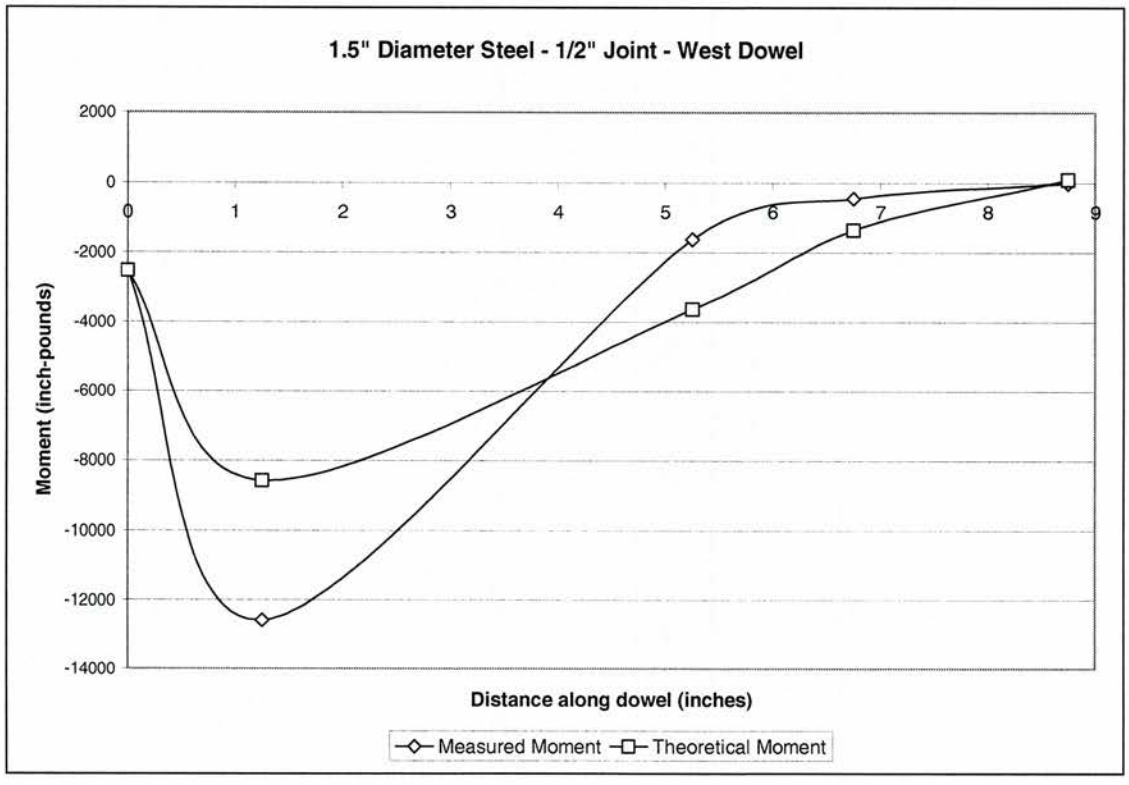

Figure C.2. Theoretical and measured moments, round steel specimen, west dowel, 1/2-inch joint

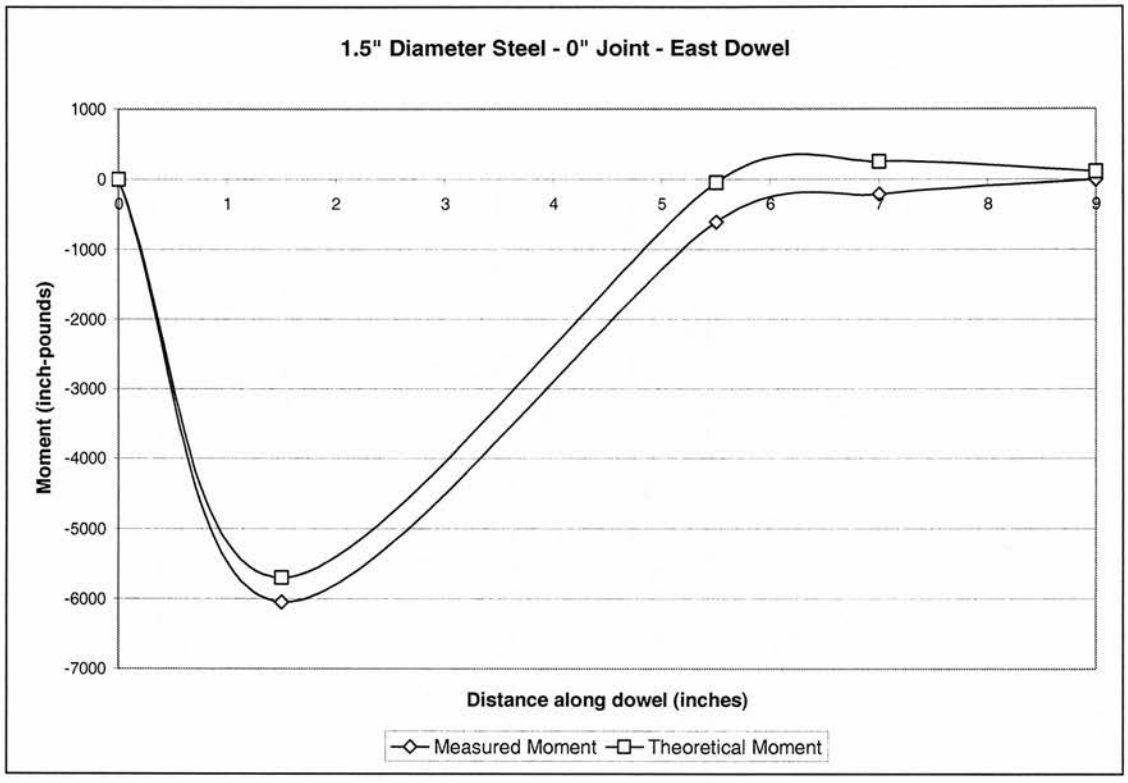

Figure C.3. Theoretical and measured moments, round steel specimen, east dowel, 0-inch joint

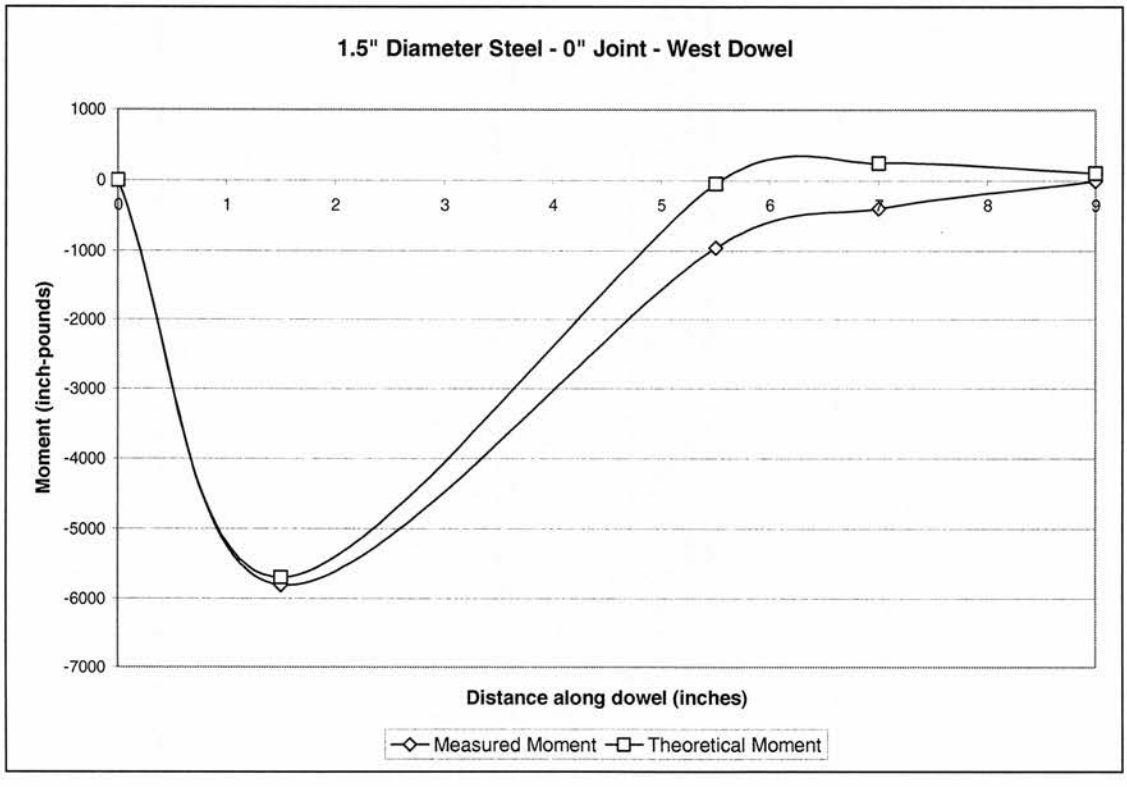

Figure C.4. Theoretical and measured moments, round steel specimen, west dowel, 0-inch joint

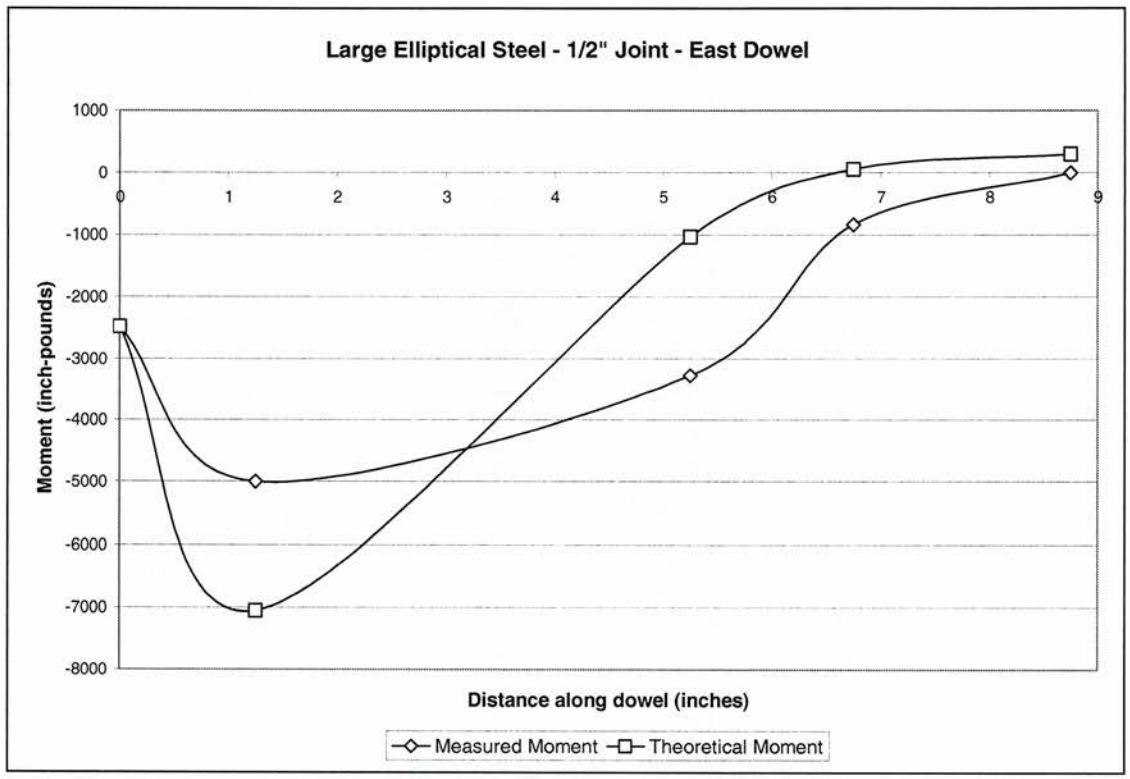

Figure C.5. Theoretical and measured moments, large elliptical steel specimen, east dowel, 1/2-inch joint

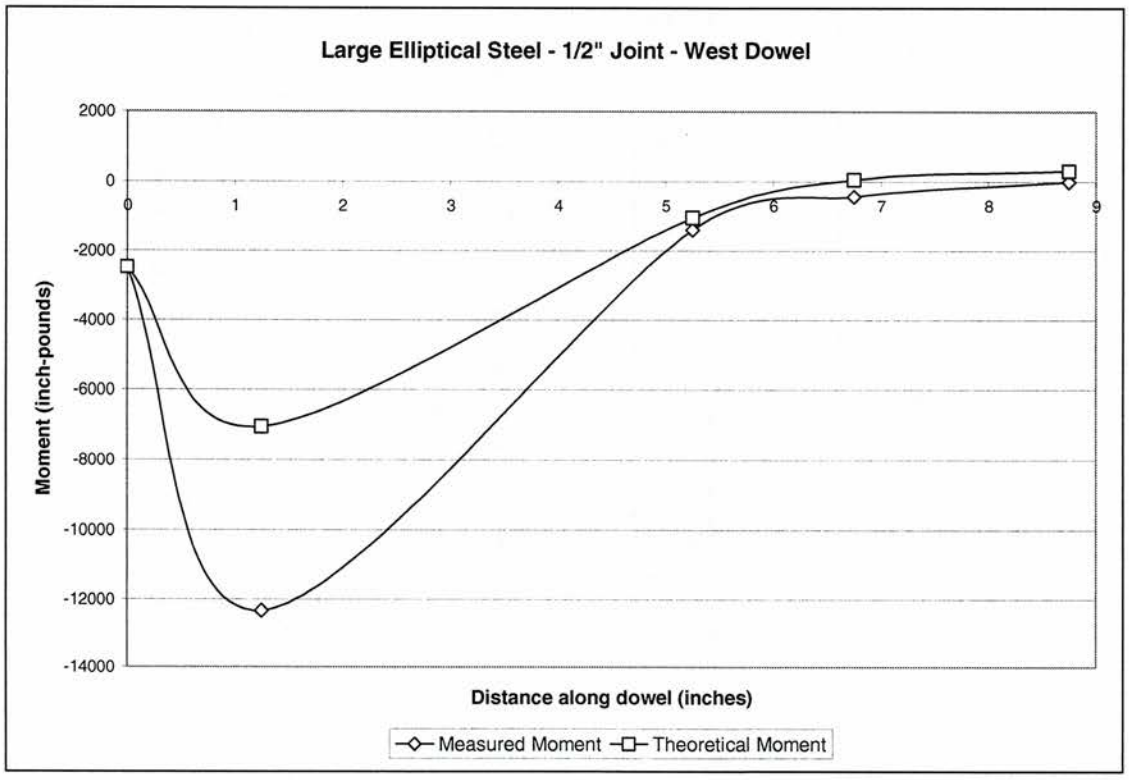

Figure C.6. Theoretical and measured moments, large elliptical steel specimen, west dowel, 1/2-inch joint

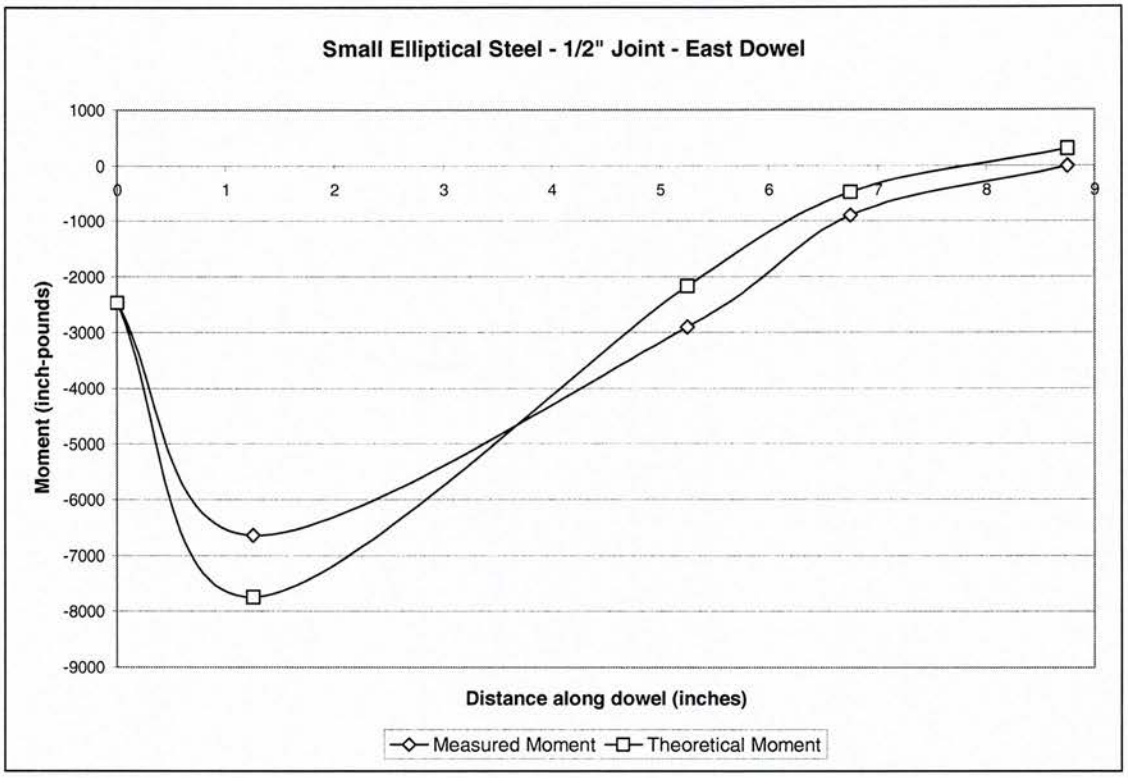

Figure C.7. Theoretical and measured moments, small elliptical steel specimen, east dowel, 1/2-inch joint

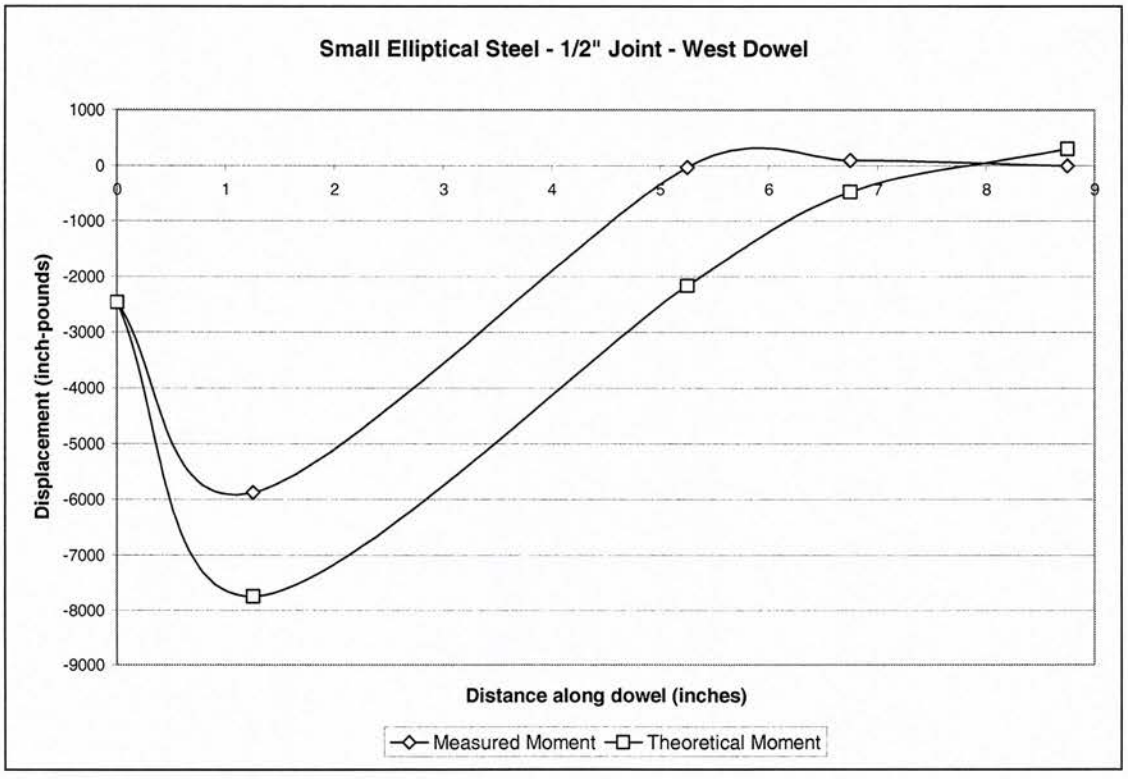

Figure C.8. Theoretical and measured moments, small elliptical steel specimen, west dowel, 1/2-inch joint

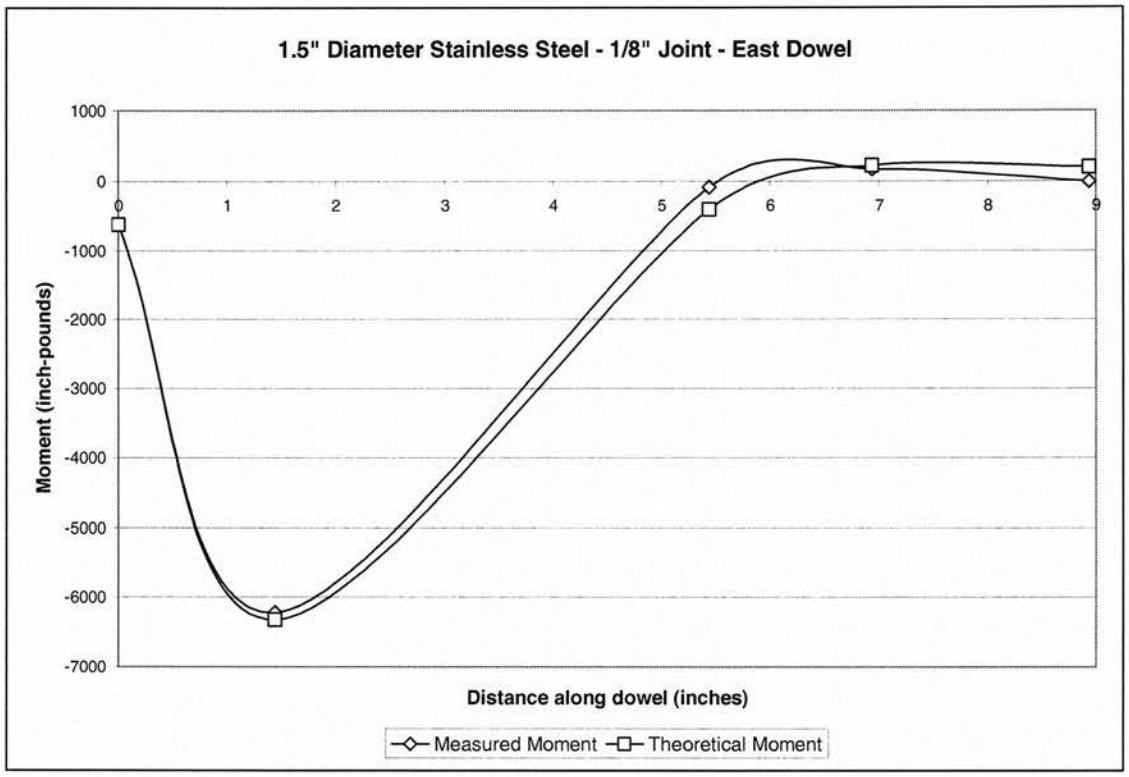

Figure C.9. Theoretical and measured moments, round stainless steel specimen, east dowel, 1/8-inch joint

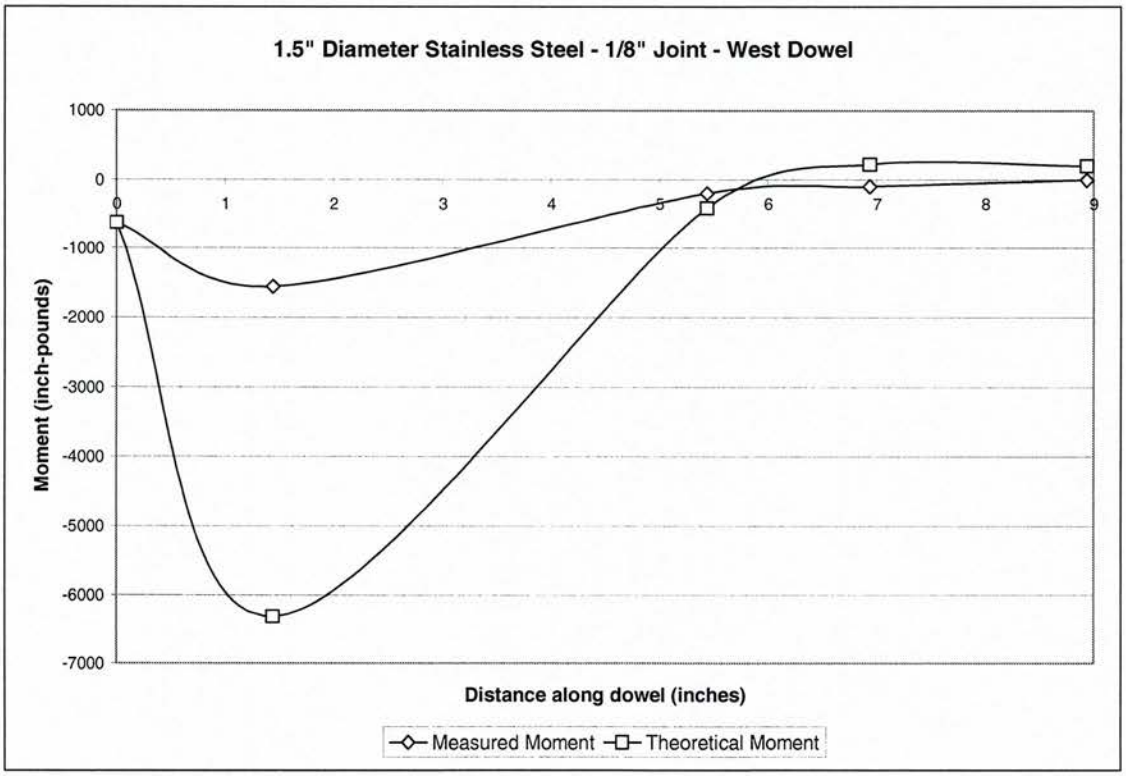

Figure C.10. Theoretical and measured moments, round stainless steel specimen, west dowel, 1/8-inch joint

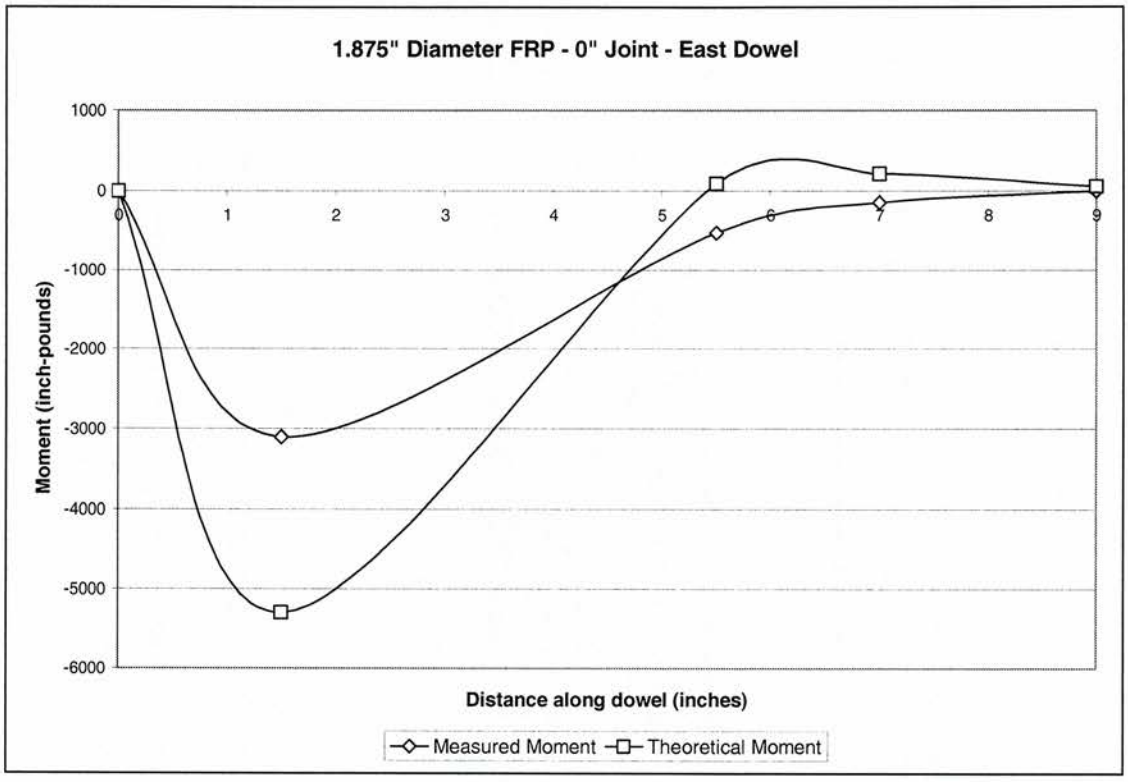

Figure C.11. Theoretical and measured moments, round GFRP specimen, east dowel, 0-inch joint

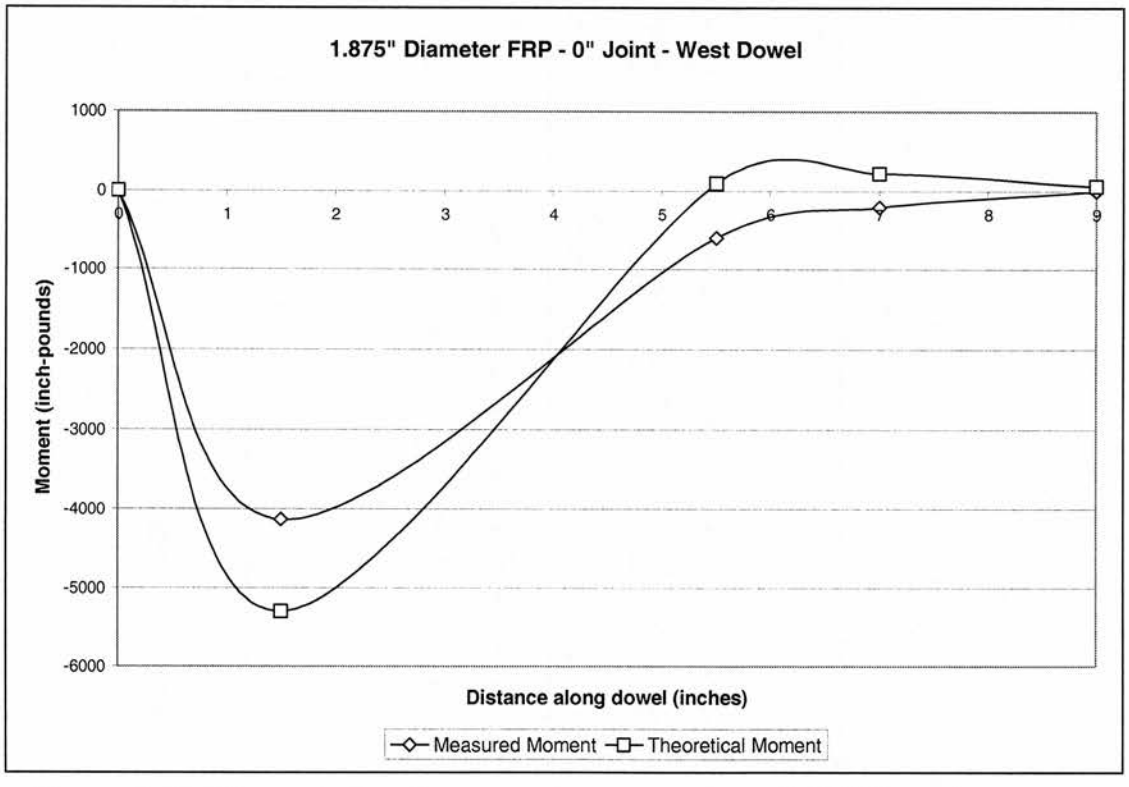

Figure C.12. Theoretical and measured moments, round GFRP specimen, west dowel, 0-inch joint

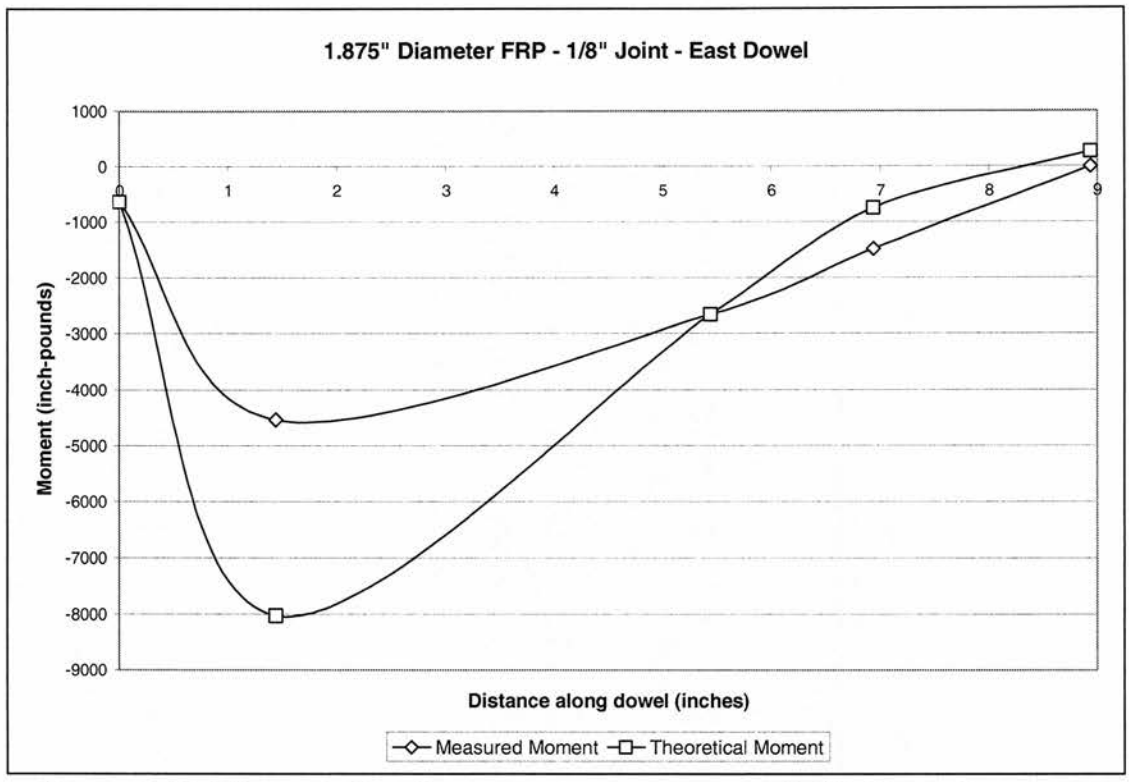

Figure C.13. Theoretical and measured moments, round GFRP specimen, east dowel, 1/8-inch joint

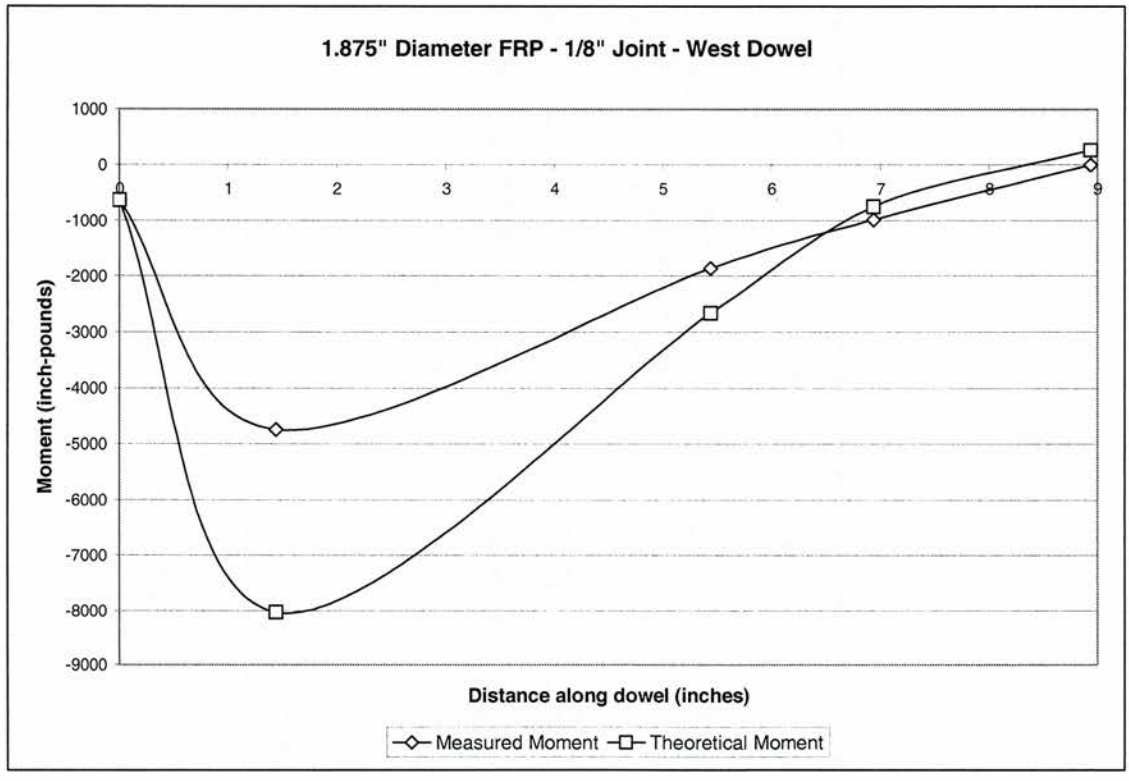

Figure C.14. Theoretical and measured moments, round GFRP specimen, west dowel, 1/8-inch joint

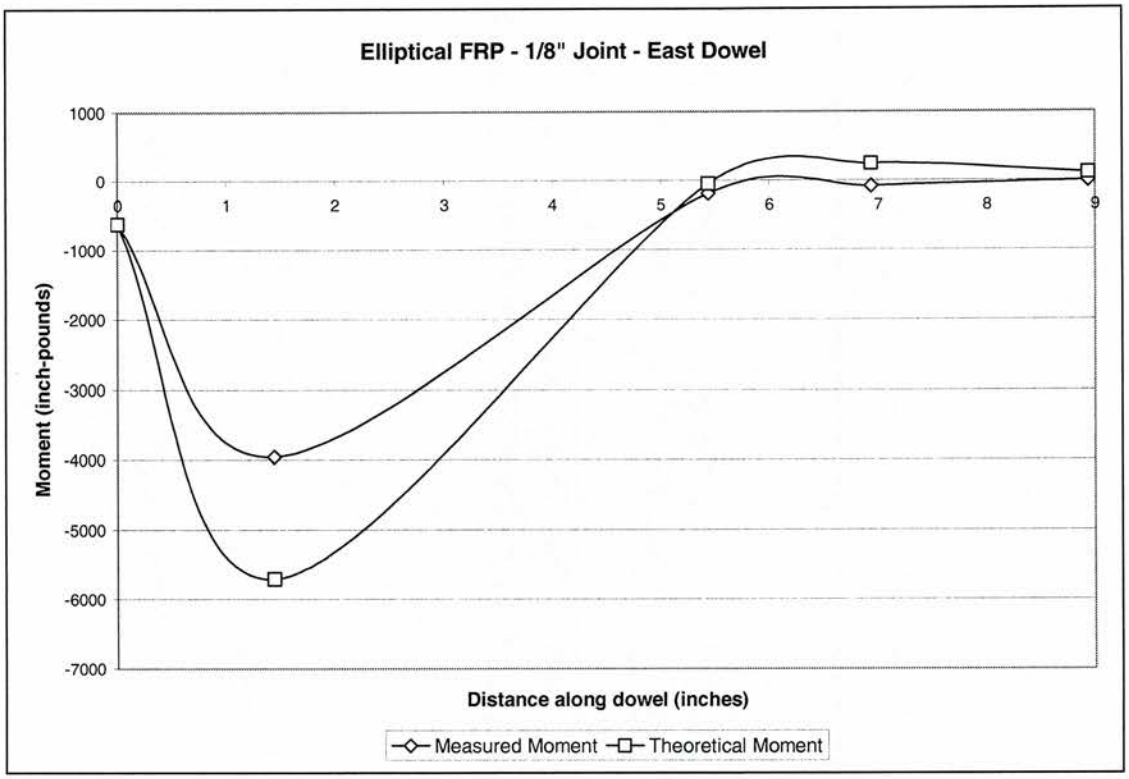

Figure C.15. Theoretical and measured moments, elliptical GFRP specimen, east dowel, 1/8-inch joint

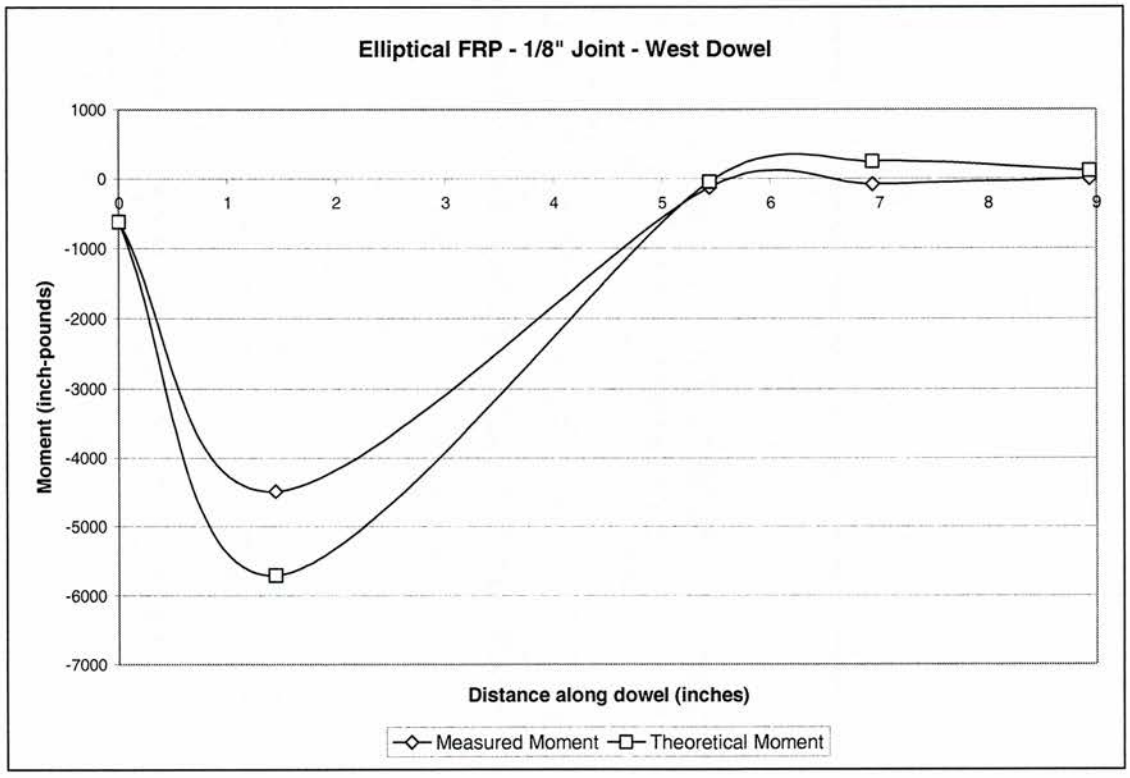

Figure C.16. Theoretical and measured moments, elliptical GFRP specimen, west dowel, 1/8-inch joint

APPENDIX D. HIGHWAY DOWEL DISPLACEMENT DIAGRAMS: THEORETICAL AND OBSERVED

Figures D.1 through D.8 show the theoretical displacement of the dowel along the length of the dowel and the observed displacement at the face of the joint, y_0. The theoretical displacement is from Timoshenko's theory (*23*) as shown in Equation 3.9. The observed y_0 is the y_0 calculated for the same load used to plot the theoretical displacement curve.

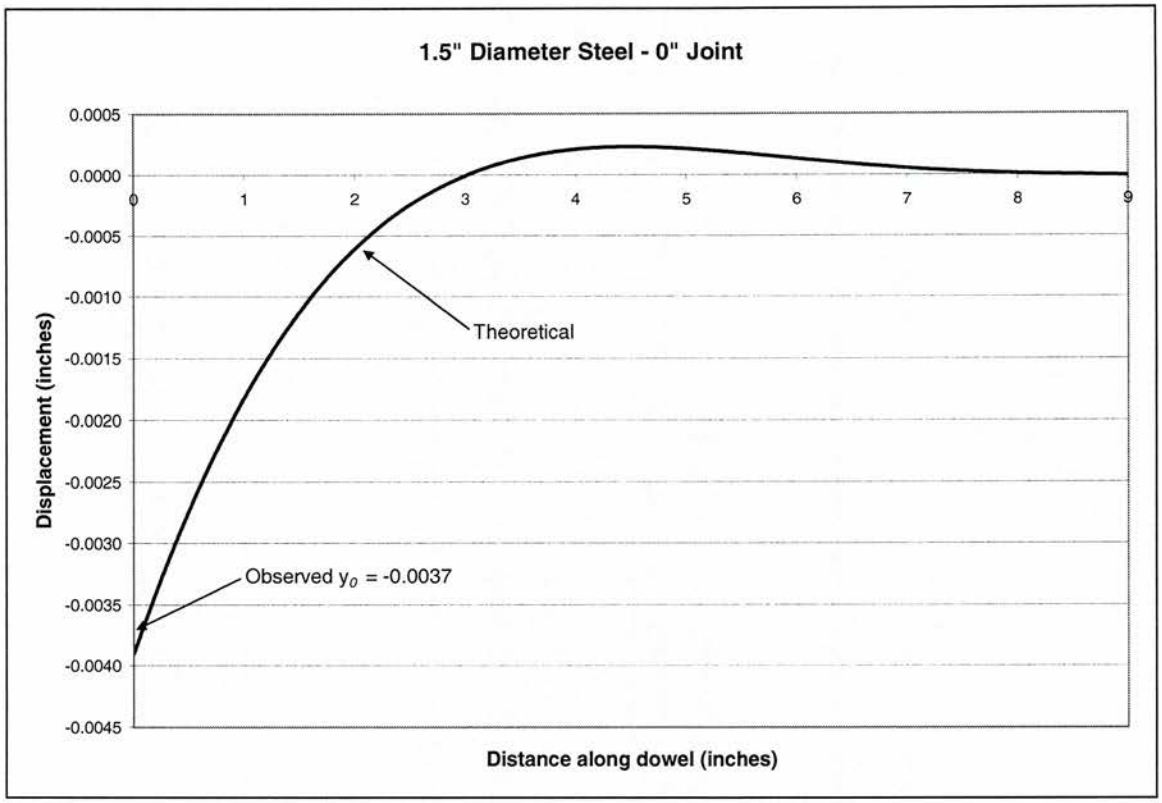

Figure D.1. Theoretical displacement of round steel dowel, 0-inch joint

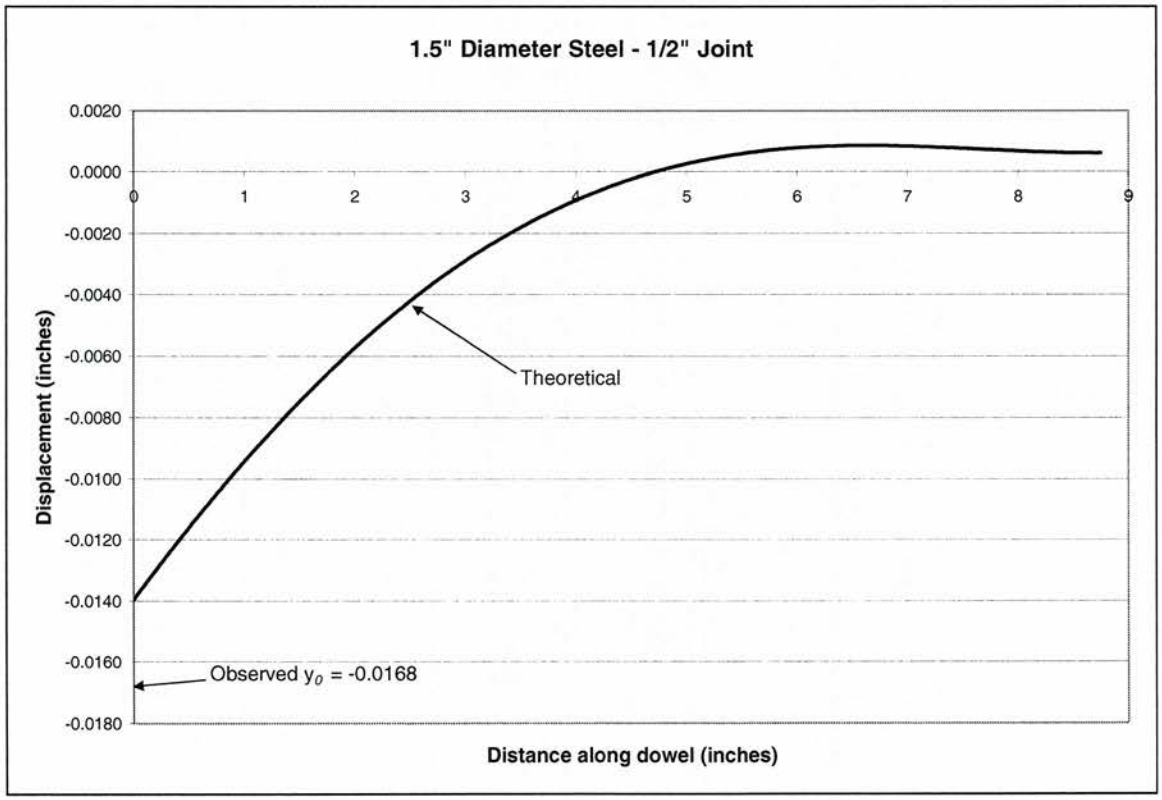

Figure D.2. Theoretical displacement of round steel dowel, 1/2-inch joint

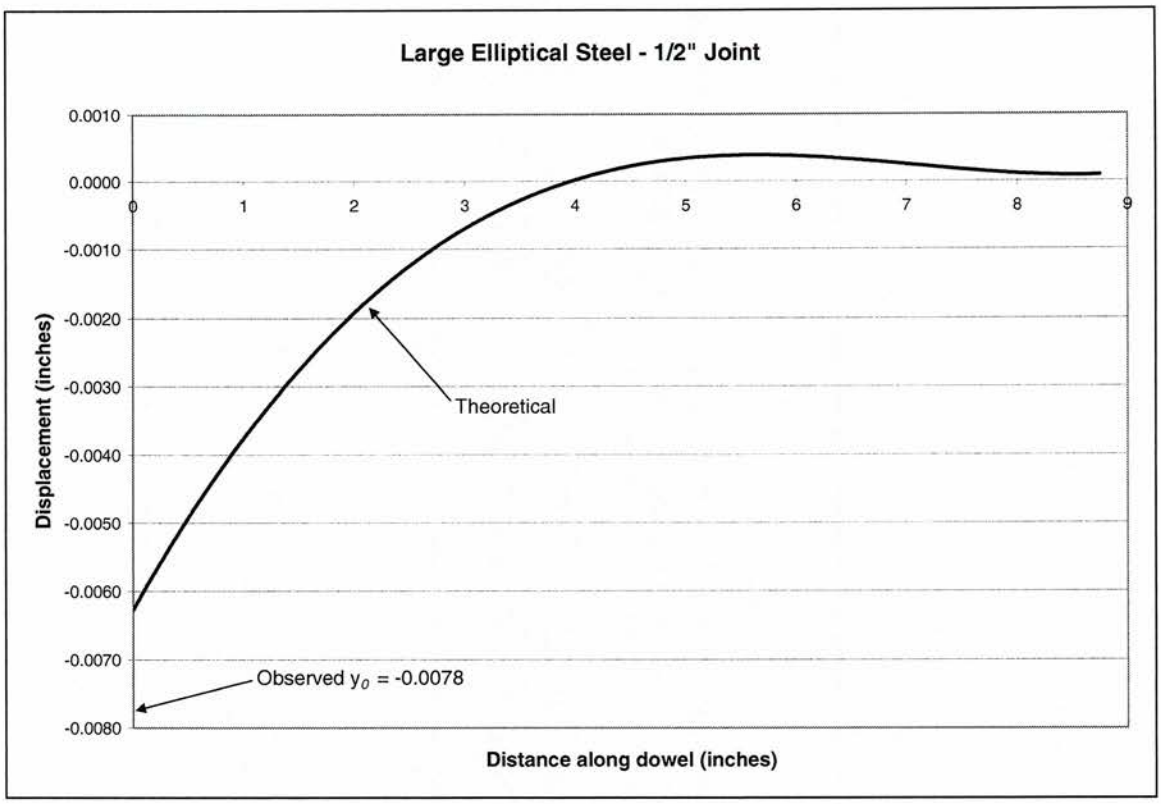

Figure D.3. Theoretical displacement of large elliptical steel dowel, 1/2-inch joint

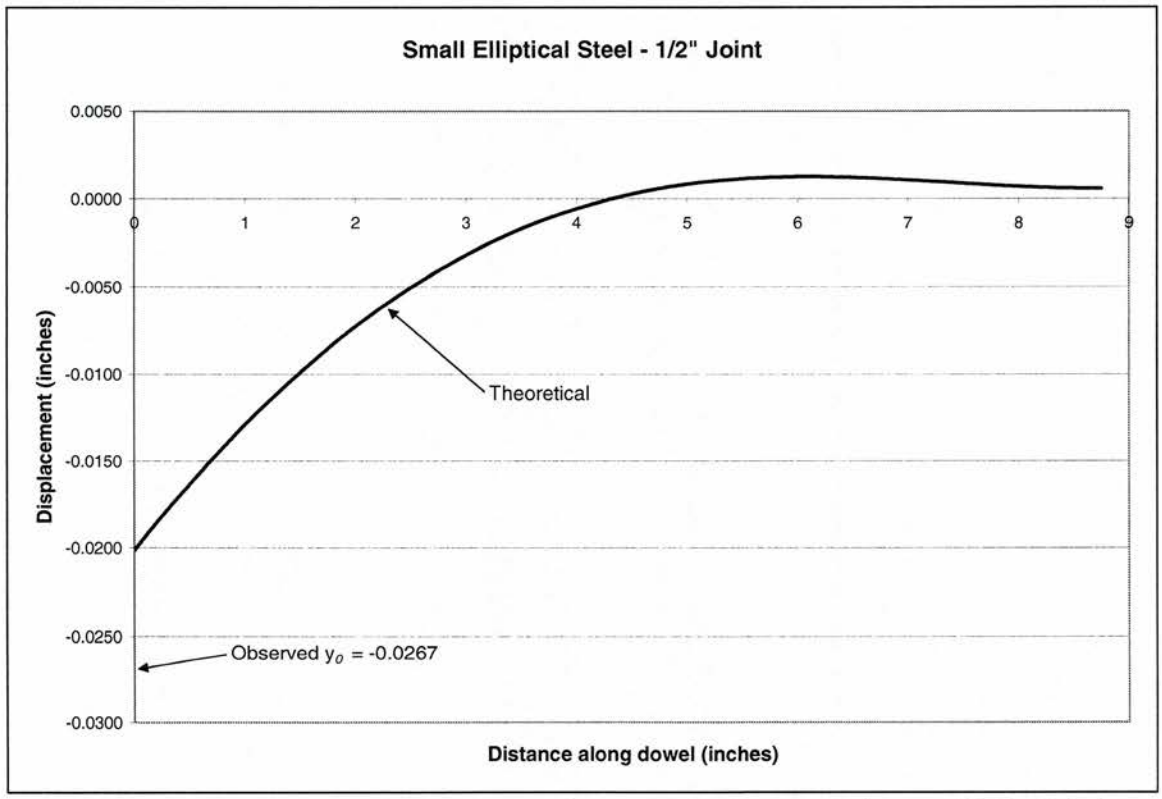

Figure D.4. Theoretical displacement of small elliptical steel dowel, 1/2-inch joint

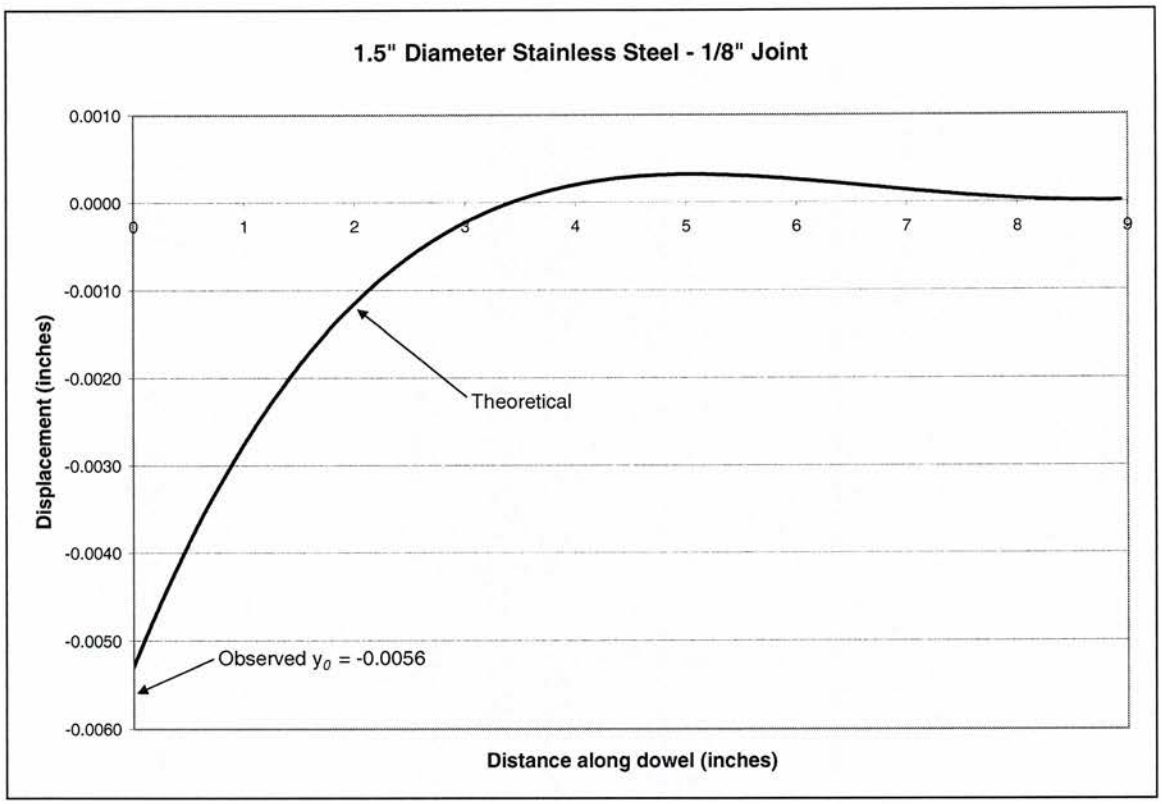

Figure D.5. Theoretical displacement of round stainless steel dowel, 1/8-inch joint

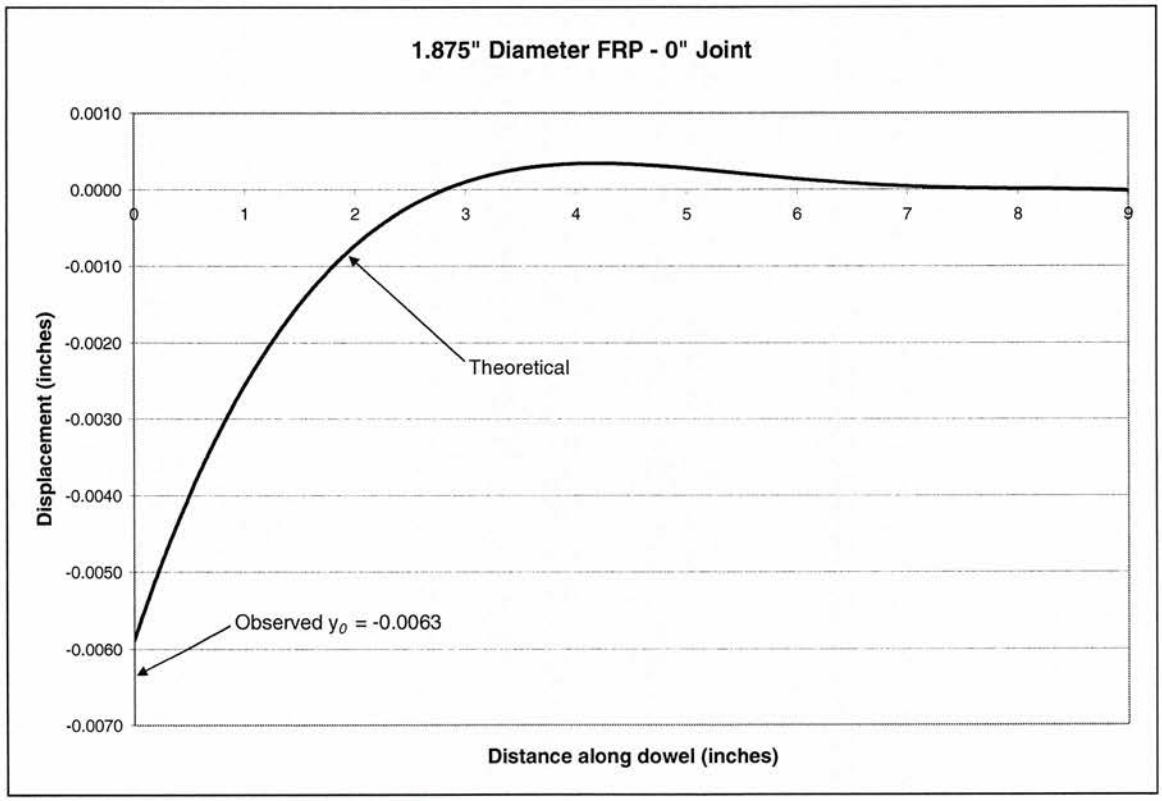

Figure D.6. Theoretical displacement of round GFRP dowel, 0-inch joint

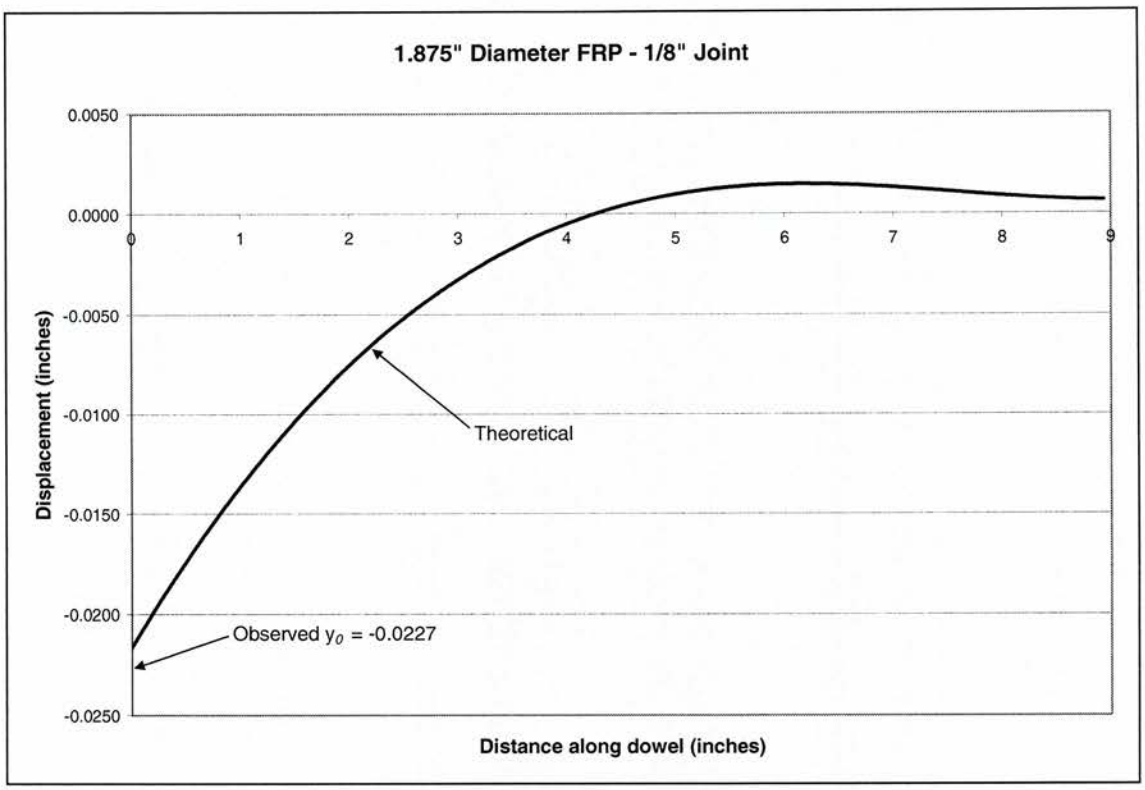

Figure D.7. Theoretical displacement of round GFRP dowel, 1/8-inch joint

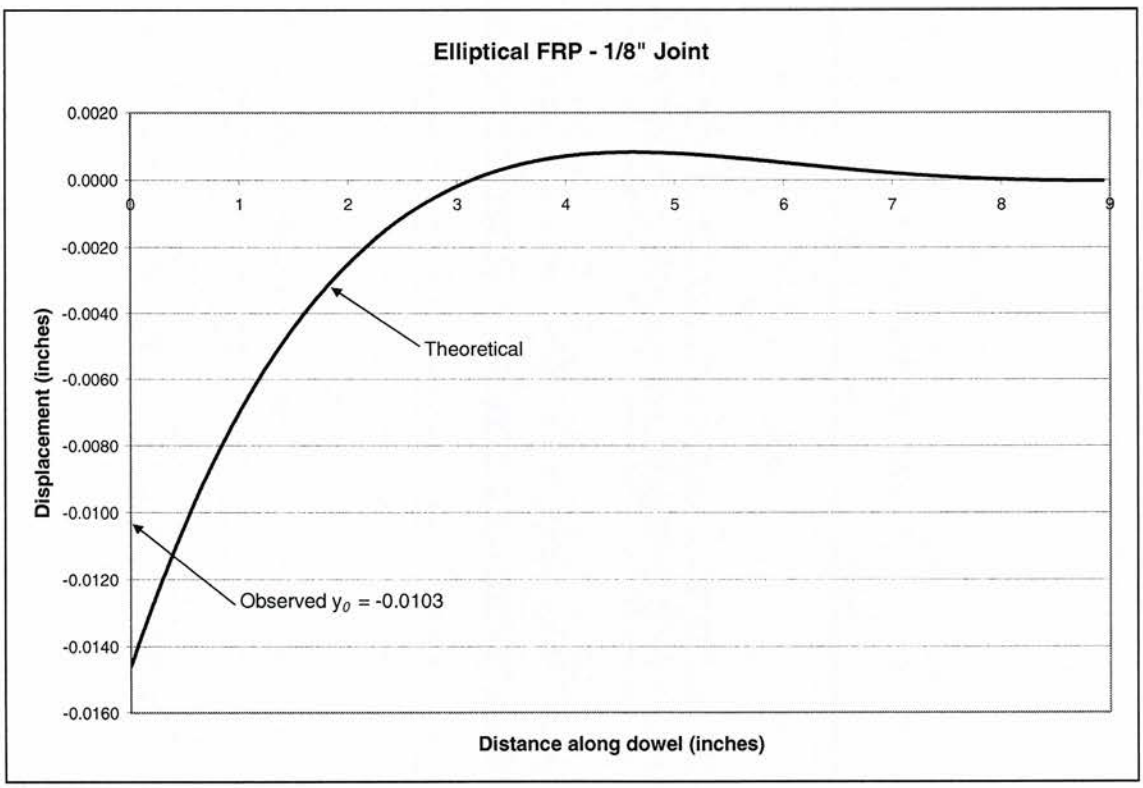

Figure D.8. Theoretical displacement of elliptical GFRP dowel, 1/8-inch joint

REFERENCES

1. Porter, M.L., E.A. Lorenz, K.P. Viswanath, B.A. Barnes, and M. Albertson. *Thermoset Composite Concrete Reinforcement: Final Report—Part II,* Project HR-325. Engineering Research Institute, Iowa State University, Ames, Iowa, October 1992.

2. Albertson, M.D. *Fibercomposite and steel pavement dowels.* Masters Thesis. Iowa State University, 1992.

3. Porter, M.L., B.W. Hughes, K.P. Viswanath, and B.A. Barnes. *Non-Corrosive Tie Reinforcing and Dowel Bars for Highway Pavement Slabs: Progress Report.* Iowa Highway Research Board Project HR-343. Department of Civil and Construction Engineering, Iowa State University, Ames, Iowa, January 1993.

4. Lorenz, E.A. *Accelerated aging of fiber composite bars and dowels.* Masters Thesis. Iowa State University, 1993.

5. Hughes, B.W. *Experimental evaluation of non-metallic dowel bars for highway pavements.* Masters Thesis. Iowa State University, 1993.

6. Porter, M.L., B.W. Hughes, and B.A. Barnes, *Fiber Composite Dowels in Highway Pavements*, Proceedings of Semisesquicentennial Transportation Conference, Iowa Department of Transportation and Iowa State University, Ames, Iowa, May 13-14, 1996.

7. Porter, M.L., and R.L. Braun. *Preliminary Assessment of the Potential Use of Alternative Materials for Concrete Highway Pavement Joints: Final Report.* Highway Innovative Technology Evaluation Center (HITEC) Report. Department of Civil and Construction Engineering, Iowa State University, Ames, Iowa, January 1997.

8. Davis, D.D. *Fatigue behavior of glass fiber reinforced polymer dowels.* Masters Thesis. Iowa State University, 2001.

9. Rohner, J.G. *Investigation of the modulus of dowel support in concrete pavements.* Masters Thesis. Iowa State University, 1999.

10. Ingram, D.N.J. *The effect of the dowel bar shape and spacing in Portland cement concrete pavements on the load transfer efficiency of the transverse joint.* Master Thesis. Iowa State University, 2004.

11. Porter, M.L., R.J. Guinn, Jr., A.L. Lundy, D.D. Davis, and J.G. Rohner. *Investigation of Glass Fiber Composite Dowel Bars for Highway Pavement Slabs: Final Report.* Iowa Highway Research Board Project TR-408. Engineering Research Institute, Iowa State University, Ames, Iowa, June 2001.

12. Porter, M.L., and R.J. Guinn. *Assessment of Highway Pavement Slab Dowel Bar Research: Final Report.* Iowa Highway Research Board Project HR-1080. Center for Transportation Research and Education, Iowa State University, Ames, Iowa, August 2002.

13. Guinn, R.J. *Assessment of highway pavement slab dowel bar research.* Masters Thesis. Iowa State University, 2002.

14. Lundy, A.L. *The effects of slope and flexural deflection on the concrete-dowel bar system.* Masters Thesis. Iowa State University, 2003.

15. Porter, M.L., R.J. Guinn, and A.L. Lundy. *Dowel Bar Optimization—Phases I and II: Final Report.* American Highway Technology Report. Center for Portland Cement Concrete Pavement Technology, Iowa State University, Ames, Iowa, October 2001.

16. Cable, J.K., M.L. Porter, J. Hoffman, L.L. Rold, and L.E. Edgar. *Demonstration and Field Evaluation of Alternative Portland Cement Concrete Pavement Reinforcement Material,* HR-1069. The Highway Division of the Iowa Department of Transportation, the Iowa Highway Research Board, and the Federal Highway Administration Demonstration Projects Program. Iowa State University, Ames, Iowa, June 2003.

17. Cable, J.K., L.E. Edgar, and J. Williams. *Field Evaluation of Elliptical Steel Dowel Performance.* Construction Report. Center for Portland Cement Concrete Pavement Technology, Iowa State University, Ames, Iowa, July 2003.

18. Porter, M.L., E.A. Lorenz, R.J. Guinn, and A.L. Lundy. *Solutions for Structural Dowel Bar Alternatives.* Center for Transportation Research and Education, Center for Portland Cement Concrete Pavement Technology, and American Highway Technology. Iowa State University, Ames, Iowa, Draft created 2004.

19. Porter, M.L, J.K. Cable, J.F. Harrington, N.J. Pierson, and A.W. Post. *Field Evaluation of Elliptical Fiber Reinforced Polymer Dowel Performance.* Center for Transportation Research and Education, Center for Portland Cement Concrete Pavement Technology, and the Federal Highway Administration, United States Department of Transportation. Iowa State, University, Ames, Iowa, June 2005.

20. Porter, M.L., J.F. Harrington, and N.J. Pierson. *Laboratory Study of Structural Behavior of Alternative Dowel Bars.* Center for Transportation Research and Education, Center for Portland Cement Concrete Pavement Technology, the Federal Highway Administration Project 7, Iowa Highway Research Board Project TR-510, and the Iowa Department of Transportation Project 04-163. Iowa State University, Ames, Iowa, April 2006.

21. Porter, M.L., J.F. Harrington, and N.J. Pierson. *Laboratory Evaluation of Concrete Slab Dowels for the Greenstreak Group.* Department of Civil, Construction & Environmental Engineering, Iowa State University, Ames, Iowa, June 2006.

22. Hughes, B.W., and M.L. Porter. Experimental Evaluation of Non-Metallic Dowel Bars in Highway Pavements. *Proceedings of Fiber Composites in Infrastructure*, edited by H. Saadatmanesh and M.R. Ehsani. First International Conference on Composites in the Infrastructure (ICCI96), January 1996.

23. Porter, M.L. FRP Dowel Bars. *Proceedings of the 1999 International Composites Expo*. Composite Institute, Harrison, New York, May 1999.

24. Porter, M.L., and D.D. Davis. Glass Fiber Reinforced Polymer Dowel Bars for Transverse Pavement Joints. *Proceedings of the FRP Symposium*, ACI Fall Convention, Baltimore, Maryland, November 2, 1999.

25. McConnel, V. FRP Reinforcement Durability and FRP Dowel Bars, *Transportation Composites Newsletter*, 1999.

26. Applied Pavement Technology, Inc. *Evaluation of Alternative Dowel Bar Materials.* Highway Innovative Technology Evaluation Center (HITEC) Draft Interim Report. Champaign, Illinois, March 2005.

27. American Association of State Highway and Transportation Officials (AASHTO). *AASHTO Guide for Design of Pavement Structures*. AASHTO, Washington, D.C., 1993.

28. Timoshenko, S., and J.M. Lessels. *Applied Elasticity*. Pennsylvania: Westinghouse Technical Night School Press, 1925.

29. Boresi, A.P., R.J. Schmidt, and O.M. Sidebottom. *Advanced Mechanics of Materials*. New York: John Wiley & Sons, Inc., 1993.

30. Friberg, B.F. Design of Dowels in Transverse Joints of Concrete Pavements. *Transactions, American Society of Civil Engineers*, Vol. 105, No. 2081, 1940.

31. Young, W.C., and Budynas, R.G. *Roark's Formulas for Stress and Strain*, 7th Edition. New York: McGraw Hill, Inc., 2002.

32. Cowper, G.R. The shear coefficient in Timoshenko's beam theory. 1966 *Journal of Applied Mechanics*, 335-340.

33. American Concrete Institute (ACI) Committee 325. Structural Design Considerations for Pavement Joints. *Journal of the American Concrete Institute*, Vol. 28, No. 1, July 1956, pp. 1–28.

34. Brown, V.L. and C.L. Bartholomew. FRP Dowel Bars in Reinforced Concrete Pavements. *Proceedings of the International Symposium on FRP Reinforcement for Concrete Structures*, American Concrete Institute (ACI), Michigan, 1993.

35. Ioannides, A.M., G.T. Korovesis. Analysis and Design of Doweled Slab-on-Grade Pavement Systems. *Journal of Transportation Engineering*, Vol. 118, No. 6, November/December 1992, pp. 745-768.

36. Eddie, Darren. *FRP Dowels for Concrete Pavements*. Masters Thesis. University of Manitoba, 1999

ACKNOWLEDGEMENTS

The research described herein was conducted at the Iowa State University Structural Engineering Laboratory in the Department of Civil, Construction & Environmental Engineering. Research was sponsored by the Federal Highway Administration, United States Department of Transportation; the Iowa Highway Research Board, Iowa Department of Transportation; the National Concrete Pavement Technology Center, Center for Transportation Research and Education; and the Greenstreak Group. Recognition should also be given to the following for providing materials: Hughes Brothers of Seward, Nebraska (dowels); Greenstreak Group of St. Louis, Missouri (dowels); EFCO Corp. of Des Moines, Iowa (forms); and Ames Read-mix Concrete of Ames, Iowa (concrete).

The author would like to acknowledge the assistance and expertise provided by Structural Engineering Laboratory Supervisor Douglas L. Wood.

Appreciation is also extended to the hourly students and volunteers who help cast the specimens used for the research. Special thanks go to Anthony W. Post and John F. Harrington for their assistance and support throughout casting and testing.

The author would also like to thank Dr. Max L. Porter for providing the research opportunity and for advising over the research and academics.